Report No. CG-D-14-98

ON PREDICTING THE LEEWAY AND DRIFT OF A SURVIVAL SUIT CLAD PERSON-IN-WATER

Tsung-Chow Su
Center for Applied Stochastics Research
Florida Atlantic University
Boca Raton, FL 33431

R. Quincy Robe
U.S. Coast Guard
Research and Development Center
1082 Shennecossett Road
Groton, CT 06340-6096

Duncan J. Finlayson
OCEANS Ltd.
31 Temperance Street
St. John's, Newfoundland, A1C 3J3, CANADA

Final Report
October 1997

Prepared for:

U.S. Department of Transportation
United States Coast Guard
Operations, (G-O)
Washington, DC 20593-0001

NOTICE

This document is disseminated under the sponsorship of the Department of Transportation in the interest of information exchange. The United States Government assumes no liability for its contents or use thereof.

The United States Government does not endorse products or manufacturers. Trade or manufacturers' names appear herein solely because they are considered essential to the object of this report.

The contents of this report reflect the views of the Coast Guard Research & Development Center. This report does not constitute a standard, specification, or regulation.

Marc B. Mandler
Technical Director
United States Coast Guard
Research & Development Center
1082 Shennecossett Road
Groton, CT 06340-6096

Technical Report Documentation Page

1. Report No. CG-D-14-98	2. Government Accession No.	3. Recipient's Catalog No.
4. Title and Subtitle On Predicting the Leeway and Drift of A Survival Suit Clad Person-In-Water		5. Report Date October 1997 6. Performing Organization Code Project No. 1012.3.7
7. Author(s) Tsung-Chow Su, R.Quincy Robe, Duncan J. Finlayson		8. Performing Organization Report No. R&DC 25/96
9. Performing Organization Name and Address U.S. Coast Guard Research and Development Center 1082 Shennecossett Road Groton, CT 06340-6096 Center for Applied Stochastics Research Florida Atlantic University Boca Raton, FL 33431 OCEANS, Ltd. 31 Temperance Street St. John's, Newfoundland, A1C 3J3, CANADA		10. Work Unit No. (TRAIS) 11. Contract or Grant No. ONR Grant N00014-91-J-1420 13. Type of Report and Period Covered Final Report
12. Sponsoring Agency Name and Address U.S. Department of Transportation United States Coast Guard Operations, (G-O) Washington, DC 20593-0001		14. Sponsoring Agency Code Commandant (G-OPR) U.S. Coast Guard Headquarters Washington, DC 20593-0001
15. Supplementary Notes This report is the twentieth in a series that documents the Improvement of Search and Rescue Capabilities (ISARC) Project at the USCG R&D Center. The R&D Center's technical point of contact is Arthur A. Allen, 860-441-2747.		

16. Abstract

Search for and rescue of persons in distress on the high seas requires the capability to accurately predict the position of the survivors. The current approach used by the U.S. Coast Guard to predict leeway drift is based on an empirical correlation between wind speed and search object motion derived from available field data. Prior to this study, no drift data were available for persons wearing survival suits which are widely used in distress situations.

As part of its ongoing program to provide more accurate methods of predicting search object drift, the U.S. Coast Guard R&D Center funded a study conducted at Florida Atlantic University in which the essential effects of environmental forces and person-in-the-water clad in a survival suit (PIW/SS) characteristics were properly modeled. This study provides a theoretical framework for and a better understanding of the dynamics of drift for a person-in-the-water clad in a survival suit, and will lead to a reliable model of drift prediction and improved efficiency in search and rescue missions. The study consisted of the development of a mathematical model for the PIW/SS drift prediction problem, laboratory studies of drag forces, field experiments to evaluate the model, and a statistical analysis of the leeway field data.

Two simple leeway models are recommended for use for manual input to "User Defined Leeway" in the current version of the U.S. Coast Guard's Computer Assisted Search Planning (CASP) tool and for use in manual search planning. Appropriate coefficients for CASP and manual solutions are provided.

17. Key Words		18. Distribution Statement
search and rescue leeway person-in-water	survival suit immersion suit exposure suit	This document is available to the U.S. public through the National Technical Information Service, Springfield, VA 22161.

19. Security Classif. (of this report)	20. SECURITY CLASSIF. (of this page)	21. No. of Pages	22. Price
UNCLASSIFIED	UNCLASSIFIED		

Form DOT F 1700.7 (8/72) Reproduction of form and completed page is authorized

METRIC CONVERSION FACTORS

Approximate Conversions to Metric Measures

Symbol	When You Know	Multiply By	To Find	Symbol
	LENGTH			
in	inches	* 2.5	centimeters	cm
ft	feet	30	centimeters	cm
yd	yards	0.9	meters	m
mi	miles	1.6	kilometers	km
	AREA			
in^2	square inches	6.5	square centimeters	cm^2
ft^2	square feet	0.09	square meters	m^2
yd^2	square yards	0.8	square meters	m^2
mi^2	square miles	2.6	square kilometers	km^2
	acres	0.4	hectares	ha
	MASS (WEIGHT)			
oz	ounces	28	grams	g
lb	pounds	0.45	kilograms	kg
	short tons (2000 lb)	0.9	tonnes	t
	VOLUME			
tsp	teaspoons	5	milliliters	ml
tbsp	tablespoons	15	milliliters	ml
fl oz	fluid ounces	30	milliliters	ml
c	cups	0.24	liters	l
pt	pints	0.47	liters	l
qt	quarts	0.95	liters	l
gal	gallons	3.8	liters	l
ft^3	cubic feet	0.03	cubic meters	m^3
yd^3	cubic yards	0.76	cubic meters	m^3
	TEMPERATURE (EXACT)			
°F	Fahrenheit temperature	5/9 (after subtracting 32)	Celsius temperature	°C

*1 in = 2.54 (exactly).

Approximate Conversions from Metric Measures

Symbol	When You Know	Multiply By	To Find	Symbol
	LENGTH			
mm	millimeters	0.04	inches	in
cm	centimeters	0.4	inches	in
m	meters	3.3	feet	ft
m	meters	1.1	yards	yd
km	kilometers	0.6	miles	mi
	AREA			
cm^2	square centimeters	0.16	square inches	in^2
m^2	square meters	1.2	square yards	yd^2
km^2	square kilometers	0.4	square miles	mi^2
ha	hectares (10,000 m^2)	2.5	acres	
	MASS (WEIGHT)			
g	grams	0.035	ounces	oz
kg	kilograms	2.2	pounds	lb
t	tonnes (1000 kg)	1.1	short tons	
	VOLUME			
ml	milliliters	0.03	fluid ounces	fl oz
l	liters	0.125	cups	c
l	liters	2.1	pints	pt
l	liters	1.06	quarts	qt
l	liters	0.26	gallons	gal
m^3	cubic meters	35	cubic feet	ft^3
m^3	cubic meters	1.3	cubic yards	yd^3
	TEMPERATURE (EXACT)			
°C	Celsius temperature	9/5 (then add 32)	Fahrenheit temperature	°F

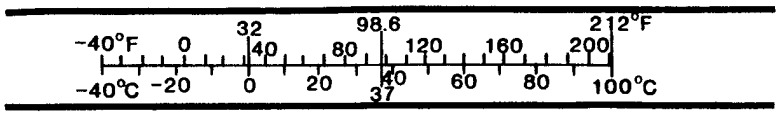

ACKNOWLEDGEMENTS

The field test was carried out in Long Key Florida with the assistance of Keys Marine Laboratory. The authors are indebted to the help of the laboratory's personnel, especially Mr. John Swanson, the Facilities Service Manager. Several graduate assistants including Messrs. Bob Milo, Q.C. Li, W. Li, H. Khuc, P. Reddy, and D. Duan, and undergraduate assistants, Messrs. G. Janssen II, P. Jean, L. Martin, M. Jaen and C. Robaina, Jr., contributed to the field test. Without their contributions, it would not have been possible to attain the objectives of the project. The authors are indebted to the outstanding performance of this field team, especially Mr. Bob Milo, the field coordinator.

Sincere thanks are due to his students L. Wei and H. Khuc for conducting laboratory experiments.

LIST OF ACRONYMS AND ABBREVIATIONS

CASP	Computer Assisted Search Planning
C_D	Drag Coefficient
C-MAN	Coastal Marine Automated Network
cm/sec	Centimeters per second
FAU	Florida Atlantic University
Hz	Hertz (1/second)
k	Spring Constant (or Stiffness)
KML	Keys Marine Laboratory
NOAA	National Oceanographic and Atmospheric Administration
PIW	Person -In-the-Water
PIW/SS	Survival Suit Clad Person-In-the-Water
R_e	Reynolds Number
SAR	Search and Rescue
$\mathbf{V}$	Drift Velocity
$\mathbf{V}_a$	True Wind Velocity (cm/sec)
$\mathbf{V}_l$	Leeway Velocity (cm/sec)
$\mathbf{V}_w$	True Surface Current (cm/sec)

TABLE OF CONTENTS

LIST OF FIGURES

LIST OF TABLES

EXECUTIVE SUMMARY

Search for and rescue of persons in distress on the high seas requires the capability to accurately predict the position of survivors. The current approach used by the U.S. Coast Guard to predict leeway drift is based on an empirical correlation between wind speed and search object motion derived from available field data. Prior to this study, no drift data were available for persons wearing survival suits, which are widely used in distress situations.

As part of its ongoing program to provide more accurate methods of predicting search object drift, the U.S. Coast Guard Research and Development (R&D) Center funded a study conducted at Florida Atlantic University (FAU) in which the essential effects of environmental forces and PIW characteristics were properly modeled. This study provides a theoretical framework for and a better understanding of the dynamics of drift for persons-in-water wearing survival suits (PIW/SS) and will lead to a reliable model of drift prediction and improved efficiency in search and rescue missions.

A theoretical analysis, laboratory experiments, and a field program were conducted at FAU to investigate the drift and leeway characteristics of a PIW/SS. A simplified leeway expression, developed from theoretical considerations, indicated that the leeway velocity should be directly proportional to the difference between the true wind velocity at the drift object and the true current at the object. This relationship should hold over a wide range of wind speeds. The constant of proportionality for a PIW/SS was evaluated in laboratory tests. Using these results, the leeway velocity, V_l, was estimated to be

$$V_l = 0.0323(V_a - V_w)$$

where the true wind velocity, V_a, should be corrected to the height of 0.2 m (0.6 ft) above mean sea level according to 1/7 power law and the true surface current, V_w, should be measured in the top half meter of the water column (nominally). For a Person-In-Water without survival suit (PIW), the constant of proportionality was found to be equal to 0.006.

A field trial was carried out to evaluate the proposed PIW/SS leeway model. To estimate surface current in the vicinity of the PIW/SS test objects, a conventional surface drift buoy method was employed using a new type of buoy designed and developed at FAU.

The evaluation concluded that, while quite good agreement was found for the total (leeway plus sea current) drift prediction, the magnitudes of the leeway vector predictions were biased on the low side.

In addition, an analysis of the derived leeway data was carried out. For this work, the interpolated wind velocities were adjusted to the standard reference height of 10 meters above the sea surface. A regression analysis of leeway speed $(|V_l|)$ on wind speed at 10 m $(|V_{a10}|)$, when constrained to pass through the origin, produced a leeway factor of 0.027; thus,

$$|V_l| = 0.027\,|V_{a10}| \quad \text{for } 5.0 \le |V_{a10}| \le 12.4 \text{ knots}$$

The standard error of the estimate was determined to be 0.133 knots.

Leeway angle analysis for the PIW/SS test models resulted in a mean leeway angle of 18 degrees to the right of the downwind direction and a standard deviation of 45 degrees. For drift durations of one hour or more in length, the envelope of leeway dispersions ranged from –25° to +38° from downwind. A bias to the right of the downwind direction was evident with the center of the dispersion being near +7°.

Two simple leeway models are recommended for use for manual input to "User Defined Leeway" in the current version of CASP and for use in manual search planning. The models are based upon: 1) a constrained linear regression of leeway upon wind speed at 10 meter height; 2) an uncertainty of leeway speed based on standard error at a wind speed of 19.6 knots; 3) maximum angle off the downwind direction; 4) the mean leeway angle. Tables in Chapter 6 provide coefficients appropriate for both CASP and manual solutions.

The field measurements made during this study relied on indirect current measurements. Recent advances in current meter technology and position determination have made it possible to measure leeway directly. The direct method should be used to continue the study of leeway for persons in the water with and without survival suits. These studies should include moderate to strong winds as well as heavy weather conditions.

CHAPTER 1

INTRODUCTION

1.1 Background

Many factors affect the drift of life rafts and disabled boats at sea. Successful Search and Rescue (SAR) missions, therefore, depend on human intelligence, on intuition and insight gained from many years at sea, and on tools developed for the task. Since 1944, numerous efforts have been made to investigate the effects of surface current (Tomczak, 1964; James, 1966; and Meyer et al., 1967) and wind velocity (Pingree, 1944; Chapline, 1960; Hufford and Broida, 1974; Morgan et al., 1977; Morgan 1978, Scobie and Thompson, 1979; Osmer, Edwards, and Breitler, 1982; and Nash and Willcox, 1985) on drifting objects. Leeway is defined as ". . . the movement of the search object through water, caused by the action of the wind on the exposed surfaces of the object." (National Search and Rescue Manual, 1991). As a vector quantity referenced to the local wind direction, leeway velocity may be expressed in terms of leeway speed and angle (the angle off the downwind direction) or, alternatively, in terms of the downwind and crosswind components. The leeway rate of a drifting object refers to the ratio of the leeway speed of the object to the local surface wind speed. Previous studies of leeway were reviewed by Hufford and Broida (1974) and by Nash and Willcox (1985). Table 1-1 summarizes the leeway information given in the National Search and Rescue Manual (1991); the table was adapted from Nash and Wilcox (1985).

While extensive field trials have been conducted to obtain empirical relationships between leeway speed and wind speed, the published results up to 1992 remain of limited value. As was pointed out by Osmer, Edwards, and Breitler (1982), the problems associated with leeway predictions are:

1. each type of craft displays different leeway characteristics;
2. a complex relationship exists between leeway motion and wind speed for wind speeds less than 5 knots;
3. the adequacy of the present leeway factors of 0.03 to 0.07 remains unknown; and,
4. the leeway angle is difficult to predict.

In an effort to help mitigate these uncertainties, Su (1986) developed a mathematical model to predict the drift of a boat and life raft for given environmental conditions. The model predictions and field test measurements resulted in excellent agreement. Subsequently, the model was simplified for operational use in search and rescue mission planning for disabled boats and drifting life rafts.

1.2 Current Work

As hydrodynamic and aerodynamic characteristics vary for different types of search objects, laboratory testing is required to provide force coefficients as inputs to mathematical models. The

models must then be verified in carefully designed field tests to assess their validity. In response to an operational need, the present study investigated the drift characteristics of a Person-In-Water (PIW) clad in a survival suit (PIW/SS).

There are three terms commonly used to describe flotation suits: exposure suits, immersion suits, and survival suits. The exposure suit is a work coverall generally made of nylon or other non-neoprene material. It is intended for working on deck in harsh weather and thus has no gloves or boots. It does, however, provide some flotation. The immersion suit and the survival suit are equivalent and are made of neoprene or other rubber-like material. They have integral gloves, boots, and hoods. Survival suits are designed to provide flotation and to retain body heat; an inflatable pillow is provided to keep a person's head above the water surface. Survival suits are carried on many boats for use in "abandon ship" situations. Persons-in-the-water clad in survival suits are the object of this study.

The PIW/SS will float in a horizontal position on the water surface rather than in an upright orientation. PIW/SS drift characteristics caused by wind loading and current drag are very different from those of a person not wearing a survival suit. A survival suit increases survival chances for a PIW/SS by reducing the effects of cold water on the victim. A better understanding of the drift characteristics of a PIW/SS will likewise increase the chances for survival by reducing search time required before sighting and rescue.

The present work was undertaken at Florida Atlantic University (FAU) and consisted of two major components. The first component dealt with the development of a mathematical model and the determination of force coefficients through laboratory measurements. In the FAU model, the essential effects of the object characteristics and environmental forces (other than in heavy weather) were properly accounted for through analysis rather than through correlation. The second component of the study included an extensive field trial to collect accurate drift object position and environmental data. For this work, a new Lagrangian drift buoy was developed from which the surface current data were derived. Post-experiment simulations were run using the data as input to the proposed model. Systematic comparisons of the measured drift tracks with the theoretical predictions for nine open water drift cases were used to evaluate the model. The resulting drift prediction model was found to be accurate and efficient.

The study was undertaken under ONR Grant N00014-91-J-1420. In terms of scientific merit, the study has provided a better understanding of the dynamical processes of drifting objects in the ocean. A reliable drift prediction model has been developed which is expected to result in improved efficiency in PIW/SS search and rescue missions. This report covers the work carried out in the study.

Table 1-1. Current Leeway Information Available In SAR Manual
(from Nash and Willcox, 1985)

Type of Craft	Wind Speed *	Leeway Speed *, †	Leeway Angle (deg)	Reference
Light-displacement cabin cruisers (no drogue)	0 - 5	0.078V		Hufford and Broida (1974)
Outboards (no drogue)	(0 - 2.6)		+/- 35	
Rafts without canopies/ballast system (no drogue)	5 - 40	0.07V + 0.04		
Rafts with canopies and ballast buckets	(2.6 - 20.6)	0.07V + 0.02		
Light-displacement cabin cruisers (with drogue)	0 - 5	0.026V		Hufford and Broida (1974)
Outboards (with drogue)	(0 - 2.6)		+/- 35	
Rafts without canopies or ballast system (with drogue)	5 - 40	0.05V - 0.12		Scobie and Thompson (1979)
Canopied raft with deep-draft ballast system	(2.6 - 20.6)	(0.05V - 0.06)		
Large cabin cruisers	0 - 40 (0 - 20.6)	0.05V	+/- 60	Chapline (1960)
Medium-displacement sailboats Fishing boats (e.g., trawlers, trollers, tuna boats)	0 - 40	0.04V	+/- 60	Chapline (1960)
Heavy-displacement, deep-draft sailing vessels	0 - 40	0.03V	+/- 45	Chapline (1960)
Surfboards	0 - 40	0.02V	+/- 35	Chapline (1960)

Note:
Leeway speed and angle information available in the National Search and Rescue Manual is listed with the most likely original source of the equations.

* Values and equations in parentheses are for meter/second (m/s), if different. All others are in knots.

† V is wind speed.

[BLANK]

CHAPTER 2

THEORETICAL ANALYSIS

2.1 Elementary Leeway Formula

A simplified analysis is presented consistent with the development of the linear leeway models currently used in search and rescue applications. A more general approach may be limited by factors of uncertainty which occur in search and rescue situations.

The forces exerted on a solid body when fluid flows by it or when it moves through a fluid are termed the drag and the lift, depending on whether the force is parallel to the motion or at right angles to it, respectively. The general expression for the drag force, $\boldsymbol{F}$, is given by

$$\boldsymbol{F} = \tfrac{1}{2} C_D \rho \; A |\boldsymbol{V}_r| \boldsymbol{V}_r \qquad (2\text{-}1)$$

where C_D is the drag coefficient, ρ is the density of the fluid, A is the cross-sectional area of the body perpendicular to the direction of the flow, and $\boldsymbol{V}_r$ is the velocity of the fluid relative to that of the drifting body. The drag coefficient is a function of body geometry and the Reynolds number. The Reynolds number, R_e, is given by

$$R_e = LV/\nu$$

where L is a characteristic length of the body in the direction of the flow, V is the relative speed, and ν is the kinematic viscosity of the fluid. Figure 2-1, adapted from Prandtl (1923) and Eisner (1930) by Daugherty and Franzini (1977), shows drag coefficients for bodies of revolution over a range of Reynolds numbers. As analytical means of obtaining drag coefficients are limited, C_D is derived largely by empirical methods.

Consider the simple case of a floating object with drift velocity $\boldsymbol{V}$, with its 'sail area' A_a exposed to a steady uniform wind of velocity $\boldsymbol{V}_a$, and its 'keel area' A_w facing a steady current of velocity $\boldsymbol{V}_w$ (Figure 2-2). The sail area is the projected area of the object above the waterline facing the wind; similarly, the keel area is the projected area below the waterline facing the water flow. Subscript 'a' refers to the air while the subscript 'w' refers to the water.

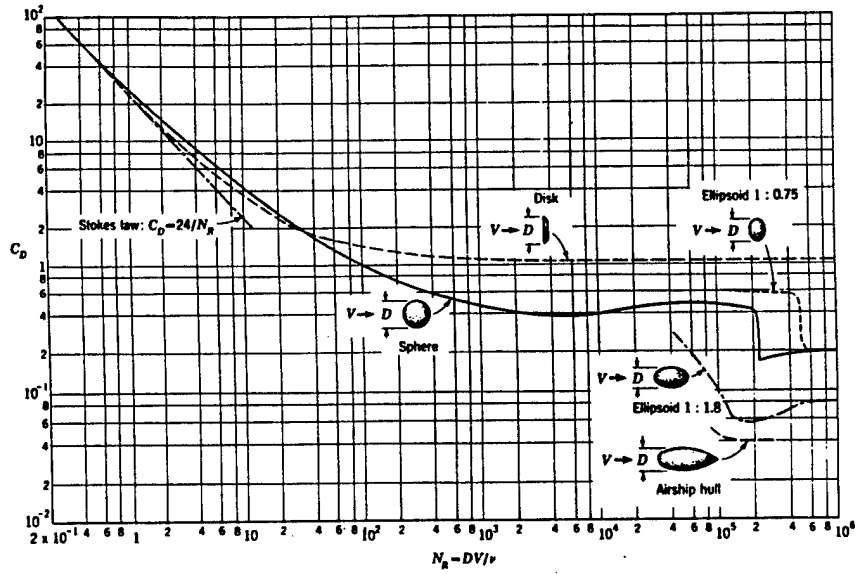

Figure 10.18. Drag coefficient for bodies of revolution. (Adapted from L. Prandtl, "Ergebnisse der aerodynamischen Versuchsanstalt zu Göttingen," p. 29, R. Oldenbourg, Munich and Berlin, 1923; and F. Eisner, "Das Widerstandsproblem," *Proc. 3d Internatn. Congr. Appl. Mech.*, p. 32, 1930.)

Figure 2-1. Drag Coefficient (Daugherty & Franzini, 1977).

Legend:

V_a = *wind velocity*
V_w = *current velocity*
V = *PIW/SS drift velocity*
V_l = *PIW/SS leeway velocity*

Note:

Lift produced by wind and current forces is not represented.

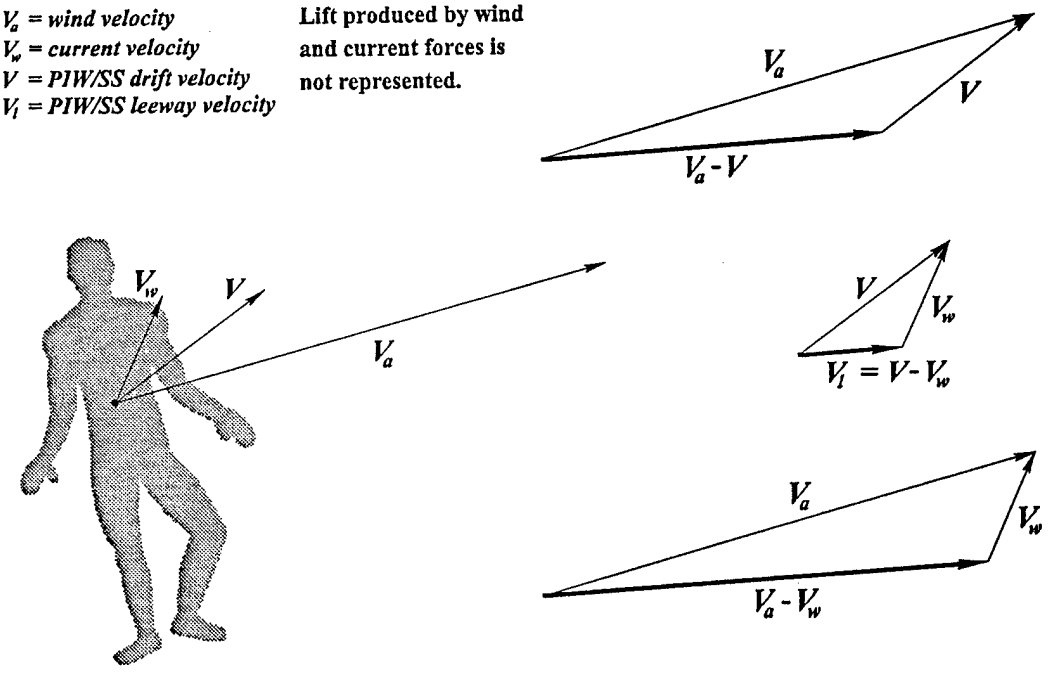

Figure 2-2. PIW/SS Drift and Leeway Velocity.

The primary forces acting on a drifting object are wind forcing and current retardation. A steady drift velocity V is achieved when the forces balance, as expressed by

$$\tfrac{1}{2} C_{D_a} \rho_a A_a |V_a - V|(V_a - V) + \tfrac{1}{2} C_{D_w} \rho_w A_w |V_w - V|(V_w - V) = 0 \qquad (2\text{-}2)$$

Assuming both Reynolds numbers, R_{e_a} and R_{e_w}, to be large, then C_{D_a} and C_{D_w} are constant. The drift velocity V can be solved easily from equation 2-2 as

$$V = \frac{\lambda}{1 + \lambda} V_a + \frac{1}{1 + \lambda} V_w \qquad (2\text{-}3)$$

in which $\lambda = \lambda_a / \lambda_w$ with $\lambda_a^2 = C_{D_a} \rho_a A_a$ and $\lambda_w^2 = C_{D_w} \rho_w A_w$.

As leeway is defined as the movement of an object through the water caused by wind acting on the object, the leeway velocity, V_l, can be computed by subtracting current velocity from the drift velocity of the object; i.e.,

$$V_l = V - V_w = \frac{\lambda}{1+\lambda} V_a + \frac{1}{1+\lambda} V_w - V_w = \frac{\lambda}{1+\lambda} (V_a - V_w) \qquad (2\text{-}4)$$

More concisely, the parameter, λ, is given by $\sqrt{C_{D_a} \rho_a A_a / C_{D_w} \rho_w A_w}$.

The expression is in agreement with the important finding of Chapline (1960) that the leeway speed of the small craft without a drogue is directly proportional to the wind velocity, at least for moderate to fresh winds. For a PIW/SS of 0.6 m (2 ft) shoulder width or larger, a wind speed of 2.5 m/s (5 knots), standard atmosphere air kinematic viscosity of 1.46 x 10^{-5} m^2/s leads to the Reynolds number $R_{e_a} \sim 10^5$. Since the current speed is typically one order of magnitude smaller than the wind speed and the kinematic viscosity of water is also one order of magnitude smaller than that of air, the corresponding R_{e_w} is expected to be of the same order of magnitude as R_{e_a}. Thus, the applicability of equation 2-4 for PIW/SS drift for wind speeds of about 2.5 m/s (5 knots) or greater is justified.

2.2 Leeway Analysis for Low Reynolds Number Flow

There are circumstances where R_{e_a} and/or R_{e_w} are not large enough to justify fully turbulent behavior corresponding to constant C_{D_a} and C_{D_w}. This may happen if the wind is less than 2.5 m/s (5 knots). For a more general treatment, the following functional dependence may be assumed

$$C_{D_a} = C'_{D_a} |V_a - V|^{-n_a}$$

with a similar expression for C_{D_w}. The drag coefficient, C'_{D_a}, is a constant. For fully turbulent conditions, $n_a = 0$ and, therefore, $C_{D_a} = C'_{D_a}$. For the case of a laminar boundary layer flow, $n_a = \frac{1}{2}$; and for very low Reynolds number flow $\left(\text{i.e., } R_{e_a} << 1\right)$, $n_a \rightarrow 1$ (Daugherty and Franzini, 1977).

Consider a case of a steady drift velocity with the wind and current flow in the same direction. The force balance leads to

$$\lambda'^2_a (V_a - V)^{2-n_a} = \lambda'^2_w (V_w - V)^{2-n_w}$$

where $\lambda'^2_a = C'_{D_a} \rho_a A_a$ and $\lambda'^2_w = C'_{D_w} \rho_w A_w$. Moreover,

$$\lambda' (V_a - V)^{1+n'} = V - V_w \tag{2-5}$$

$$\text{with } \lambda' = \left(\lambda'_a / \lambda'_w\right)^{\frac{2}{2-n_w}} \text{ and } n' = \frac{n_w - n_a}{2 - n_w} \tag{2-6}$$

From the definition of leeway in which $V_l = V - V_w$, equation 2-5 can be written as

$$V_l = \lambda' \left(V_a - \left(V_w + V_l\right)\right)^{1+n'}$$

As the wind speed is typically considerably greater than the search object drift speed $\left(\text{i.e.,}|V_a| >> |(V_w + V_l)|\right)$, the following binomial expansion is valid,

$$V_l = \left(\lambda' V_a^{1+n'} \left(1 - \frac{V_w + V_l}{V_a} \right)^{1+n'} \Big/ \lambda' V_a^{1+n'} \left(1 - (1+n') \frac{V_w + V_l}{V_a} \right) \right)$$

Therefore

$$V_l = \left(\frac{\lambda'}{1+\lambda'(1+n')V_a^{n'}} \right) V_a^{1+n'} - \left(\frac{\lambda'(1+n')V_a^{n'}}{1+\lambda'(1+n')V_a^{n'}} \right) V_w \qquad (2\text{-}7)$$

Aside from the transition range, R_{e_a} and R_{e_w} are generally of the same order and $n_a = n_w$, therefore $n' = 0$. Hence, equation 2-7 can be reduced to

$$V_l = \frac{\lambda'}{1+\lambda'} V_a - \frac{\lambda'}{1+\lambda'} V_w = \frac{\lambda'}{1+\lambda'} (V_a - V_w)$$

where λ' is defined according to equation 2-6.

For fully turbulent, or high Reynolds number, flow as typically occurs in moderate to fresh wind, $n_w = 0$ and,

$$\lambda' = \left(\frac{C'_{D_a} \rho_a A_a}{C'_{D_w} \rho_w A_w} \right)^{\frac{1}{2}}$$

For laminar flow with moderate Reynolds number, $n_w = \frac{1}{2}$, and

$$\lambda' = \left(\frac{C'_{D_a} \rho_a A_a}{C'_{D_w} \rho_w A_w} \right)^{\frac{2}{3}}$$

For very low Reynolds number flow, $n_w = 1$, and

$$\lambda' = \left(\frac{C'_{D_a} \rho_a A_a}{C'_{D_w} \rho_w A_w} \right)$$

We note that the basic solution (equation 2-4) can be generalized to deal with the low wind speed cases, provided that the leeway factor λ' is used instead of λ .

2.3 Wave Effect

Hufford and Broida (1974) reported that small craft leeway appears to increase up to about 15% with increasing sea state. The relationship has not yet been quantitatively established, however. This section contains a simple derivation to account for the wave effect on drift.

The wave drift force can be expressed by

$$F = \tfrac{1}{2} C_w \rho_w g L a^2 \qquad (2\text{-}8)$$

where C_w denotes the wave drift coefficient, g is the acceleration due to gravity, L is a characteristic length of the drifting object, and a is the wave amplitude which is equal to one-half the wave height. The force acts in the direction of the wave propagation. The wave drift coefficient in a regular wave pattern is a function of the frequency of the incoming waves and may reach a value of order 1 in some cases. Including the wave drift force in the balance equation 2-2, and assuming that the wind, current, and wave forces act in the same direction, we obtain

$$\tfrac{1}{2} C_{D_a} \rho_a A_a (V_a - V)^2 + \tfrac{1}{2} C_{D_w} \rho_w A_w (V_w - V)^2 + \tfrac{1}{2} C_w \rho_w g L a^2 = 0 \qquad (2\text{-}9)$$

This quadratic equation can be solved to yield

$$V = V_o - \frac{V_o - V_w}{1 - \lambda} + \left(\left(\frac{V_o - V_w}{1 - \lambda} \right)^2 + \frac{\alpha}{1 - \lambda^2} \right)^{\frac{1}{2}} \qquad (2\text{-}10)$$

where V_o is the solution of equation 2-10 when a = 0; thus,

$$V_o = \frac{\lambda}{1+\lambda} V_a + \frac{1}{1+\lambda} V_w$$

and

$$\alpha = \frac{C_w g L a^2}{C_{D_w} A_w}$$

For large α, the effect of wave drift is considerable as indicated in equation 2-10. With small α, assuming $\alpha << |V_o - V_w|$, equation 2.10 can be reduced to yield

$$V = V_o + \frac{1}{2} \frac{\alpha}{(1+\lambda)(V_o - V_a)}$$

so that

$$V_l = \frac{\lambda}{1+\lambda}(V_a - V_w) + \frac{1}{2} \frac{\alpha}{\lambda(V_a - V_w)} \qquad (2\text{-}11)$$

For α equal to zero, equation 2-11 reduces to equation 2-4, as expected. From equation 2-11, it is apparent that the wave effect on leeway is negligible if

$$\left(\left(\frac{1}{2} \frac{\alpha}{\lambda(V_a - V_w)} \right) \Big/ \left(\frac{\lambda}{1+\lambda} (V_a - V_w) \right) \right) << 1$$

or

$$\frac{1}{2} \left(\frac{1+\lambda}{\lambda^2} \right) \frac{1}{(V_a - V_w)^2} \frac{gLC_w a^2}{A_w C_{D_w}} << 1$$

Since $\lambda << 1$, $V_a >> V_w$ normally, and $A_w = L^2$ approximately, wave forces will be negligible when

$$\frac{a}{L} << \lambda \left(\frac{2\, C_{D_w}}{C_w} \right)^{\frac{1}{2}} \frac{|V_a - V_w|}{\sqrt{gL}} \qquad (2\text{-}12)$$

This condition may not generally be satisfied. For example, for $\lambda = 0.03$, $C_{D_w} = 1$, $C_w = 0.01$, $V_w = 0$, $V_a = 20$ knots (10.28 m/s), g = 9.81 m/s^2, the condition (2-12) requires the wave amplitude to be much less than 1.87 m while the significant wave amplitude at a such sea state is 1.2 m. It is therefore concluded that wave drift needs to be included in the drift prediction for severe weather search.

2.4 Drift Object Orientation

A vessel in which the hull and superstructure are balanced fore and aft will, in general, lie beam on to the wind and sea. Field observations indicated that this is also true for a PIW/SS. Figure 2-3(a) illustrates a floating body abeam to the wind; in this orientation, the relative current drag directly opposes the wind drag force and an equilibrium condition results. The 'S' in the figure denotes the flow stagnation points where velocities of the flows are zero and the maximum pressures occur. Figure 2-3(b) shows a small perturbation of the previous condition. The streamline pattern has changed and the locations of maximum pressure have shifted along the body. This couple acts to return the boat back to its equilibrium position.

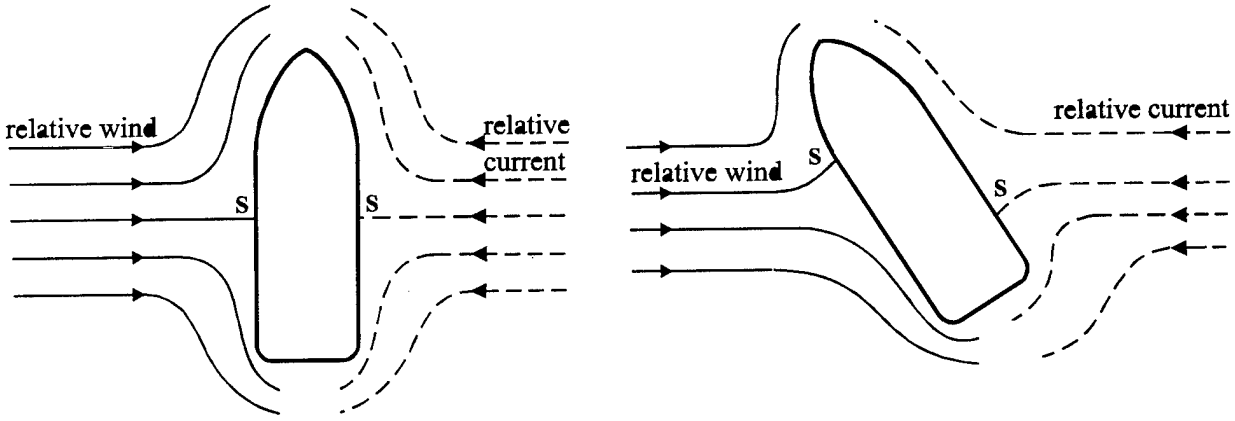

(a) (b)

Figure 2-3. Flow Pattern and Fluid Forcing.

Figure 2-4(a) illustrates a vessel with its bow facing into a steady wind. Figure 2-4(b) shows that a small perturbation will have a destabilizing effect which will turn the vessel further away from its original undisturbed orientation. Thus, given a balanced hull and superstructure arrangement, the vessel will turn its beam to the wind.

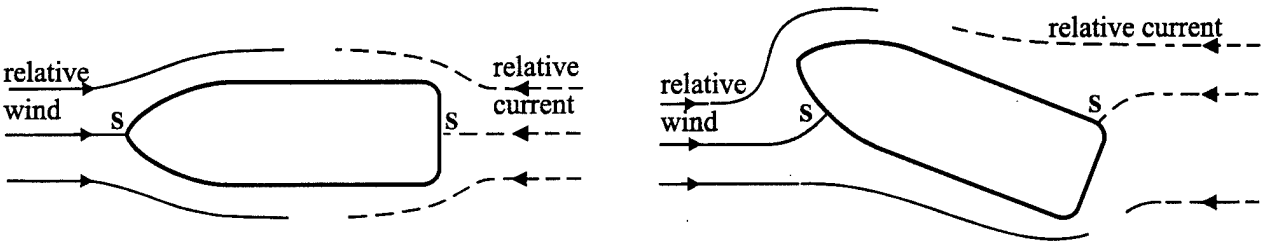

(a) (b)

Figure 2-4. Flow Pattern and Fluid Forcing.

The following chapter documents the laboratory work that was undertaken to determine the air and water drag coefficients of a PIW/SS test model. With these values, a model for predicting PIW/SS leeway velocity is put forward. The model is based on equation 2-4, valid for fully turbulent, high Reynolds number flow.

[BLANK]

CHAPTER 3

LABORATORY MEASUREMENTS

3.1 Experiment Overview

Laboratory tests were carried out at the Water Channel Test Facility of the Center for Applied Stochastics Research at Florida Atlantic University. The objectives of the experiments required that a PIW/SS model be subjected to wind and current, and that the drag forces on the model be measured. In order to do this, the model was secured to a cantilever beam and placed in a partially submerged, face-up position in the Water Channel. The force exerted by the water current was measured to obtain a force coefficient on the submerged portion of the model. To estimate the wind drag coefficient, the model was placed in a face-down position. The current force on the model could then be measured to obtain a force coefficient for the above-water portion of the body.

3.2 Water Channel Test Facility

The Water Channel at FAU is fabricated of Plexiglas to facilitate visual observation (Figures 3-1 and 3-2). Water is circulated by a variable-pitch propeller driven by a 3-horsepower DC motor. The DC motor is controlled by a SCR (Silicon-Controlled Rectifier) type control unit which converts the 230V AC power to a DC voltage. The DC voltage is adjustable from 0 to 180V with a maximum current of 16A. By changing the input voltage to the motor, the rotation speed of the propeller can be adjusted to give longitudinal flow speeds ranging from 0 to 0.5 m/s (0 to 1 knot). Higher speeds can be obtained by varying the pitch of the propeller. To observe the flow and to facilitate speed calibration, hydrogen bubbles are generated from a straight, 25 μ m diameter, platinum wire connected to the cathode of a pulsating electric current source. Flow speeds are calibrated by measuring the distance between adjacent lines of bubbles. These distances, together with the corresponding time intervals at which the bubbles are generated, are used to compute the flow speeds. The relationship between the DC motor input voltage and the corresponding average flow speed was found to be nearly linear.

Transducers of the non-contact eddy-current type were used to measure the force on the PIW/SS model by detecting small displacements of an elastic linkage which supported the model. The transducer sensing elements were 5 mm in diameter, with the following specifications:

1. measuring range of 1.25 to 2 mm;
2. sensitivity of 8 mV/μ m;
3. accuracy within 5%;
4. deviation from exact linearity within 20 μ m;
5. frequency response between 0 and 1000 Hz;
6. temperature range of -10 to 100°C; and,
7. output voltage range of 0 to 16V.

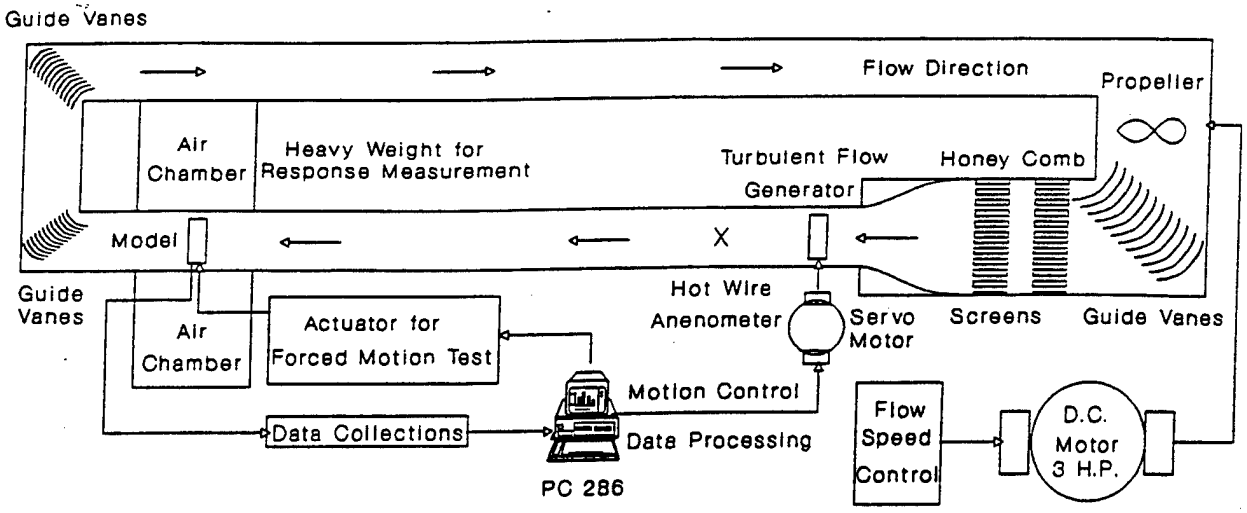

Figure 3-1. Sketch of Water Channel Test facility at the Center for Applied Stochastics Research at Florida Atlantic University.

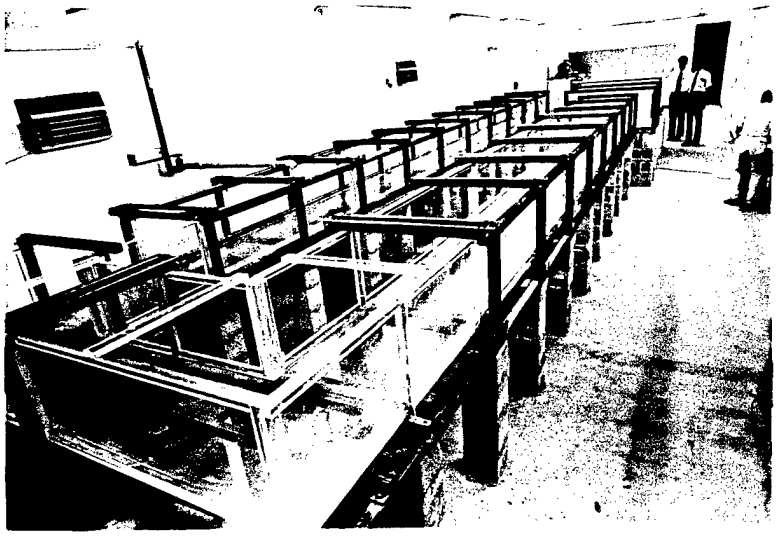

Figure 3-2. Overview of the FAU Water Channel Test Facility.

The output of each transducer was transmitted through a shielded multi-conductor cable to a data acquisition board on a microcomputer for recording and processing. The data acquisition board, National Instrument Model AT-MIO-16L-9, has an eight channel differential mode analog-to-digital converter and is capable of collecting data up to 100,000 samples/s with a 12-bit precision. This is equivalent to an error range of ±0.025%. Since the highest input voltage of the board is limited to 10V, the output from the transducer, ranging up to 16V in amplitude, is reduced by one-half, using a register-divider for each channel.

Several programs were written in the C language for recording data interactively as well as in batch mode using the LabWindows Data Acquisition Library. These programs were then compiled with Microsoft Quick C for DOS. A program configuration file defined the sampling rate, recording channels, and scale factors, so that the readings reflect the displacement in mm rather than in volts. The data were stored on computer disk for subsequent processing using other programs, such as DADiSP, GnuPlot on a PC, and IMSL/FORTRAN on a DEC station 5000.

3.3 Test Arrangement

The test arrangement used in the experiment was based on a cantilever beam approach in which a force applied to the load end of a beam resulted in a deflection of the beam. In the set up, the test model was fixed to the end of a rigid aluminum bar which was secured vertically below a horizontal aluminum block using a single bolt. The bolt also served as a pivot allowing for angular adjustment. The aluminum block was itself secured to a thin steel plate that acted as a leaf spring. When water flowed past the test model, a force was exerted on the model in the direction of the flow, deflecting the leaf spring. A transducer, positioned near the fixed end of the leaf spring, detected the amount of deflection; the measurements were subsequently recorded.

3.4 Calibration of the Leaf Spring

Calibration was accomplished in the following manner. Initially, the unloaded position of the leaf spring was recorded as a reference point. Next, a horizontal force was applied to the vertically mounted cantilever bar using a 50 g mass connected by a wire running through a fixed pulley. The position of the leaf spring was then measured by the transducer and recorded. Three trials were conducted. The procedure was repeated using a mass of 100 g and, finally, with 200 g. Subsequently, the spring displacements were calculated for each trial and then the mean displacement for each of the individual loads was computed. The results are given in Table 3-1.

The relationship between the force and the mean displacement was found to be approximately linear over the range of displacements observed. Moreover, the spring stiffness, k, was determined to be 6944 N/m. With the spring constant and a measured deflection, the applied force on the object caused by the fluid flow can be readily computed.

Table 3-1. Calibration Results showing Mass and Force vs. Displacement

		x-position			x-displacement			Mean disp.
Mass (g)	Force (N)	Trial 1 x (mm)	Trial 2 x (mm)	Trial 3 x (mm)	Trial 1 δx (mm)	Trial 2 δx (mm)	Trial 3 δx (mm)	$\overline{\delta x}$ (mm)
0.0	0.0	0.739	0.740	0.740	0.000	0.000	0.000	0.000
50.0	0.4905	0.813	0.814	0.814	0.074	0.074	0.074	0.074
100.0	0.9810	0.876	0.885	0.881	0.137	0.145	0.141	0.141
200.0	1.9620	1.005	1.006	1.019	0.266	0.266	0.279	0.270

3.5 Test Model and Configurations

In the Water Channel, a rubber mannequin dressed in a scale model survival suit was used as the test model. It was approximately 30 cm (12 inches) in length and 8 cm (3 inches) across the shoulders. The model was secured to the load end of the cantilever beam. (Figures 3-3 and 3-4).

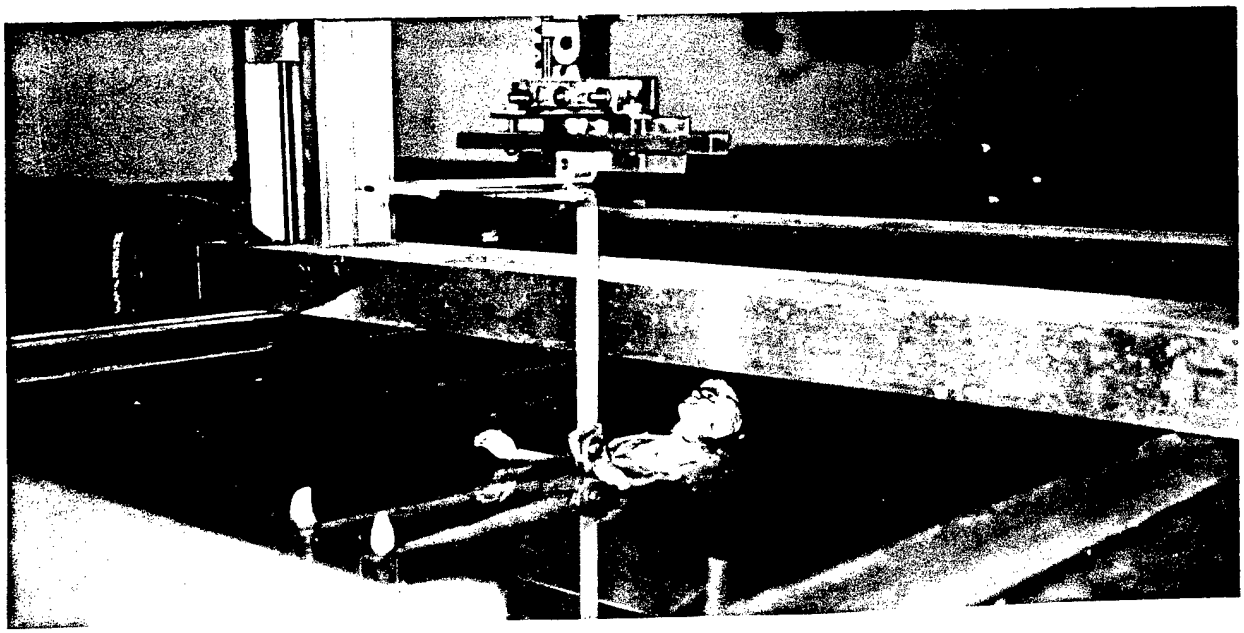

Figure 3-3. Model of a PIW/SS in the Water Channel Test Facility.

Figure 3-4. Model of PIW without Survival Suit.

The first test was conducted with the model partially submerged and oriented in the natural face-up position of a person floating in water. The model was also tested in other orientations, including face-down, vertical, and sideways to the current flow. Each configuration was tested with controlled water current speeds of 0, 10, 20, 30, and 40 cm/s. In addition to each orientation, five angular positions with respect to the current flow were tested; specifically, at 0, 30, 45, 60, and 90 degrees to the current direction.

3.6 Results Obtained

The resulting force was normalized to obtain the drag coefficient using

$$C_{D_w} = \frac{F}{\frac{1}{2}\rho_w L T V^2}$$

where: F is the drag force (N) given by $(k)(\delta x)$;

k is the spring constant (6944 N/m);

δx is the spring deflection in meters;

ρ_w is the water density (1000 kg/m^3);

L is the length or height of model (0.30 m);

T is average width of model (0.08 m); and,

V is the velocity of water flow in m/s.

Drag coefficients were determined for the various configurations described in Section 3.5. As expected, the coefficients were found to be higher, in general, for model configurations positioned 90° to the flow than for the other angles. Moreover, in line with the arguments presented in Section 2.4, this is the preferred orientation with respect to the flow direction. This being the case, the drag coefficients tabulated in Table 3-2 are for PIW and PIW/SS configurations positioned perpendicular to the flow. Computed drag coefficients are given for the above- and below-water portions of the PIW test model oriented vertically, and for the PIW/SS model floating horizontally on the surface. The results are given for water flow speeds of 10, 20, 30, and 40 cm/s.

Table 3-2. Drag Coefficients for PIW and PIW/SS Test Models Oriented Perpendicular (90°) to the Flow.

	Water flow speed (cm/s)			
Test Model, body segment, orientation	10	20	30	40
Head of PIW, vertical orientation	0.110	0.110	0.112	0.131
PIW model, below-water portion, vertical orientation	1.198	1.032	1.012	0.989
PIW/SS model, above-water portion, horizontal	0.697	0.654	0.686	0.690
PIW/SS model, below-water portion, horizontal,	0.822	0.773	0.744	0.757

The effect of the current speed variation (i.e., Reynolds number effect) is considered small in light of other uncertainties involved in the PIW/SS or PIW cases. For the case of V equal to 40 cm/s, L equal to 30 cm, and μ for water at 20°C equal to $1 \times 10^{-6}\ m^2/s$, the Reynolds number is approximately 1.2×10^5. Leeway velocity coefficients were computed for both the PIW/SS and PIW using the appropriate air and water drag coefficients determined at a water flow speed of 40 cm/s. These cases are detailed below, concluding with the corresponding leeway model equations. In these calculations, the density of air, ρ_a, is taken to be equal 1.224 kg/m^3

Model 1 - Person-In-Water with survival suit (PIW/SS), floating horizontally:

$C_{D_a} = 0.690, \quad C_{D_w} = 0.757$

$A_a = A_w$, approximately

$\lambda = \sqrt{C_{D_a} \rho_a A_a / C_{D_w} \rho_w A_w} = 0.0334$

$\lambda / (1 + \lambda) = 0.0323$

Therefore, the PIW/SS leeway velocity is estimated to be:

$$V_l = 0.0323 (V_a - V_w) \tag{3-1}$$

Model 2 - Person-In-Water without survival suit (PIW), floating upright:

$C_{D_a} = 0.131, \quad C_{D_w} = 0.989$

$A_a = 0.2 A_w$, approximately

$\lambda = \sqrt{C_{D_a} \rho_a A_a / C_{D_w} \rho_w A_w} = 0.006$

$\lambda / (1 + \lambda) = 0.006$

Therefore, the PIW leeway velocity is estimated to be:

$$V_l = 0.006 (V_a - V_w) \tag{3-2}$$

[BLANK]

CHAPTER 4

FIELD PROGRAM

4.1 Introduction

A field program was designed and carried out with the primary objective of collecting a data set in order to calibrate and evaluate the theoretical PIW/SS leeway prediction model (equation 3-1). The secondary objective of the work was to obtain a better understanding and appreciation of the leeway of a PIW/SS as it pertains to search and rescue operations. Field experiments were conducted on February 27 and 28 and on March 6 and 7 in 1993 along the coast of Long Key, Florida. The work in February took place in Florida Bay near the Keys Marine Laboratory (KML); the March tests were conducted in the Atlantic Ocean along the Long Key Viaduct. The Keys Marine Laboratory, a joint operation of the Florida Marine Research Institute, the Florida Department of Natural Resources, and the Florida Institute of Oceanography provided logistical support. KML was the staging area for the field trials. Two 24 foot T-Craft boats having a 7-person capacity were provided by KML.

4.2 Experiment Design

4.2.1 Experiment Area

A one nautical mile square area, centered in Florida Bay off KLM, served as the tracking range on February 27 and 28, 1993 (Figure 4-1). A 1 x 1 nautical mile area, in the Atlantic Ocean off the northern end of the Long Key Viaduct, was the tracking range used on March 6 and 7, 1993 (Figure 4-2).

4.2.2 PIW/SS Drift Objects

Three mannequins were dressed in survival suits to simulate PIW/SS drifting bodies (Figures 4-3a and 4-3b). Mr. George Janssen II, a senior in mechanical engineering at FAU, volunteered in the real person drift test on February 27, 1993 (Figure 4-4).

4.2.3 Test Procedure and Position Measurement

Two independent boat crews deployed and recovered the drift objects during the trials. Each boat had a captain, one graduate research assistant, and two undergraduate assistants. Individual tests began with the rapid deployment of a PIW/SS model along with three Lagrangian drift buoys in the immediate vicinity. The specific locations chosen for the deployment of the test objects and drift buoys were determined by the expected tidal current and wind conditions for the day. With time, the model and associated buoys tended to drift apart due to the greater leeway of the PIW/SS. Whenever appropriate, the drift buoys were recovered and redeployed near the PIW/SS model.

The positions of the drift objects were obtained by triangulation using survey transits. Two land-based tracking teams were each equipped with two transits. The teams consisted of four graduate research assistants; each team was responsible for tracking one PIW/SS model and the accompanying three drift buoys. Communication by portable radio ensured that the survey measurements were synchronized.

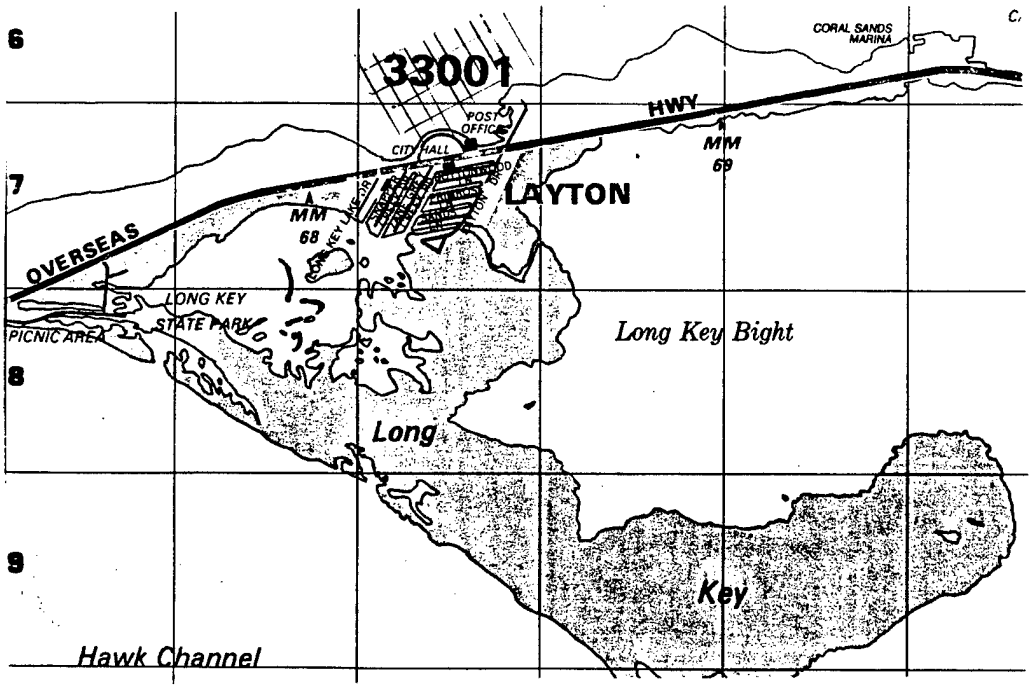

Figure 4-1. Experiment Area - February 27 and 28, 1993.

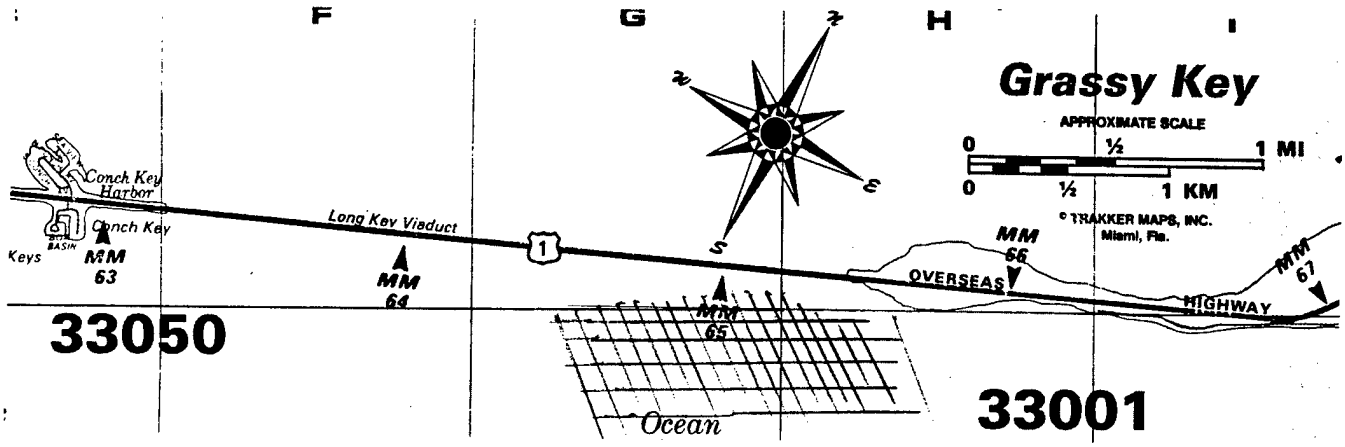

Figure 4-2. Experiment Area - March 6 and 7, 1993.

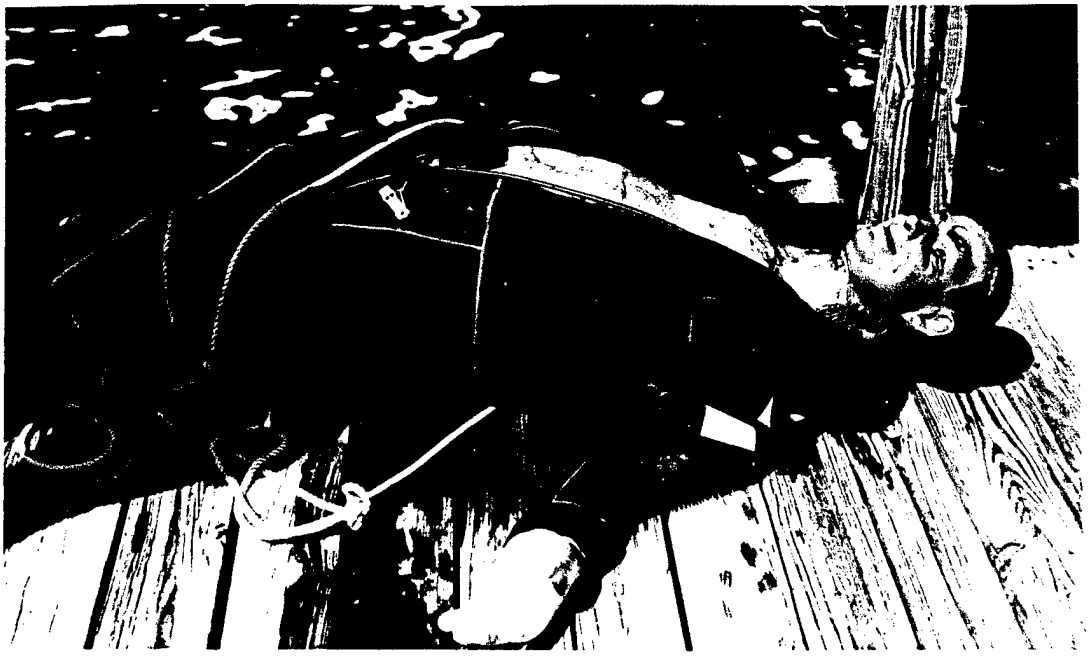

Figure 4-3(a). Mannequin in Survival Suit.

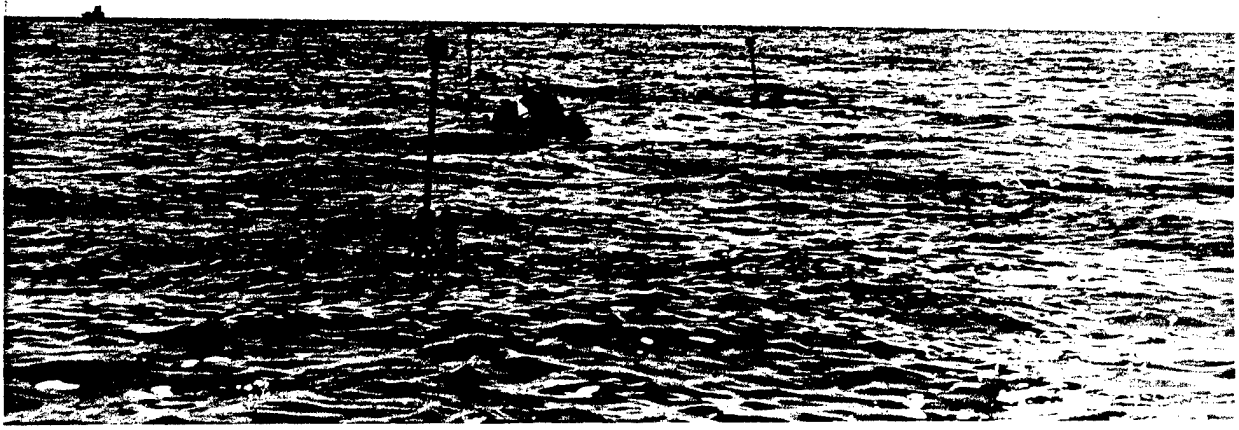

Figure 4-3(b). Mannequin in Survival Suit

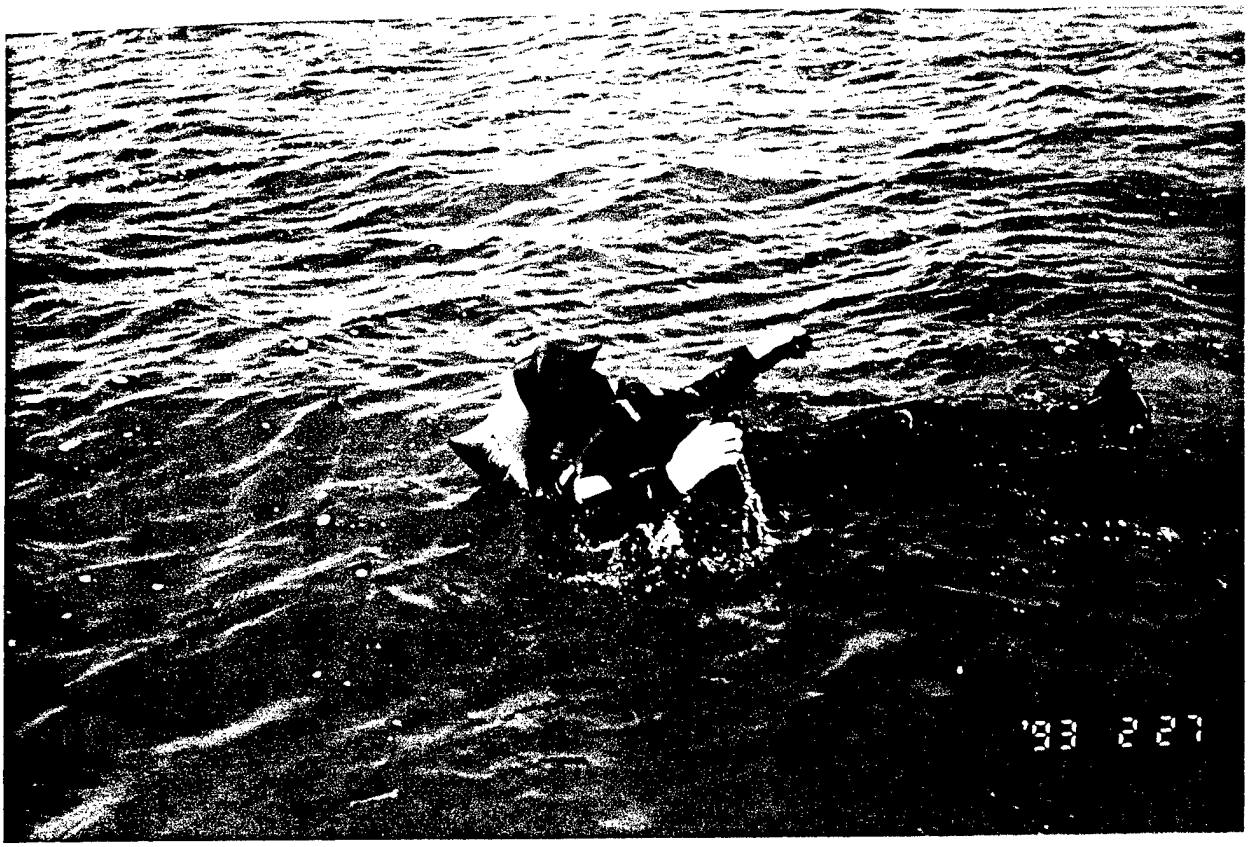

Figure 4-4. Mr. George Janssen II in Survival Suit.

Normally, measurements were made and recorded at ten minute intervals during the full period that the PIW/SS model remained within the tracking range.

4.2.4 Surface Current Measurement

The currents in the vicinity of the PIW/SS model were determined using Lagrangian drift buoy position data. For this experiment, a new buoy design, having relatively low leeway characteristics, was developed at FAU. The design made use of the property of flow stagnation operating on a narrow, 'plank-on-edge' drag plate; this acts to keep the plate perpendicular to the direction of the current (see Figure 2-3). The proper orientation in the vertical plane and constant depth below the water surface were assured by using two small floats mounted on the top edge of the plate and a counterweight secured to the center of the lower edge. The buoys were equipped with an instrument and power supply housing, a flashing light, and whip antenna. The design is illustrated in Figure 4-5 and shown in Figures 4-6 to 4-8.

Seven buoys were fabricated and tested at FAU. Constructed primarily of plywood, the low cost buoys were deemed to be expendable. They were light weight but strongly built, and were easily deployed and recovered by one person (Figures 4-9 to 4-12). Tests showed that a set of drift buoys deployed near one another moved together in parallel (Figure 4-13), substantiating the design concept. They tilted rhythmically in the waves, as shown in Figure 4-14, rather than being slammed about. With an on-board flow sensor, this periodic motion could be measured and recorded to produce a local wave record. There was no loss of, or damage to, the buoys during the test.

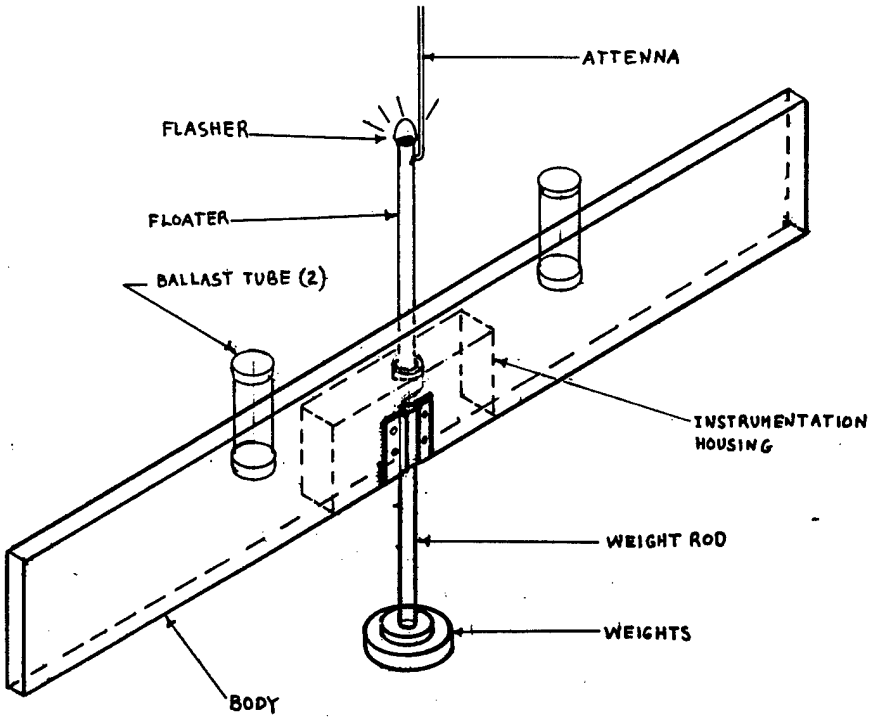

Figure 4-5. FAU Drift Buoy Assembly.

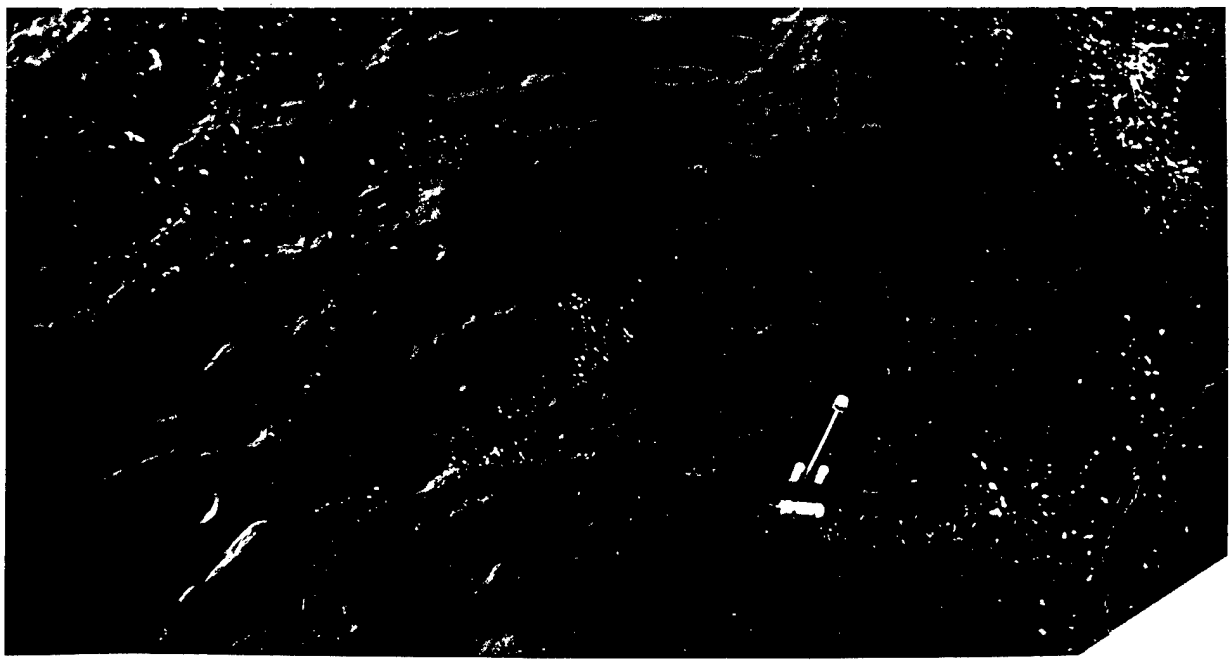

Figure 4-6. FAU Designed Drift Buoy in Action.

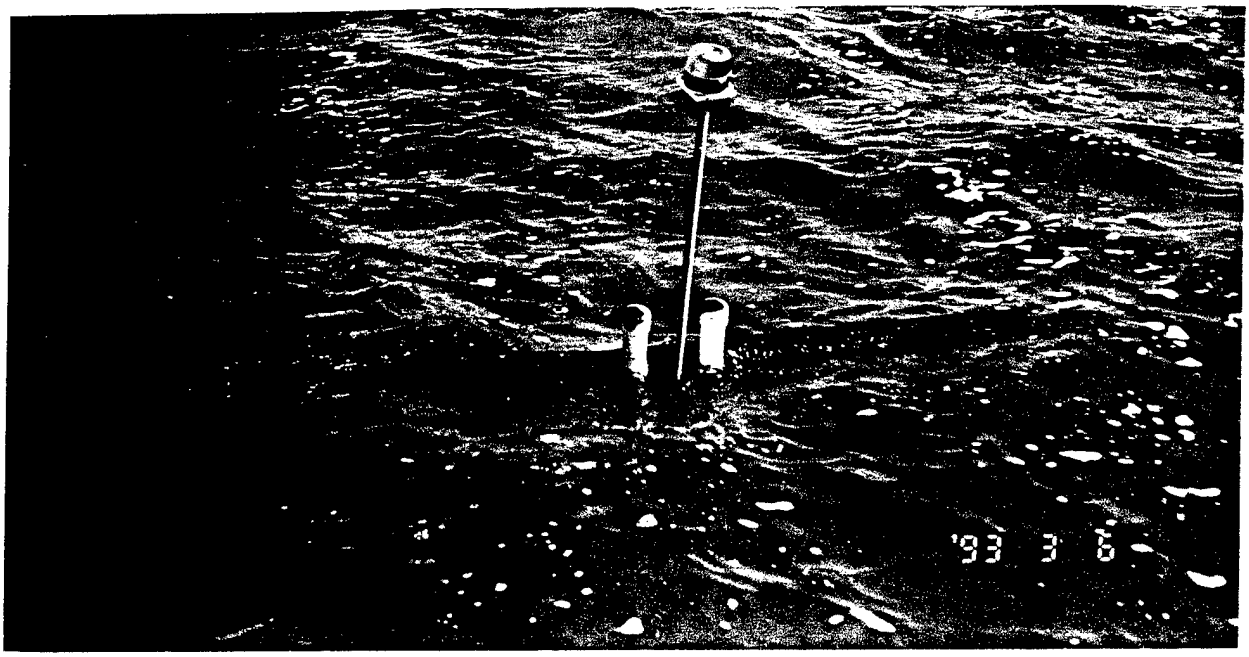

Figure 4-7. FAU Drift Buoy in Action.

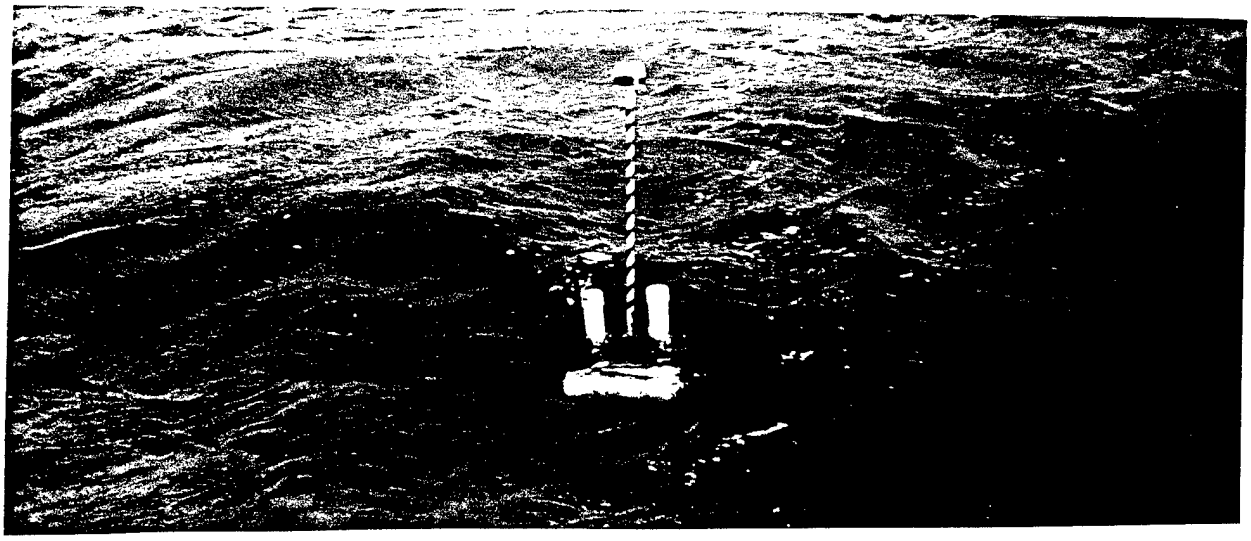

Figure 4-8. FAU Drift Buoy in Action.

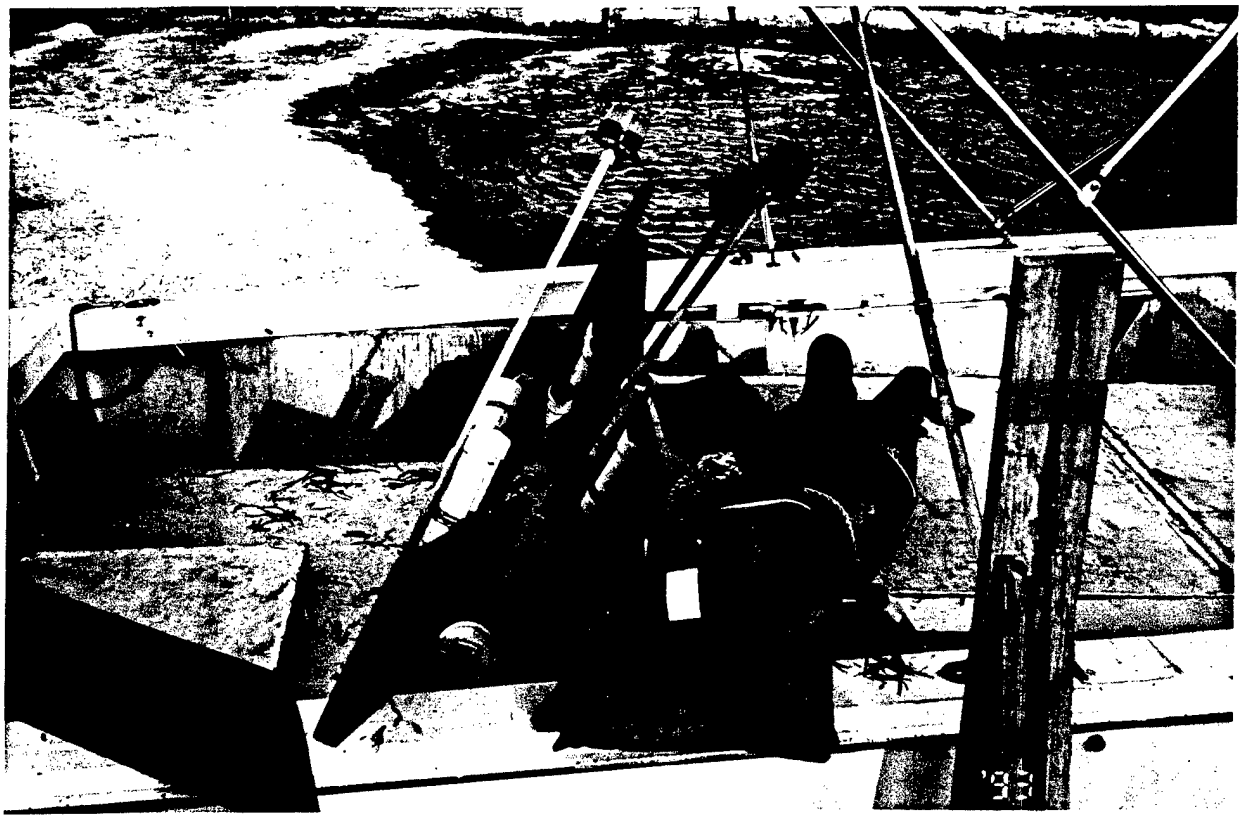

Figure 4-9. Transport of a FAU Drift Buoy.

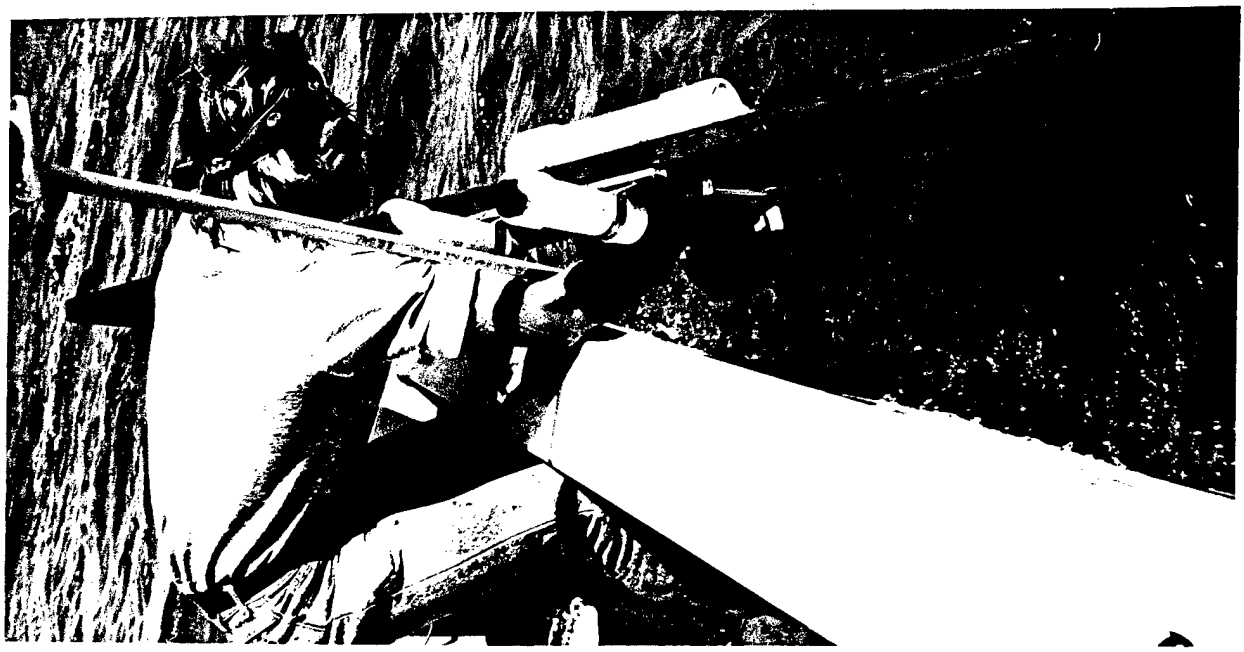

Figure 4-10. Deployment of a FAU Drift Buoy.

Figure 4-11. Release of a FAU Drift Buoy.

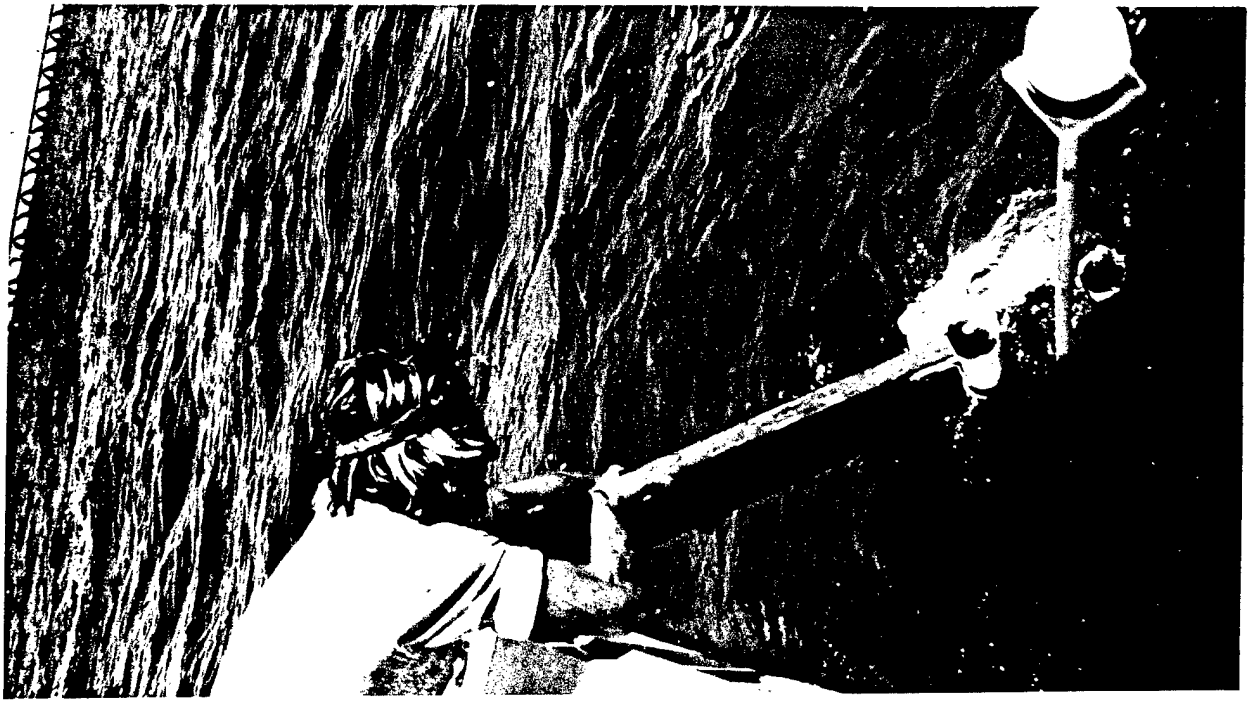

Figure 4-12. Recovery of a FAU Drift Buoy.

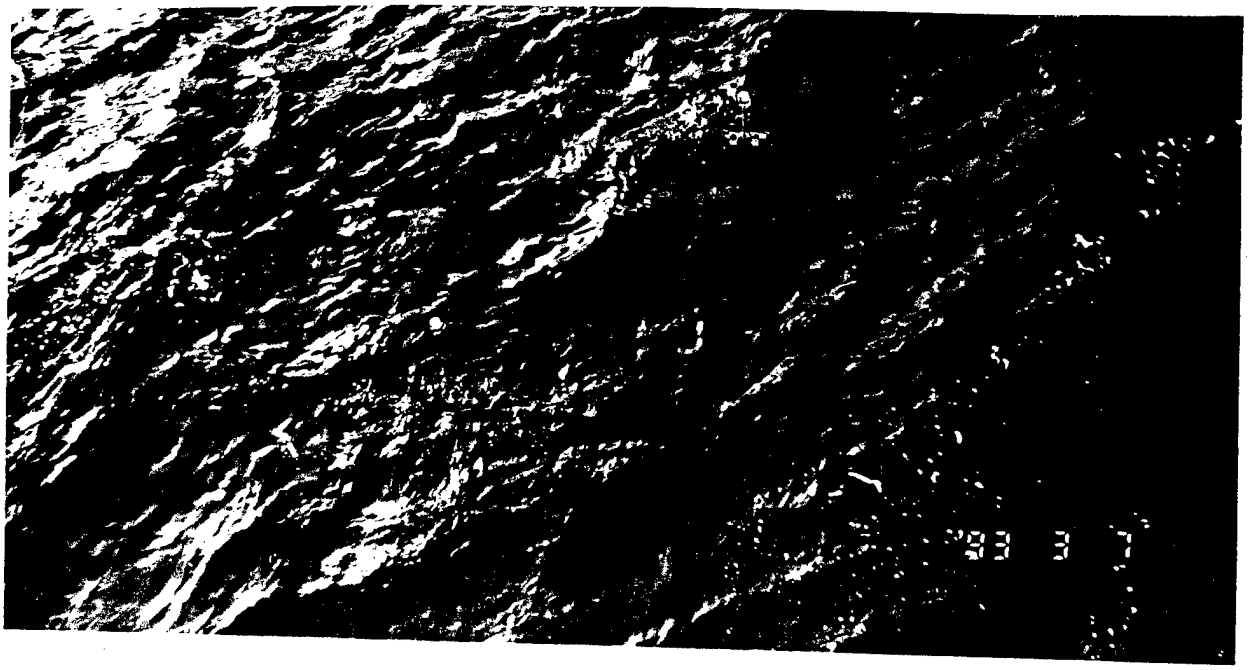

Figure 4-13. FAU Buoys Drift in Parallel in a Uniform Current.

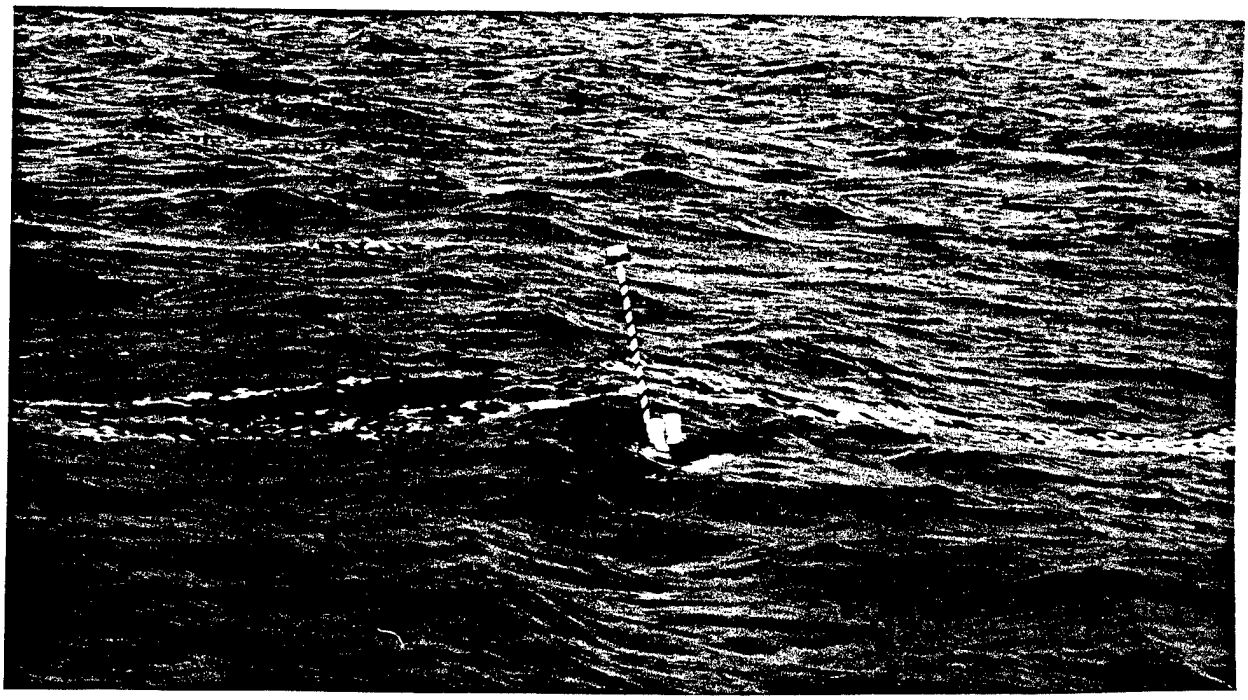

Figure 4-14. FAU Buoy Tilting in Waves.

4.2.5 Wind Velocity Measurements

Hourly wind records were available form the nearby environmental monitoring station LONF (identifier S-16) located one mile offshore in latitude 24°52′N, longitude 080°51′W. The station is part of the NOAA Coastal-Marine Automated Network (C-MAN Users Guide, 1992). The wind velocity sensor at the station was positioned 6 m (20 ft) above mean sea level. Appendix A contains the wind data that was observed during the field trials.

4.3 Drift Run Data Set Summary

A total of nineteen drift sequences were obtained during the trials. Test B3-B was conducted with Mr. George Janssen II volunteering as the PIW/SS; all the other trials were conducted using mannequins dressed in survival suits. Visual observations made during the drift runs confirmed that the PIW/SS models tended to lie broadside to the wind direction. Nine data sets were selected for analysis and evaluation and are summarized in Table 4-1.

Table 4-1. Field Data Set Summary

Test	Date (1993)	Time (start)	Time (end)	Duration (minutes)
A5-O	Mar 06	0955	1145	110
A6-O	Mar 06	1220	1440	140
A7-O	Mar 07	0905	0935	30
A8-O	Mar 07	0950	1350	240
B7-O	Mar 06	0940	1035	55
B8-O	Mar 06	1055	1215	80
B9-O	Mar 06	1242	1434	112
B10-O	Mar 07	0935	1020	45
B11-O	Mar 07	1035	1303	148

Appendix B contains tables of the PIW/SS position coordinates, as well as current and wind velocity components, for the nine (9) drift tests conducted in the Atlantic Ocean on March 06 and 07, 1993. The data collected during these open water runs were used to evaluate the proposed PIW/SS leeway model. Appendix C contains drift track plots for each of these tests.

CHAPTER 5

PIW/SS LEEWAY MODEL EVALUATION

5.1 Introduction

The PIW/SS drift trajectory data, along with the wind and current velocity data gathered during the field program, were used to evaluate the theoretical drift prediction model (equation 2-3) and leeway model (equation 3-1). The current data from the Florida Bay trials indicated the presence of small scale eddies which, unfortunately, precluded accurate interpolation of the currents in the vicinity of the PIW/SS test object. A more uniform current field was found over the Atlantic Ocean tracking range; consequently, only the nine drift tests carried out at this site were used in the evaluation.

5.2 Wind Speed Adjustment

In this work, it has been assumed that the wind velocities recorded at the nearby C-MAN station were representative of the conditions over the tracking range. However, as the wind data were recorded at a height of 6 m above sea level, it was necessary to adjust the observed wind speed to obtain an estimate of the true speed of the wind acting on the PIW/SS test object. For simplicity, it was assumed that the wind profile in the surface boundary layer obeyed the 1/7th power law (Panofsky and Dutton, 1984). This is given by

$$V_a(z) = (z / z_r)^{1/7} V_{ar} \qquad (5\text{-}1)$$

where V_{ar} is the wind velocity at a specified reference height, z_r, above the sea surface. Assuming that the wind profile in the surface boundary layer is logarithmic to a height of 10 m, the exponent (1/7) implies a *roughness length* of 0.005 m, approximately. *Roughness length* is a measure of the roughness of surface.

The height of the PIW/SS was approximately 0.2 m (0.6 ft). Therefore, using equation 5-1, the true wind speed at the PIW/SS test object was estimated to be equal to 0.6 of the measured wind speed at 6 m above sea level. Since the components of wind stress in the surface boundary layer are invariant with height, the direction of the wind near the surface is constant. The wind direction at the PIW/SS was, therefore, taken to be the same as the observed wind direction. The wind velocity data were interpolated to the times of the position observations.

5.3 Current Data Reduction

The position data for the drift buoys were used to compute the 10-minute mean current velocities for each of the buoys. The data for the three drift buoys accompanying each PIW/SS test object were then interpolated to produce estimates of the true current velocity at the object at each of the position observation times.

5.4 PIW/SS Test Object Position Data

Appendix B contains listings of the processed data for each of the nine drift trajectories over the Atlantic Ocean tracking range. Two tables are presented for each drift run. The first table, identified as Table 1, presents the position coordinates of the PIW/SS test objects along with the interpolated wind and current velocity components at corresponding times. In the tables, time is given in hours and minutes, position coordinates are given in meters, and velocity components are given in meters/second. In Appendix C, plots are shown for each of the drift tracks. While the scales of the individual plots are different, the grid lines are shown at 200 m intervals in all cases.

5.5 Model Evaluation

Two approaches were used to compare model predictions with the observed data. First, the drift of the PIW/SS test objects was predicted using equation 2-3 with λ set equal to the laboratory determined value of 0.03341. The results for each drift run are listed in Table 1 of Appendix B. Secondly, equation 3-1 was used to predict the PIW/SS test object leeway. Table 2 of Appendix B lists the predicted and derived leeway velocity components as well as the predicted and derived progressive leeway displacement coordinates for each drift run. For each set of predictions, the drift length and leeway distance segment percent errors were computed and the mean percent error for each run was calculated. Drift segment durations were nominally ten minutes long. These error statistics are given in the tables as well. Appendix C contains two series of plots corresponding to Tables 1 and 2 of Appendix B. It is apparent that the difference between the predicted and observed drift trajectories is due to the error of the predicted leeway.

Table 5-1 summarizes the mean percent error of the predicted drift and leeway trajectory segments for each of the drift runs. Evidently, there is a negative bias in the leeway predictions. However, even though individual drift run prediction errors differ widely, the results indicate that overall there is a small positive bias for the total drift distance predictions.

5.6 PIW/SS Test Object Leeway Analysis

The derived leeway data for the PIW/SS test objects were subjected to simple statistical analyses in order to summarize the combined data set. As well, linear regression analyses of leeway speed on wind speed were performed. For this summary, the interpolated wind speeds were adjusted to the standard reference height of 10 m above the sea surface using equation 5-1.

Leeway rate, speed, and angle statistics for the PIW/SS test objects are presented in Table 5-2. While a total of 74 samples were collected in total, a number displayed rather large leeway rates. As this is believed to be due to sampling errors, only those cases in which the leeway rate was less than 0.075 were included in the analyses. Eliminating the outliers reduced the data set to 65 samples. The mean leeway rate for this reduced data set was determined to be 0.029, while the standard deviation was found to be 0.016. Following normal operational practice, the leeway speed and wind speed statistics are given in knots.

Table 5-1. Mean Percent Errors of Predicted Drift and Leeway Distances

Drift Run	Mean Percent Error of Drift	Mean Percent Error of Leeway
	(%)	(%)
A5-O	-8.1	-21.5
A6-O	1.9	-46.1
A7-O	-14.5	-28.7
A8-O	26.4	-4.5
B7-O	-35.4	-42.1
B8-O	17.1	-10.1
B9-O	-14.7	-49.0
B10-O	68.5	-55.4
B11-O	-8.1	-8.7

Leeway angle is the angle off the downwind direction, with positive angles to the right and negative angles to the left. The statistics indicate a bias to the right of the downwind direction, with the mean and median leeway angles being 18 and 13 degrees, respectively. With a standard deviation of 45°, the dispersion of leeway angles, based on the 10-minute drift segment records, is quite large.

Table 5-2. PIW/SS Test Object Leeway Statistics

Number of cases: 65	Wind speed range at 10 m: 5.0 to 12.4 knots				
	Minimum	Maximum	Mean	Std. dev.	Median
Leeway rate	0.007	0.072	0.029	0.016	0.024
Leeway speed (knots)	0.04	0.71	0.24	0.13	0.21
Leeway angle (degrees off downwind, positive to right)	-74	162	18	45	13

A progressive vector diagram of leeway displacements for each drift run, after rotating the wind directions into the south, is shown as Figure 5-1. The large variability in leeway angles for individual drift segment intervals is readily seen. However, looking at drift durations of one hour or more reveals a smaller range of leeway angle dispersions. Using this criteria, the envelope of leeway angles ranges from -25° to +38°. Again, there is a bias to the right of the downwind direction which is centered about +7°. Short period variations may, in fact, be largely due to sampling errors.

The linear regression analysis of leeway speed on the 10 m height wind speed produced the following equation:

$$|V_l| = 0.114 + 0.014\,|V_{a10}| \qquad (5\text{-}2)$$

This result is based on 65 samples in wind speeds at 10 m ranging from 5.0 knots to 12.4 knots. The standard error of the estimate was determined to be 0.130 knots; the variance accounted for was only 0.061, however.

Constraining the regression to pass through the origin resulted in

$$|V_l| = 0.027\,|V_{a10}| \qquad (5\text{-}3)$$

valid over the same range of wind speeds as given above. The standard error of the estimate was determined to be 0.133 knots.

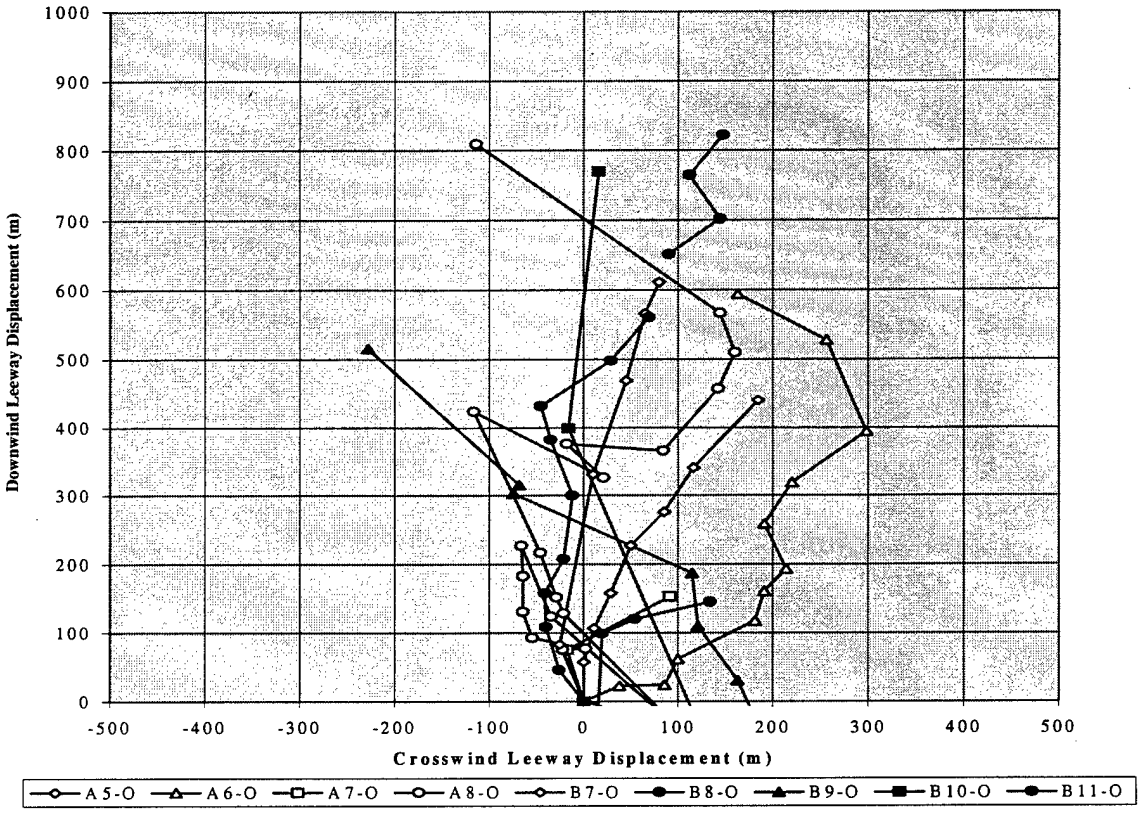

Figure 5-1. PIW/SS Leeway Displacement (all winds rotated into the south).

[BLANK]

CHAPTER 6

CONCLUSIONS AND RECOMMENDATIONS

6.1 Conclusions

A theoretical analysis, laboratory experiments, and a field program were conducted to investigate the drift and leeway characteristics of a Person-In-Water clad in a survival suit (PIW/SS). The study has resulted the following conclusions:

1. A simplified leeway formula, developed from theoretical considerations, indicates that the leeway velocity is directly proportional to the difference between the true wind velocity at the drift object and the true current at the object over a wide range of wind speeds.

2. The constant of proportionality for a PIW/SS was evaluated in laboratory tests. With this, the leeway velocity vector was estimated to be

$$V_l = 0.0323(V_a - V_w) \qquad (3\text{-}1)$$

   The constant (the leeway factor) was found to be 0.006 for a Person-In-Water without survival suit (PIW). For these models, the true wind velocity, V_a, should be adjusted to the height of 0.2 m (0.6 ft) above mean sea level according to 1/7 power law (Equation 5-1); V_w is the true surface current of the water column (top half meter, approximately).

3. A field trial was carried out to evaluate the proposed PIW/SS drift model (equation 2-3) and leeway model (equation 3-1). Quite good agreement was found for the total drift prediction. In assessing the leeway predictions, however, it was found that the magnitudes of the leeway vector predictions were biased on the low side.

4. A statistical analysis of the ratio of leeway speed to the wind speed adjusted to 10 m height for the PIW/SS test objects produced a mean value of 0.029 with a standard deviation of 0.016. A regression analysis of leeway speed on wind speed constrained to pass through the origin produced a leeway factor of 0.027; thus,

$$|V_l| = 0.027\,|V_{a10}| \quad \text{for } 5.0 \le |V_{a10}| \le 12.4 \text{ knots}$$

   The standard error of the estimate was determined to be 0.133 knots.

5. Leeway angle analysis for the PIW/SS test models using the 10-minute drift segment data resulted in a mean leeway angle of 18 degrees to the right of the downwind direction and a standard deviation of 45 degrees. For drift durations of one hour or more in length, the

envelope of leeway dispersions ranged from –25° to +38°. A bias to the right of the downwind direction was evident, with the center of the dispersion being near +7°.

6. The procedure for leeway prediction established in the present study can be extended to other search and rescue drift objects.

7. A new type of drift buoy was developed and field tested for surface current measurement. It offers certain advantages over traditional designs.

6.2 Recommendations

6.2.1 Interim Coast Guard Search Planning Guidance

Two simple leeway models are recommended for use for manual input to "User Defined Leeway" in the current version of CASP and for use in manual search planning. The models are based upon: 1) a constrained linear regression of leeway speed upon wind speed at 10 meter height; 2) an uncertainty of leeway speed based on standard error at a wind speed of 19.6 knots; 3) maximum angle off downwind direction; 4) the mean leeway angle.

Table 6-1 provides recommended coefficients for simple equations that model the leeway of PIW/SS. The coefficients are presented in a format suitable for direct input into CASP "User Defined Leeway" input. The wind speed and leeway speed in this table are in knots. The present version of CASP has no provision to input a mean leeway angle. The "User Defined Leeway" mean leeway angle is fixed directly downwind or at zero degrees, hence divergence is relative to downwind.

Table 6-1
Summary of CASP "User Defined Leeway" Equations Coefficients
(Leeway speed and 10 m wind speed measured in knots.)

CLASS	CRAFT	Multiplier	Speed Uncertainty	Divergence (degrees)
Person-in-Water (PIW)	Survival Suit (SS)	0.027 (1)	0.49 (1)	38° (2)

NOTES

1. The terms Multiplier, Speed Uncertainty, and Divergence are as described in Allan and Staubs (1997). The Multiplier and Speed Uncertainty values are based on the constrained (through zero) linear regression of leeway speed upon wind speed at 10 meters (Eq. 5-3). The standard error of the estimate was determined to be 0.133 knots.
2. Divergence is defined here as the maximum angle off downwind, either positive or negative, for drifts of more than one hour.

Table 6-2 presents the manual equation coefficients recommended for use in manual search planning. The same data sources were used, but in Table 6-2 the wind speed is in meters per second and the leeway speed is in centimeters per second. The mean angle is relative to the downwind direction. It is anticipated that the divergence of leeway angles will decrease once further field trials are conducted.

Table 6-2
Summary of Manual Equations Coefficients
$\mathbf{V}_l$ (cm/s) = Multiplier * $\mathbf{V}_{a10}$ (m/s)
$\mathbf{V}_l$ max (cm/s) = Max Slope * $\mathbf{V}_{a10}$ (m/s)
$\mathbf{V}_l$ min (cm/s) = Min Slope * $\mathbf{V}_{a10}$ (m/s)

CLASS	CRAFT	Multiplier $\mathbf{V}_l$ (cm/s) $\mathbf{V}_{a10}$ (m/s)	Uncertainty Range (Max & Min Slopes)	Mean Angle (degree)	Divergence (Max & Min Leeway Angles)
Person-in-Water (PIW)	Survival Suit (SS)	2.7 (1)	4.0 1.4 (2)	7°	+38° -25° (3)

NOTES

1. The Multiplier and Uncertainty values are based on the constrained linear regression of leeway speed on wind speed at 10 meters (Equation 5-3). The standard error of the estimate was determined to be 6.85 cm/s.

2. Uncertainty Range is defined as Slope Uncertainty Range = Multiplier +/- (Multiplier * Uncertainty).

3. Divergence is defined as maximum and minimum leeway angles for drifts greater than one hour.

6.2.2 Future Research

The field experiments reported here were conducted under light wind conditions. Investigation of PIW/SS leeway under moderate to strong winds and in heavy weather is also needed. It is recommended that wind velocity be referenced to a standard height of 10 meters rather than to leeway target height.

Recent advances in current meter technology and position determination have made it possible to make direct measurements of leeway. The direct method should be used to determine leeway of persons in the water with and without survival suits under a variety of wind conditions.

[BLANK]

REFERENCES

Allen, A.A., and P. Staubs, 1997. "CASP User Defined Input for Maritime Life Rafts", Coast Guard Report, 5 pp.

Chapline, W.E., 1960. "Estimating the Drift of Distressed Small Craft", Coast Guard Alumni Association Bulletin, U.S. Coast Guard Academy, New London, CT., Vol. 22, No. 2, March-April 1960, pp. 39-42.

Coastal Marine Automated Network (C-MAN) Users Guide, 1992. National Data Buoy Center, National Oceanic and Atmospheric Administration Report No. 1203-01.04-2B.

Daugherty, R.L., and J.B. Franzini, 1977. "Fluid Mechanics with Engineering Applications", 7th edition, McGraw-Hill.

Hufford, G.L., and S. Broida, 1974. "Determination of Small Craft Leeway", U.S. Coast Guard, Report No. CGR & DC 39/74.

James, R., 1966. "Ocean Thermal Structure Forecasting" U.S. Naval Oceanographic Office, Washington, D.C.

Meyers, J.J., C.H. Holm, and R.F. McAllister, 1967. Handbook of Ocean and Underwater Engineering, McGraw-Hill, New York.

Morgan, C.W., 1978. "Seven-Man Life Raft Leeway Study". U.S. Coast Guard Oceanographic Unit Technical Report 78-1, Washington, D.C.

Morgan, C.W., S.E. Brown, and R.C. Murrell, 1977. "Experiments in Small Craft Leeway", U.S. Coast Guard Oceanographic Unit Technical Report 77-2, Washington, D.C.

Nash, L., and J. Willcox, 1985. "Summer 1983 Leeway Drift Experiment", U.S. Coast Guard Report No. CG-D-35-85.

Osmer, S.R., N.C. Edwards, Jr., and A.L. Breitler, 1982. "An Evaluation of Life Raft Leeway, February 1982.", U.S. Coast Guard Report No. CG-D-10-82.

Panofsky, H.A., and J.A. Dutton, 1984. Atmospheric Turbulence, Models and Methods for Engineering Applications, John Wiley & Sons, New York.

Pingree, F.W., 1944. "Forethought on Rubber Rafts", Woods Hole Oceanographic Institution, 26 pp.

Scobie, R.W., and D.L. Thompson, 1979. "Life Raft Study", U.S. Coast Guard, Oceanographic Unit Technical Report No. 79-1.

Su, T.C., 1986. "On Predicting the Boat's Drift for Search and Rescue", U.S. Department of Transportation, Report No. DOT/OST/P-34/87/059.

Tomczak, C., 1964. "Investigations with Drift Cards to Determine the Influence of the Wind on Surface Currents", Studies on Oceanography, University of Tokyo Press, Japan

APPENDIX A

Wind Velocity Data

The table given in this appendix lists the hourly wind data observed at station LONF (identifier S-16) during the field trials. The station, part of the NOAA Coastal-Marine Automated Network (C-MAN Users Guide, 1992), is located in latitude 24°52′N, longitude 080°51′W. The wind velocity sensor was positioned 6 m (20 ft) above mean sea level.

Table A-1. Hourly Wind Direction and Speed Data

Date	Time	Wind Direction (degrees True)	Wind Speed (m/s)
Feb 27, 1993	0800	343	9.7
	0900	352	8.1
	1000	360	7.9
	1100	355	6.1
	1200	345	3.7
	1300	329	2.2
	1400	343	3.0
	1500	297	4.6
	1600	302	3.8
Feb 28, 1993	0800	020	7.5
	0900	020	7.9
	1000	020	7.4
	1100	007	5.4
	1200	020	4.4
	1300	024	3.8
	1400	014	3.1
	1500	350	1.5
	1600	012	1.3
Mar 06, 1993	0800	360	4.6
	0900	019	5.5
	1000	031	4.9
	1100	013	3.1
	1200	020	3.4
	1300	053	2.5
	1400	047	2.5
	1500	043	2.4
	1600	112	3.0
Mar 07, 1993	0800	023	5.7
	0900	054	6.1
	1000	052	5.4
	1100	078	5.1
	1200	079	5.0
	1300	075	3.8
	1400	054	2.7
	1500	033	2.4
	1600	205	1.3

APPENDIX B

PIW/SS Leeway and Drift Test Data

This appendix contains data tables for the nine PIW/SS drift tests that were conducted in the Atlantic Ocean in early March 1993. Two tables are given for each drift run. In Table 1, the observed position coordinates as well as the current and wind velocity components at ten (10) minute intervals (nominally) are given. In addition, Table 1 lists the PIW/SS model predicted coordinates and percent errors for each drift segment. Table 2 lists the derived and predicted leeway velocity components and the derived and predicted progressive leeway displacement coordinates for the individual drift segments. Segmented Percent Errors are also given in Table 2. Note that calculations were made using original data values while values presented in all tables have been rounded.

Definitions of Terms Used in Tables

Predicted Leeway is based on Eq. 3-1. The wind component at the PIW/SS is estimated as 0.6 the measured wind speed (as discussed inCh. 5). Thus

$$\text{Predicted Leeway}_x = 0.0323\ (_x\text{wind} * 0.6 - {}_x\text{current})$$

$$\text{Predicted Leeway}_y = 0.0323\ (_y\text{wind} * 0.6 - {}_y\text{current}) \quad \text{where}$$

$$_x\text{wind} = (_x\text{wind}_{n-1} + {}_x\text{wind}_n)/2$$

$$_y\text{wind} = (_y\text{wind}_{n-1} + {}_y\text{wind}_n)/2$$

$$_x\text{current} = (_x\text{current}_{n-1} + {}_x\text{current}_n)/2$$

$$_y\text{current} = (_y\text{current}_{n-1} + {}_y\text{current}_n)/2$$

The Derived Leeway is drift over the ten minute interval minus the average current. Thus

$$\text{Derived Leeway}_x = [(\text{E-W coordinates}_{n+1} - \text{E-W coordinates}_n)/\text{time interval}] - {}_x\text{current}$$

$$\text{Derived Leeway}_y = [(\text{N-S coordinates}_{n+1} - \text{N-S coordinates}_n)/\text{time interval}] - {}_y\text{current}$$

where $_x$current and $_y$current are as defined above and time interval is in seconds.

The Computed Position is the previous computed position plus a portion (0.9677) of the average current over the time interval plus the wind portion (0.0323) over the time interval. Thus

$$\text{Computed E-W Position} = \text{E-W Position}_{n-1} + (_x\text{current} * \text{time interval} * 0.9677) + (_x\text{wind} * 0.6 * \text{time interval} * 0.0323)$$

$$\text{Computed N-S Position} = \text{N-S Position}_{n-1} + (_y\text{current} * \text{time interval} * 0.9677) + (_y\text{wind} * 0.6 * \text{time interval} * 0.0323)$$

where wind_x, wind_y, current_x, and current_y are as defined above.

The Segment Percent Error is the difference between the computed distance and the observed distance divided by the observed distance. Thus

Segment % Error =

$$100\% * \left[\frac{\sqrt{\left(\Delta x_{computed}\right)^2 + \left(\Delta y_{computed}\right)^2} - \sqrt{\left(\Delta x_{observed}\right)^2 + \left(\Delta y_{observed}\right)^2}}{\sqrt{\left(\Delta x_{observed}\right)^2 + \left(\Delta y_{observed}\right)^2}} \right]$$

where $\Delta x_{computed}$ = (E-W Coordinate $_{n-1}$ - E-W Coordinate $_n$)

$\Delta y_{computed}$ = (N-S Coordinate $_{n-1}$ - N-S Coordinate $_n$)

$\Delta x_{observed}$ = (E-W Coordinate $_{n-1}$ - E-W Coordinate $_n$)

$\Delta y_{observed}$ = (N-S Coordinate $_{n-1}$ - N-S Coordinate $_n$)

Table1 Drift Run A5-O

PIW/SS Field Data and Predicted Coordinates

Date: March 06, 1993

		Observed data						Computed data			
		PIW/SS position		Current		Wind			PIW/SS position		
Drift segment number	Time of measurement	E-W coordinate	N-S coordinate	x-component	y-component	x-component	y-component	Drift period	E-W coordinate	N-S coordinate	Segment percent error
	(local)	(m)	(m)	(m/s)	(m/s)	(m/s)	(m/s)	hh:mm	(m)	(m)	(%)
1	9:55	616	-817	-0.10	0.00	-2.46	-4.27		616	-817	
2	10:05	526	-866	-0.10	0.00	-2.33	-4.11	0:10	529	-864	-3.3
3	10:15	429	-922	-0.11	-0.06	-1.97	-3.96	0:10	441	-928	-3.6
4	10:25	338	-985	-0.07	-0.03	-1.65	-3.79	0:10	369	-998	-9.1
5	10:35	257	-1076	-0.05	-0.09	-1.34	-3.59	0:10	318	-1075	-24.4
6	10:45	200	-1193	0.02	-0.18	-1.06	-3.37	0:10	296	-1194	-6.6
7	10:55	165	-1355	0.02	-0.18	-0.81	-3.13	0:10	297	-1337	-13.7
8	11:25	222	-1902	0.14	-0.34	-0.88	-3.07	0:30	411	-1899	4.3
									Average percent error (%)		-8.1

Table 2 Drift Run A5-O

Derived and Predicted PIW/SS Leeway Velocities and Progressive Vector Coordinates

Date: March 06, 1993

			Derived leeway		Predicted lwy		Derived leeway		Predicted leeway		
Drift segment number	Time of measurement		x-component	y-component	x-component	y-component	E-W coordinate	N-S coordinate	E-W coordinate	N-S coordinate	Segment percent error
1	9:55						616	-817	616	-817	
2	10:05		-0.05	-0.08	-0.04	-0.08	587	-867	590	-865	-5.1
3	10:15		-0.05	-0.06	-0.04	-0.08	554	-905	567	-912	2.5
4	10:25		-0.06	-0.06	-0.03	-0.07	516	-943	548	-956	-9.6
5	10:35		-0.08	-0.09	-0.03	-0.07	471	-1000	532	-998	-38.3
6	10:45		-0.08	-0.06	-0.02	-0.06	422	-1035	518	-1036	-32.9
7	10:55		-0.08	-0.09	-0.02	-0.06	374	-1088	507	-1070	-49.8
8	11:25		-0.05	-0.04	-0.02	-0.05	282	-1166	472	-1163	-17.5
									Average percent error (%)		-21.5

Table 1 Drift Run A6-O

PIW/SS Field Data and Predicted Coordinates

Date: March 06, 1993

		Observed data						Computed data			
		PIW/SS position		Current		Wind			PIW/SS position		
Drift segment number	Time of measurement	E-W coordinate	N-S coordinate	x-component	y-component	x-component	y-component	Drift period	E-W coordinate	N-S coordinate	Segment percent error
	(local)	(m)	(m)	(m/s)	(m/s)	(m/s)	(m/s)	hh:mm	(m)	(m)	(%)
1	12:20	1081	-293	0.28	-0.61	-1.57	-2.62		1081	-293	
2	12:30	1207	-655	0.28	-0.61	-1.73	-2.34	0:10	1226	-674	6.3
3	12:40	1316	-926	0.21	-0.39	-1.84	-2.05	0:10	1348	-990	16.1
4	12:50	1414	-1182	0.24	-0.40	-1.92	-1.76	0:10	1456	-1244	0.5
5	13:00	1428	-1363	0.13	-0.29	-1.96	-1.48	0:10	1539	-1463	29.4
6	13:10	1462	-1523	0.12	-0.19	-1.94	-1.52	0:10	1588	-1617	-0.9
7	13:20	1489	-1622	0.10	-0.14	-1.92	-1.56	0:10	1629	-1730	17.1
8	13:30	1512	-1763	0.10	-0.13	-1.90	-1.59	0:10	1665	-1826	-28.3
9	13:40	1522	-1877	0.16	-0.19	-1.88	-1.63	0:10	1715	-1939	7.6
10	13:50	1490	-1966	0.10	-0.14	-1.86	-1.67	0:10	1767	-2053	33.1
11	14:20	1543	-2297	0.06	-0.11	-2.18	-1.14	0:30	1831	-2315	-19.7
12	14:40	1582	-2537	0.06	-0.11	-2.36	-0.52	0:20	1845	-2460	-40.1
									Average percent error (%)		1.9

Table 2 Drift A6-O

Derived and Predicted PIW/SS Leeway Velocities and Progressive Vector Coordinates

Date: March 06, 1993

			Derived leeway		Predicted lwy		Derived leeway		Predicted leeway		
Drift segment number	Time of measurement		x-component	y-component	x-component	y-component	E-W coordinate	N-S coordinate	E-W coordinate	N-S coordinate	Segment percent error
	(local)		(m/s)	(m/s)	(m/s)	(m/s)	(m)	(m)	(m)	(m)	(%)
1	12:20						1081	-293	1081	-293	
2	12:30		-0.07	0.00	-0.04	-0.03	1036	-291	1056	-310	-32.1
3	12:40		-0.06	0.05	-0.04	-0.03	998	-261	1030	-325	-37.9
4	12:50		-0.06	-0.03	-0.04	-0.02	962	-278	1004	-340	-24.7
5	13:00		-0.16	0.04	-0.04	-0.02	867	-252	978	-352	-70.9
6	13:10		-0.07	-0.03	-0.04	-0.02	827	-270	953	-365	-35.8
7	13:20		-0.07	0.00	-0.04	-0.02	787	-271	928	-380	-27.5
8	13:30		-0.06	-0.10	-0.04	-0.03	751	-332	904	-395	-59.0
9	13:40		-0.11	-0.03	-0.04	-0.03	686	-349	880	-411	-57.0
10	13:50		-0.18	0.02	-0.04	-0.03	579	-340	855	-427	-73.2
11	14:20		-0.05	-0.06	-0.04	-0.02	493	-451	781	-469	-39.2
12	14:40		-0.03	-0.09	-0.05	-0.01	462	-561	726	-484	-50.1
									Average percent error (%)		-46.1

Table 1 Drift Run A7-O

PIW/SS Field Data and Predicted Coordinates

Date: March 07, 1993

		Observed data						Computed data			
		PIW/SS position		Current		Wind			PIW/SS position		
Drift segment number	Time of measurement	E-W coordinate	N-S coordinate	x-component	y-component	x-component	y-component	Drift period	E-W coordinate	N-S coordinate	Segment percent error
	(local)	(m)	(m)	(m/s)	m/s	(m/s)	(m/s)	hh:mm	(m)	(m)	(%)
1	9:05	722	-518	-0.24	0.39	-4.86	-3.56		722	-518	
2	9:15	525	-340	-0.24	0.39	-4.75	-3.52	0:10	525	-330	2.6
3	9:25	257	-88	-0.23	0.31	-4.64	-3.48	0:10	333	-167	-31.5
										Average percent error (%)	-14.5

Table 2 Drift A7-O

Derived and Predicted PIW/SS Leeway Velocities and Progressive Vector Coordinates

Date: March 07, 1993

			Derived leeway		Predicted lwy		Derived leeway		Predicted leeway		
Drift segment number	Time of measurement		x-component	y-component	x-component	y-component	E-W coordinate	N-S coordinate	E-W coordinate	N-S coordinate	Segment percent error
	(local)		(m/s)	(m/s)	(m/s)	(m/s)	(m)	(m)	(m)	(m)	(%)
1	9:05						722	-518	722	-518	
2	9:15		-0.09	-0.10	-0.09	-0.08	670	-576	670	-566	-9.5
3	9:25		-0.21	0.07	-0.08	-0.08	545	-535	620	-614	-47.9
										Average percent error (%)	-28.7

Table 1 Drift Run A8-O

PIW/SS Field Data and Predicted Coordinates

Date: March 07, 1993

		Observed data						Computed data			
		PIW/SS position		Current		Wind			PIW/SS position		
Drift segment number	Time of measurement	E-W coordinate	N-S coordinate	X-component	Y-component	X-component	Y-component	Drift period	E-W coordinate	N-S coordinate	Segment percent error
	local	m	m	m/s	m/s	m/s	m/s	hh:mm	m	m	%
1	9:50	1392	-1064	-0.35	0.04	-4.37	-3.37		1392	-1064	
2	10:00	1135	-1104	-0.35	0.04	-4.26	-3.33	0:10	1139	-1080	-2.4
3	10:10	910	-1013	-0.35	0.20	-4.46	-2.97	0:10	885	-1047	5.5
4	10:20	764	-988	-0.19	0.07	-4.64	-2.61	0:10	675	-1001	44.9
5	10:30	618	-957	-0.20	0.12	-4.78	-2.23	0:10	507	-974	14.0
6	10:40	456	-918	-0.18	0.08	-4.89	-1.85	0:10	340	-939	2.0
7	10:50	307	-886	-0.18	0.08	-4.98	-1.46	0:10	179	-912	7.7
8	11:00	189	-898	-0.52	-0.31	-5.03	-1.07	0:10	-83	-994	130.9
9	11:10	72	-894	-0.39	-0.33	-5.01	-1.05	0:10	-405	-1192	223.4
10	11:20	-19	-916	0.18	0.37	-4.99	-1.03	0:10	-524	-1192	27.2
11	11:30	-132	-970	-0.10	-0.05	-4.97	-1.01	0:10	-559	-1111	-29.6
12	11:40	-195	-1027	-0.04	-0.10	-4.95	-0.99	0:10	-657	-1166	32.7
13	11:50	-279	-1158	-0.04	-0.24	-4.93	-0.97	0:10	-738	-1276	-12.3
14	12:00	-490	-1492	-0.03	-0.51	-4.92	-0.96	0:10	-816	-1505	-38.8
15	12:10	-418	-1503	0.04	-0.04	-4.70	-0.97	0:10	-869	-1676	145.7
16	12:20	-437	-1672	0.03	-0.36	-4.48	-0.98	0:10	-902	-1804	-22.6
17	12:30	-441	-1852	0.00	-0.58	-4.27	-0.98	0:10	-944	-2088	59.6
18	13:00	-543	-2862	0.00	-0.58	-3.63	-0.97	0:30	-1082	-3132	3.8
19	13:20	-515	-3371	0.14	-0.27	-3.14	-1.29	0:20	-1079	-3652	2.0
20	13:30	-483	-3619	0.12	-0.43	-2.89	-1.41	0:10	-1039	-3871	-11.0
21	13:40	-514	-4215	0.09	-0.42	-2.64	-1.50	0:10	-1010	-4135	-55.6
									Average percent error (%)		26.4

Table 2 Drift A8-O

Derived and Predicted PIW/SS Leeway Velocities and Progressive Vector Coordinates

Date: March 07, 1993

			Derived leeway		Predicted lwy		Derived leeway		Predicted leeway		
Drift segment number	Time of measurement		x-component	y-component	x-component	y-component	E-W coordinate	N-S coordinate	E-W coordinate	N-S coordinate	Segment percent error
	(local)		(m/s)	(m/s)	(m/s)	(m/s)	(m)	(m)	(m)	(m)	(%)
1	9:50						1392	-1064	1392	-1064	
2	10:00		-0.08	-0.11	-0.07	-0.07	1345	-1128	1349	-1104	-25.9
3	10:10		-0.03	0.03	-0.07	-0.06	1330	-1109	1305	-1143	142.5
4	10:20		0.03	-0.09	-0.08	-0.06	1346	-1165	1257	-1178	1.6
5	10:30		-0.05	-0.04	-0.08	-0.05	1317	-1191	1206	-1208	51.9
6	10:40		-0.08	-0.03	-0.09	-0.04	1269	-1212	1153	-1233	11.6
7	10:50		-0.07	-0.03	-0.09	-0.03	1228	-1228	1100	-1254	31.3
8	11:00		0.15	0.09	-0.09	-0.02	1320	-1171	1048	-1267	-51.1
9	11:10		0.26	0.33	-0.08	-0.01	1476	-975	999	-1273	-80.1
10	11:20		-0.05	-0.06	-0.09	-0.02	1448	-1009	943	-1285	30.5
11	11:30		-0.23	-0.25	-0.10	-0.02	1311	-1159	884	-1300	-70.2
12	11:40		-0.04	-0.02	-0.09	-0.02	1290	-1171	828	-1310	136.6
13	11:50		-0.10	-0.05	-0.09	-0.01	1230	-1200	771	-1318	-14.1
14	12:00		-0.32	-0.18	-0.09	-0.01	1040	-1309	714	-1322	-74.1
15	12:10		0.12	0.26	-0.09	-0.01	1109	-1155	658	-1328	-66.6
16	12:20		-0.07	-0.08	-0.09	-0.01	1069	-1204	604	-1336	-13.7
17	12:30		-0.02	0.17	-0.09	0.00	1056	-1102	553	-1338	-50.2
18	13:00		-0.06	0.02	-0.08	0.00	954	-1068	415	-1338	28.2
19	13:20		-0.05	0.00	-0.07	-0.01	898	-1067	334	-1348	46.4
20	13:30		-0.08	-0.06	-0.06	-0.01	852	-1105	296	-1357	-35.3
21	13:40		-0.16	-0.57	-0.06	-0.01	758	-1446	262	-1366	-90.0
									Average percent error (%)		-4.5

Table 1 Drift Run B7-O

PIW/SS Field Data and Predicted Coordinates

Date: March 06, 1993

		Observed data						Computed data			
		PIW/SS position		Current		Wind			PIW/SS position		
Drift segment number	Time of measurement	E-W coordinate	N-S coordinate	x-component	y-component	x-component	y-component	Drift period	E-W coordinate	N-S coordinate	Segment percent error
	(local)	(m)	(m)	(m/s)	(m/s)	(m/s)	(m/s)	hh:mm	(m)	(m)	(%)
1	9:40	-721	-728	-0.11	0.13	-2.31	-4.54		-721	-728	
2	9:50	-804	-735	-0.11	0.13	-2.42	-4.36	0:10	-812	-704	13.3
3	10:05	-978	-822	0.06	0.12	-2.33	-4.11	0:15	-876	-669	-62.9
4	10:15	-1038	-855	0.06	0.12	-1.97	-3.96	0:10	-866	-647	-63.8
5	10:25	-1112	-907	-0.11	-0.03	-1.65	-3.78	0:10	-901	-665	-55.5
6	10:35	-1182	-958	-0.02	-0.02	-1.34	-3.59	0:10	-956	-723	-8.1
									Average percent error (%)		-35.4

Table 2 Drift B7-O

Derived and Predicted PIW/SS Leeway Velocities and Progressive Vector Coordinates

Date: March 06, 1993

			Derived leeway		Predicted lwy		Derived leeway		Predicted leeway		
Drift segment number	Time of measurement		x-component	y-component	x-component	y-component	E-W coordinate	N-S coordinate	E-W coordinate	N-S coordinate	Segment percent error
	(local)		(m/s)	(m/s)	(m/s)	(m/s)	(m)	(m)	(m)	(m)	(%)
1	9:40						-721	-728	-721	-728	
2	9:50		-0.03	-0.14	-0.04	-0.09	-738	-813	-746	-782	-30.9
3	10:05		-0.17	-0.22	-0.05	-0.09	-889	-1013	-787	-860	-65.1
4	10:15		-0.16	-0.18	-0.04	-0.08	-985	-1118	-813	-909	-60.8
5	10:25		-0.10	-0.13	-0.03	-0.08	-1045	-1197	-834	-955	-49.0
6	10:35		-0.05	-0.06	-0.03	-0.07	-1076	-1233	-850	-997	-4.6
										Average percent error (%)	-42.1

Table 1 Drift Run B8-O

PIW/SS Field Data and Predicted Coordinates

Date: March 06, 1993

		Observed data						Computed data			
		PIW/SS position		Current		Wind			PIW/SS position		
Drift segment number	Time of measurement	E-W coordinate	N-S coordinate	x-component	y-component	x-component	y-component	Drift period	E-W coordinate	N-S coordinate	Segment percent error
	(local)	(m)	(m)	(m/s)	(m/s)	(m/s)	(m/s)	hh:mm	(m)	(m)	(%)
1	10:55	-250	-1228	0.03	-0.10	-0.81	-3.13		-250	-1228	
2	11:05	-247	-1281	0.03	-0.10	-0.73	-3.02	0:10	-242	-1322	77.5
3	11:15	-246	-1490	0.07	-0.27	-0.80	-3.05	0:10	-221	-1465	-31.0
4	11:25	-242	-1702	0.07	-0.40	-0.88	-3.07	0:10	-191	-1695	9.5
5	11:35	-242	-1971	0.21	-0.49	-0.95	-3.10	0:10	-120	-1989	12.5
									Average percent error (%)		17.1

Table 2 Drift B8-O

Derived and Predicted PIW/SS Leeway Velocities and Progressive Vector Coordinates

Date: March 06, 1993

			Derived leeway		Predicted lwy		Derived leeway		Predicted leeway		
Drift segment number	Time of measurement		x-component	y-component	x-component	y-component	E-W coordinate	N-S coordinate	E-W coordinate	N-S coordinate	Segment percent error
	(local)		(m/s)	(m/s)	(m/s)	(m/s)	(m)	(m)	(m)	(m)	(%)
1	10:55						-250	-1228	-250	-1228	
2	11:05		-0.03	0.01	-0.02	-0.06	-265	-1221	-260	-1262	112.3
3	11:15		-0.05	-0.16	-0.02	-0.05	-294	-1319	-269	-1294	-67.5
4	11:25		-0.06	-0.02	-0.02	-0.05	-332	-1330	-281	-1323	-21.3
5	11:35		-0.14	0.00	-0.02	-0.05	-416	-1332	-294	-1350	-63.9
									Average percent error (%)		-10.1

Table 1 Drift Run B9-O

PIW/SS Field Data and Predicted Coordinates

Date: March 06, 1993

		Observed data						Computed data			
		PIW/SS position		Current		Wind			PIW/SS position		
Drift segment number	Time of measurement	E-W coordinate	N-S coordinate	x-component	y-component	x-component	x-component	Drift period	E-W coordinate	N-S coordinate	Segment percent error
	(local)	(m)	(m)	(m/s)	(m/s)	(m/s)	(m/s)	hh:mm	(m)	(m)	(%)
1	12:42	69	-721	0.16	-0.98	-1.86	-1.99		69	-721	
2	12:52	82	-1112	0.16	-0.98	-1.93	-1.70	0:10	140	-1311	52.0
3	13:02	86	-1566	0.06	-0.21	-1.96	-1.49	0:10	181	-1675	-19.3
4	13:12	86	-1813	0.06	-0.34	-1.94	-1.53	0:10	193	-1853	-28.1
5	13:32	108	-2250	0.07	-0.30	-1.90	-1.60	0:20	224	-2261	-6.5
6	13:42	185	-2649	0.07	-0.30	-1.87	-1.64	0:10	243	-2454	-52.3
7	13:52	211	-2785	0.06	-0.14	-1.85	-1.68	0:10	259	-2601	6.8
8	14:02	228	-3209	0.14	-0.43	-1.87	-1.65	0:10	295	-2786	-55.6
									Average percent error (%)		-14.7

Table 2 Drift B9-O

Derived and Predicted PIW/SS Leeway Velocities and Progressive Vector Coordinates

Date: March 06, 1993

			Derived leeway		Predicted lwy		Derived leeway		Predicted leeway		
Drift segment number	Time of measurement		x-component	y-component	x-component	y-component	E-W coordinate	N-S coordinate	E-W coordinate	N-S coordinate	Segment percent error
	(local)		(m/s)	(m/s)	(m/s)	(m/s)	(m)	(m)	(m)	(m)	(%)
1	12:42						69	-721	69	-721	
2	12:52		-0.14	0.33	-0.04	0.00	-14	-524	44	-723	-88.2
3	13:02		-0.10	-0.16	-0.04	-0.01	-76	-621	19	-730	-77.7
4	13:12		-0.06	-0.14	-0.04	-0.02	-112	-703	-5	-743	-70.1
5	13:32		-0.05	-0.04	-0.04	-0.02	-168	-756	-52	-767	-31.4
6	13:42		0.06	-0.37	-0.04	-0.02	-133	-975	-75	-780	-88.0
7	13:52		-0.02	-0.01	-0.04	-0.03	-146	-979	-98	-795	101.3
8	14:02		-0.07	-0.42	-0.04	-0.02	-189	-1232	-122	-809	-89.4
									Average percent error (%)		-49.0

Table 1 Drift Run B10-O

PIW/SS Field Data and Predicted Coordinates

Date: March 07, 1993

		Observed data						Computed data			
		PIW/SS position		Current		Wind			PIW/SS position		
Drift segment number	Time of measurement	E-W coordinate	N-S coordinate	x-component	y-component	x-component	y-component	Drift period	E-W coordinate	N-S coordinate	Segment percent error
	(local)	(m)	(m)	(m/s)	(m/s)	(m/s)	(m/s)	hh:mm	(m)	(m)	(%)
1	9:35	-1143	-1364	-0.27	-0.05	-4.53	-3.44		-1143	-1364	
2	9:45	-1279	-1267	-0.27	-0.05	-4.42	-3.40	0:10	-1352	-1433	31.6
3	9:55	-1470	-1063	-0.12	0.77	-4.32	-3.35	0:10	-1516	-1263	-15.5
4	10:09	-1562	-864	0.54	0.57	-4.45	-3.01	0:14	-1417	-770	129.3
5	10:19	-1570	-691	0.54	0.57	-4.62	-2.64	0:10	-1156	-472	128.7
									Average percent error (%)		68.5

Table 2 Drift B10-O

Derived and Predicted PIW/SS Leeway Velocities and Progressive Vector Coordinates

Date: March 07, 1993

			Derived leeway		Predicted lwy		Derived leeway		Predicted leeway		
Drift segment number	Time of measurement		x-component	y-component	x-component	y-component	E-W coordinate	N-S coordinate	E-W coordinate	N-S coordinate	Segment percent error
	(local)		(m/s)	(m/s)	(m/s)	(m/s)	(m)	(m)	(m)	(m)	(%)
1	9:35						-1143	-1364	-1143	-1364	
2	9:45		0.04	0.21	-0.08	-0.06	-1117	-1237	-1190	-1403	-53.1
3	9:55		-0.12	-0.02	-0.08	-0.08	-1191	-1249	-1237	-1449	-12.0
4	10:09		-0.32	-0.43	-0.09	-0.08	-1459	-1613	-1314	-1519	-77.0
5	10:19		-0.55	-0.28	-0.11	-0.07	-1791	-1782	-1377	-1563	-79.3
									Average percent error (%)		-55.4

Table 1 Drift Run B11-O

PIW/SS Field Data and Predicted Coordinates

Date: March 07, 1993

		Observed data						Computed data			
		PIW/SS position		Current		Wind			PIW/SS position		
Drift segment number	Time of measurement	E-W coordinate	N-S coordinate	x-component	y-component	x-component	y-component	Drift period	E-W coordinate	N-S coordinate	Segment percent error
	(local)	(m)	(m)	(m/s)	(m/s)	(m/s)	(m/s)	hh:mm	(m)	(m)	(%)
1	10:34	115	-997	-0.18	0.14	-4.83	-2.08		115	-997	
2	10:44	-28	-954	-0.18	0.14	-4.93	-1.69	0:10	-47	-937	16.1
3	10:54	-185	-911	-0.15	0.11	-5.00	-1.30	0:10	-202	-883	0.7
4	11:04	-317	-865	-0.13	0.09	-5.02	-1.06	0:10	-342	-841	4.8
5	11:18	-473	-816	-0.12	0.01	-5.00	-1.03	0:14	-524	-819	11.5
6	11:28	-636	-820	-0.12	0.01	-4.98	-1.02	0:10	-651	-825	-21.9
7	11:38	-772	-877	-0.08	-0.07	-4.96	-1.00	0:10	-767	-854	-18.9
8	11:48	-854	-940	-0.03	-0.07	-4.94	-0.98	0:10	-858	-908	1.8
9	12:01	-951	-1064	-0.01	-0.40	-4.89	-0.96	0:13	-950	-1100	35.9
10	12:11	-1029	-1276	-0.01	-0.40	-4.68	-0.97	0:10	-1013	-1342	10.7
11	12:21	-1031		0.02	-0.39	-4.46	-0.98	0:10	-1065	-1581	-80.9
12	12:31	-1094	-1766	0.05	-0.47	-4.25	-0.99	0:10	-1097	-1841	-85.2
13	12:43	-1148	-2055	-0.02	-0.44	-3.99	-0.99	0:12	-1146	-2173	14.3
14	12:53	-1213	-2368	-0.02	-0.44	-3.78	-0.98	0:10	-1204	-2443	-13.7
15	13:03	-1328	-2721	-0.14	-0.80	-3.56	-1.03	0:10	-1294	-2814	2.9
									Average percent error (%)		-8.7

Table 2 Drift B11-O

Derived and Predicted PIW/SS Leeway Velocities and Progressive Vector Coordinates

Date: March 07, 1993

			Derived leeway		Predicted lwy		Derived leeway		Predicted leeway		
Drift segment number	Time of measurement		x-component	y-component	x-component	y-component	E-W coordinate	N-S coordinate	E-W coordinate	N-S coordinate	Segment percent error
	(local)		(m/s)	(m/s)	(m/s)	(m/s)	(m)	(m)	(m)	(m)	(%)
1	10:34						115	-997	115	-997	
2	10:44		-0.06	-0.07	-0.09	-0.04	82	-1038	62	-1021	10.3
3	10:54		-0.09	-0.05	-0.09	-0.03	25	-1069	8	-1041	-10.3
4	11:04		-0.08	-0.02	-0.09	-0.03	-22	-1081	-48	-1057	17.8
5	11:18		-0.06	0.01	-0.09	-0.02	-75	-1072	-126	-1075	49.6
6	11:28		-0.15	-0.02	-0.09	-0.02	-167	-1082	-182	-1087	-37.9
7	11:38		-0.13	-0.07	-0.09	-0.02	-242	-1121	-238	-1098	-33.3
8	11:48		-0.08	-0.03	-0.09	-0.02	-290	-1141	-294	-1108	11.2
9	12:01		-0.10	0.08	-0.09	-0.01	-369	-1080	-368	-1117	-25.2
10	12:11		-0.12	0.04	-0.09	-0.01	-438	-1054	-423	-1121	-25.4
11	12:21		-0.01	0.83	-0.09	-0.01	-442		-476	-1124	-89.3
12	12:31		-0.14	-0.83	-0.09	-0.01	-525	-1053	-528	-1127	-89.8
13	12:43		-0.09	0.06	-0.08	0.00	-587	-1013	-585	-1131	-21.7
14	12:53		-0.09	-0.08	-0.07	0.00	-639	-1058	-630	-1133	-35.5
15	13:03		-0.11	0.03	-0.07	0.00	-705	-1040	-671	-1133	-39.9
									Average percent error (%)		-22.8

APPENDIX C

PIW/SS Leeway Displacement and Drift Plots

Appendix C contains trajectory plots for each of the nine drift runs conducted over the Atlantic Ocean tracking range in March 1993. Two plots are shown for each drift run In the first, the derived and predicted progressive leeway displacement vectors are shown. In the second plot, the observed and predicted drift trajectories of the PIW/SS test objects are shown. While the scale of the individual plots vary, the grid lines are drawn at intervals of 200 meters in all cases. The position coordinates used to generate the plots are listed in Appendix B.

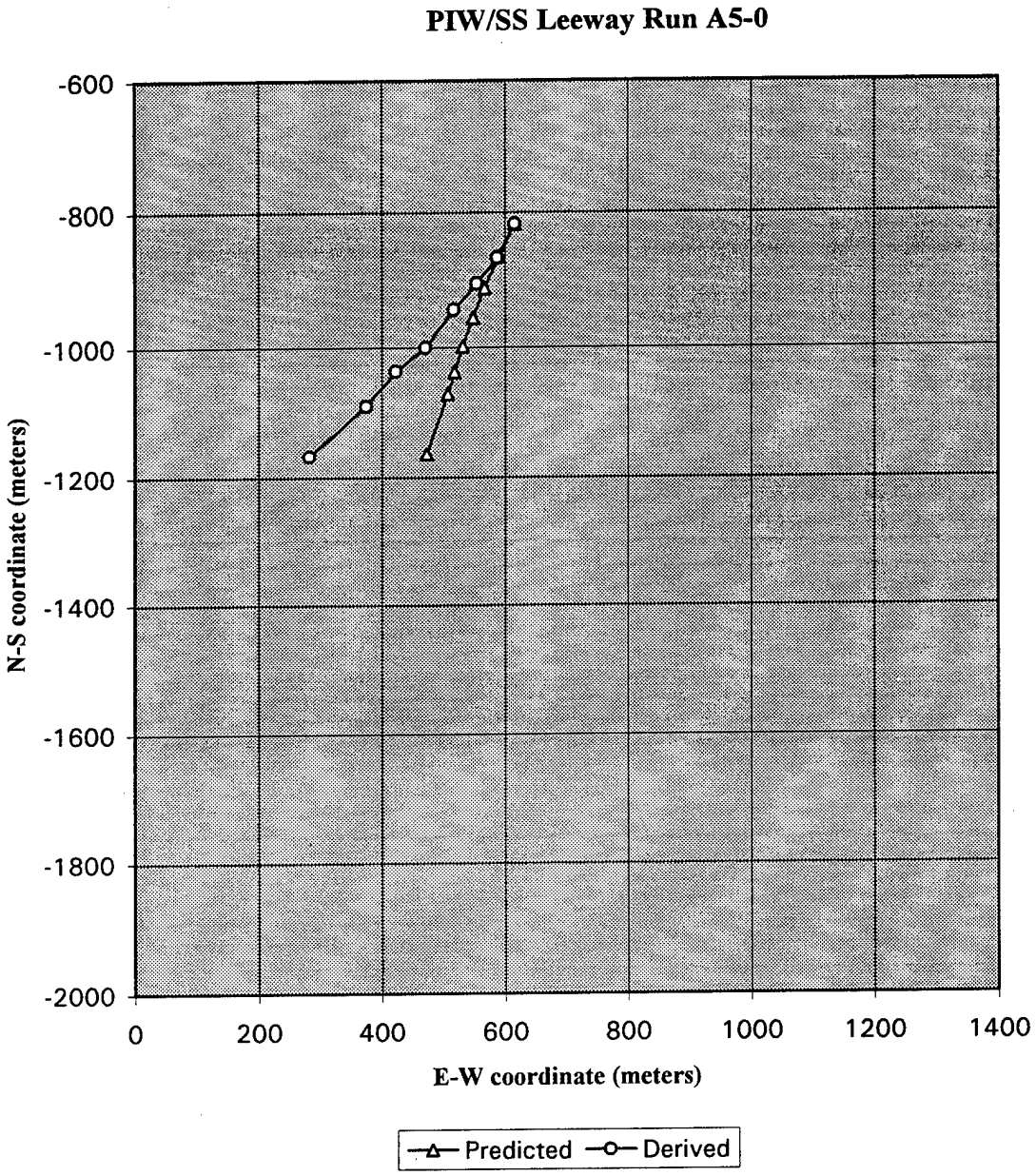
PIW/SS Leeway Run A5-0
-600
-800
-1000
-1200
-1400
-1600
-1800
-2000
N-S coordinate (meters)
0
200
400
600
800
1000
1200
1400
E-W coordinate (meters)
Predicted
Derived

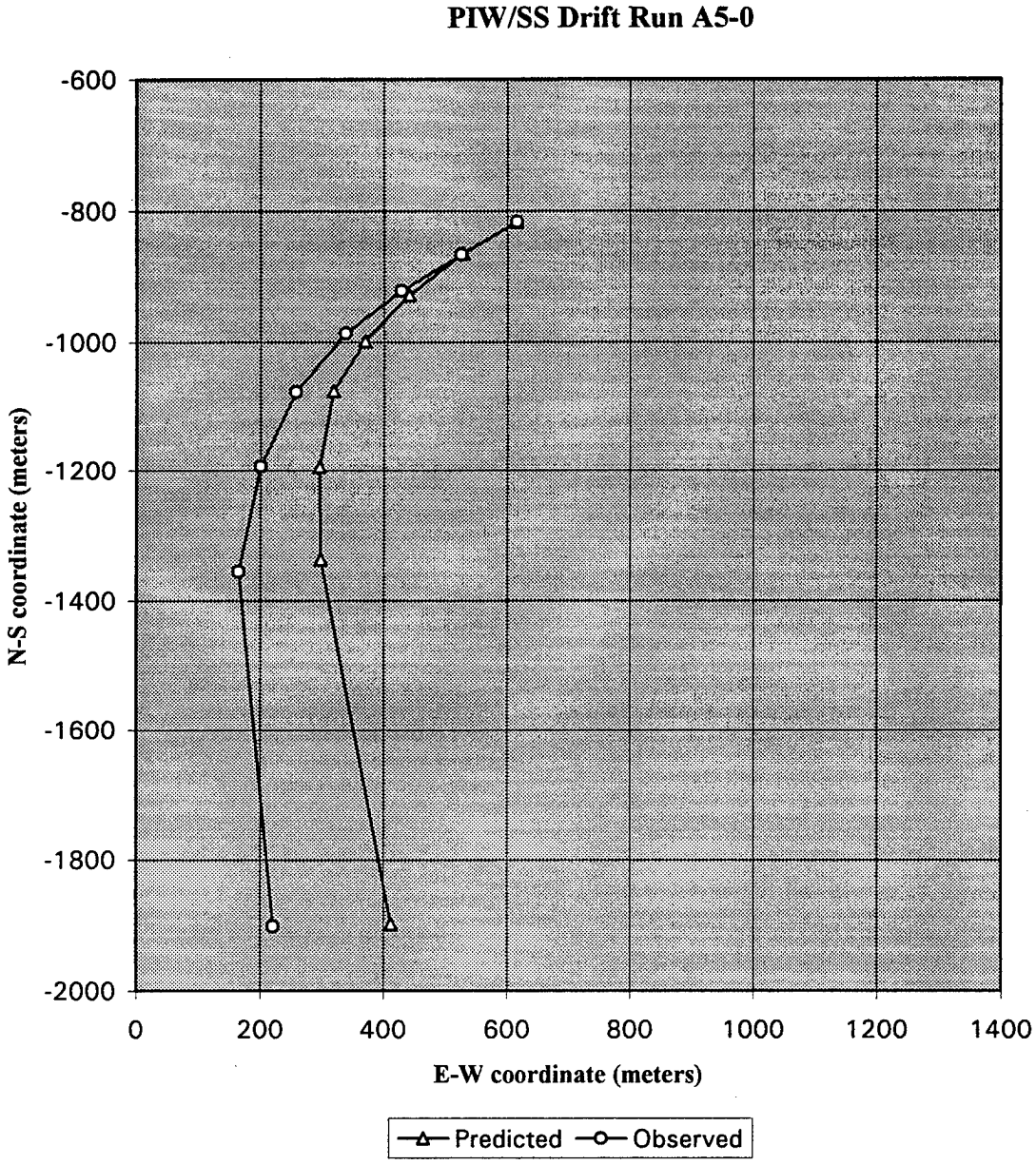
PIW/SS Drift Run A5-0
-600
-800
-1000
-1200
-1400
-1600
-1800
-2000
N-S coordinate (meters)
0
200
400
600
800
1000
1200
1400
E-W coordinate (meters)
Predicted
Observed

PIW/SS Leeway Run A6-0

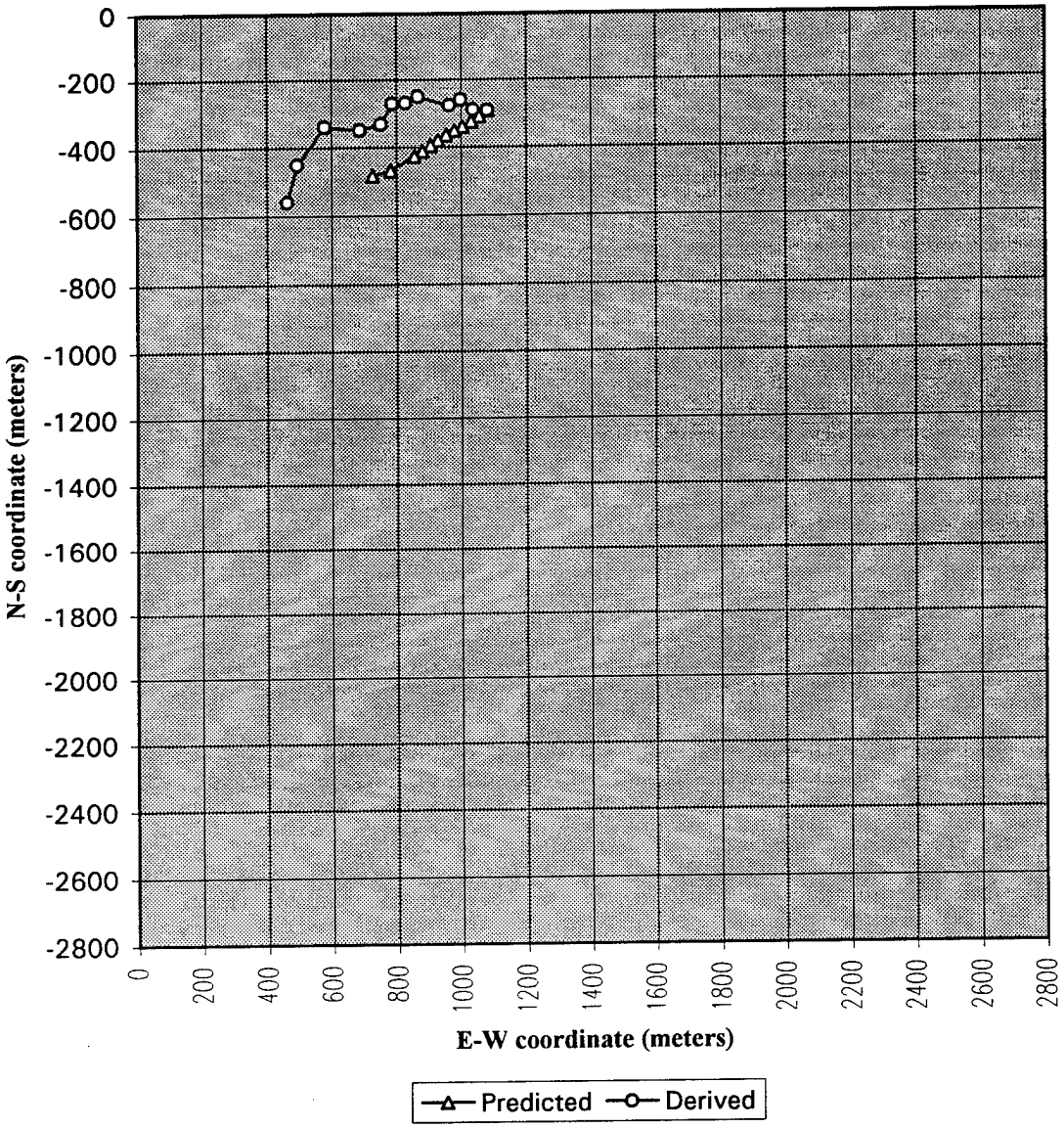

PIW/SS Drift Run A6-0

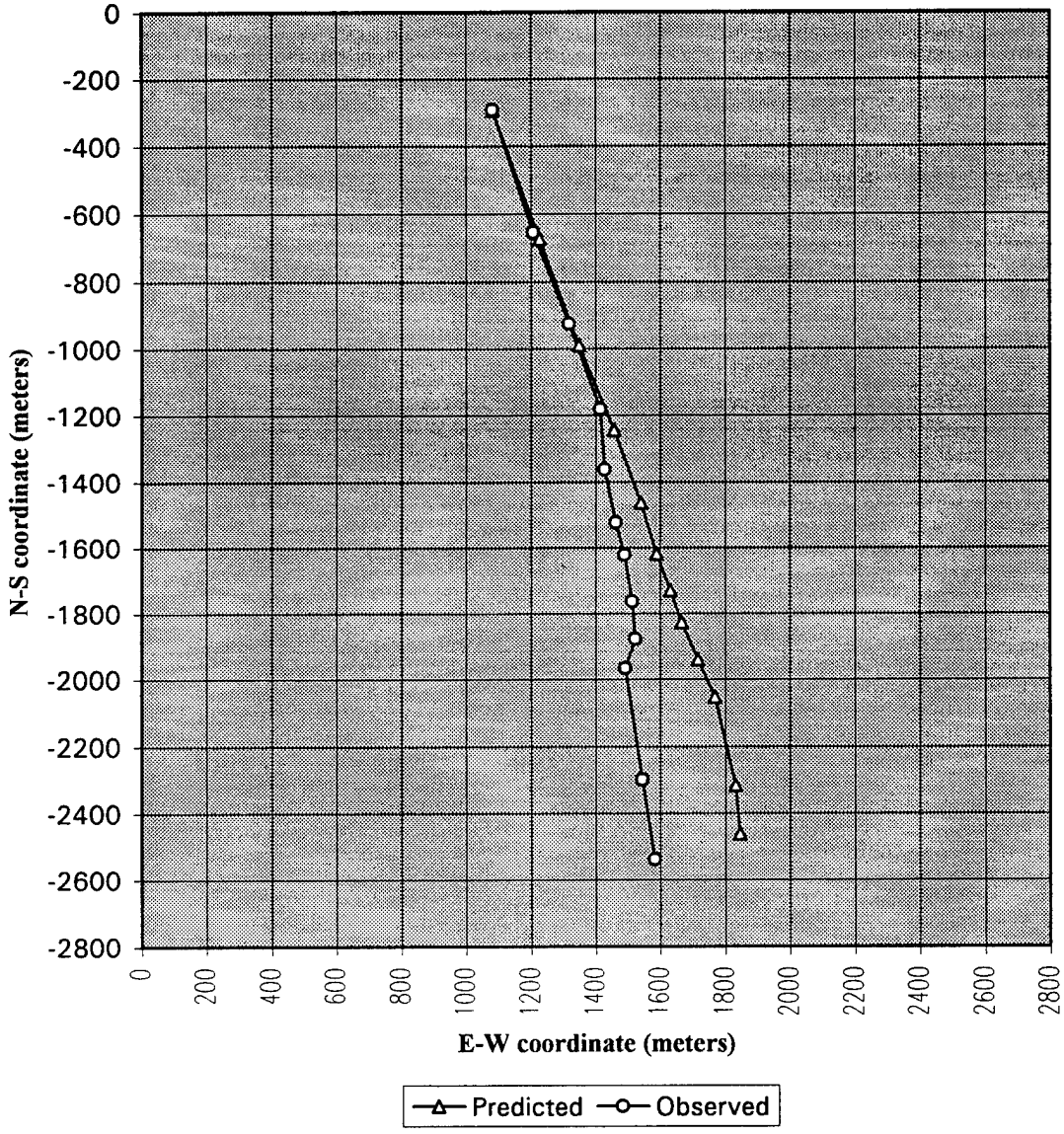

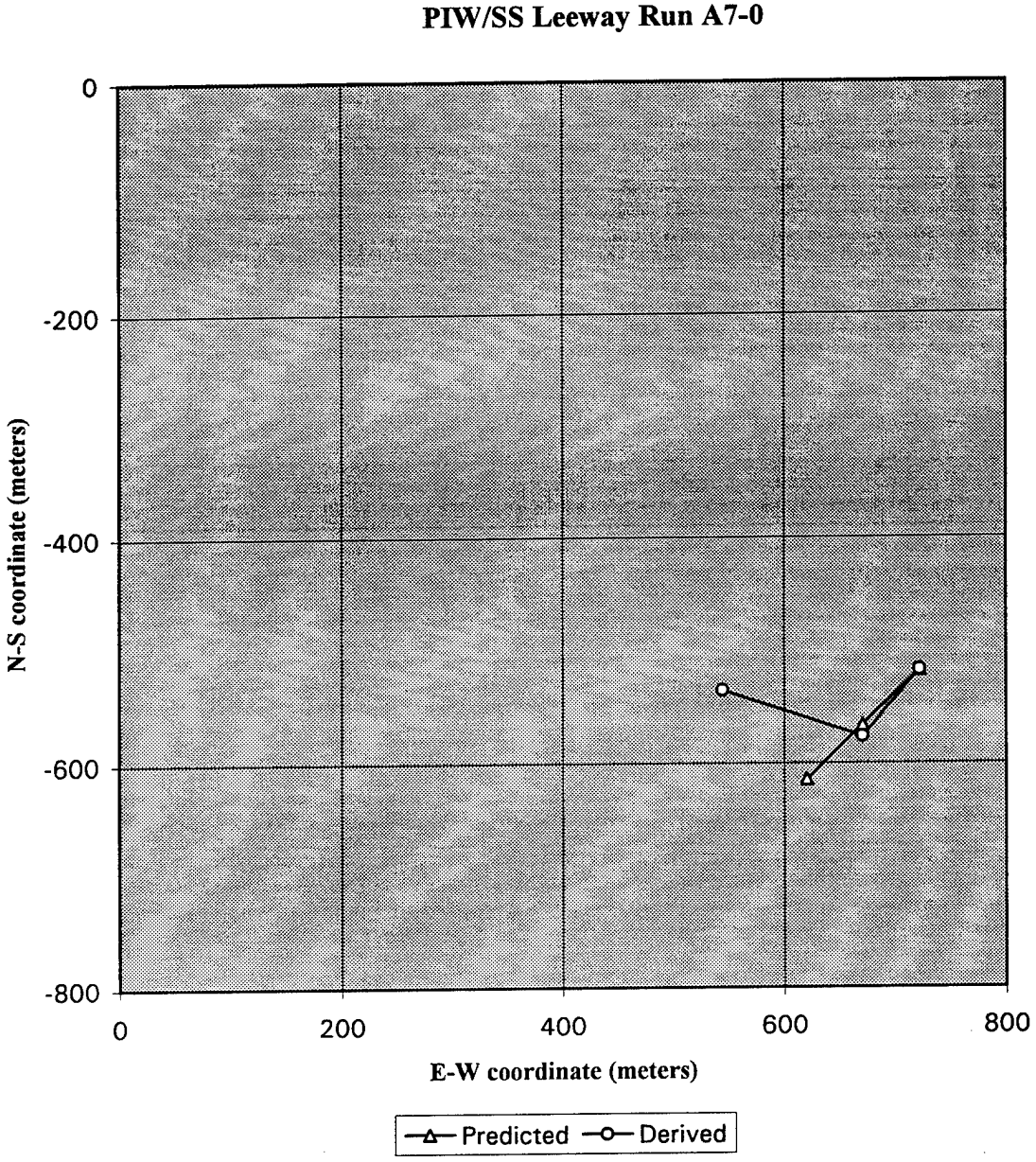
PIW/SS Leeway Run A7-0
0
-200
-400
-600
-800
N-S coordinate (meters)
0
200
400
600
800
E-W coordinate (meters)
Predicted
Derived

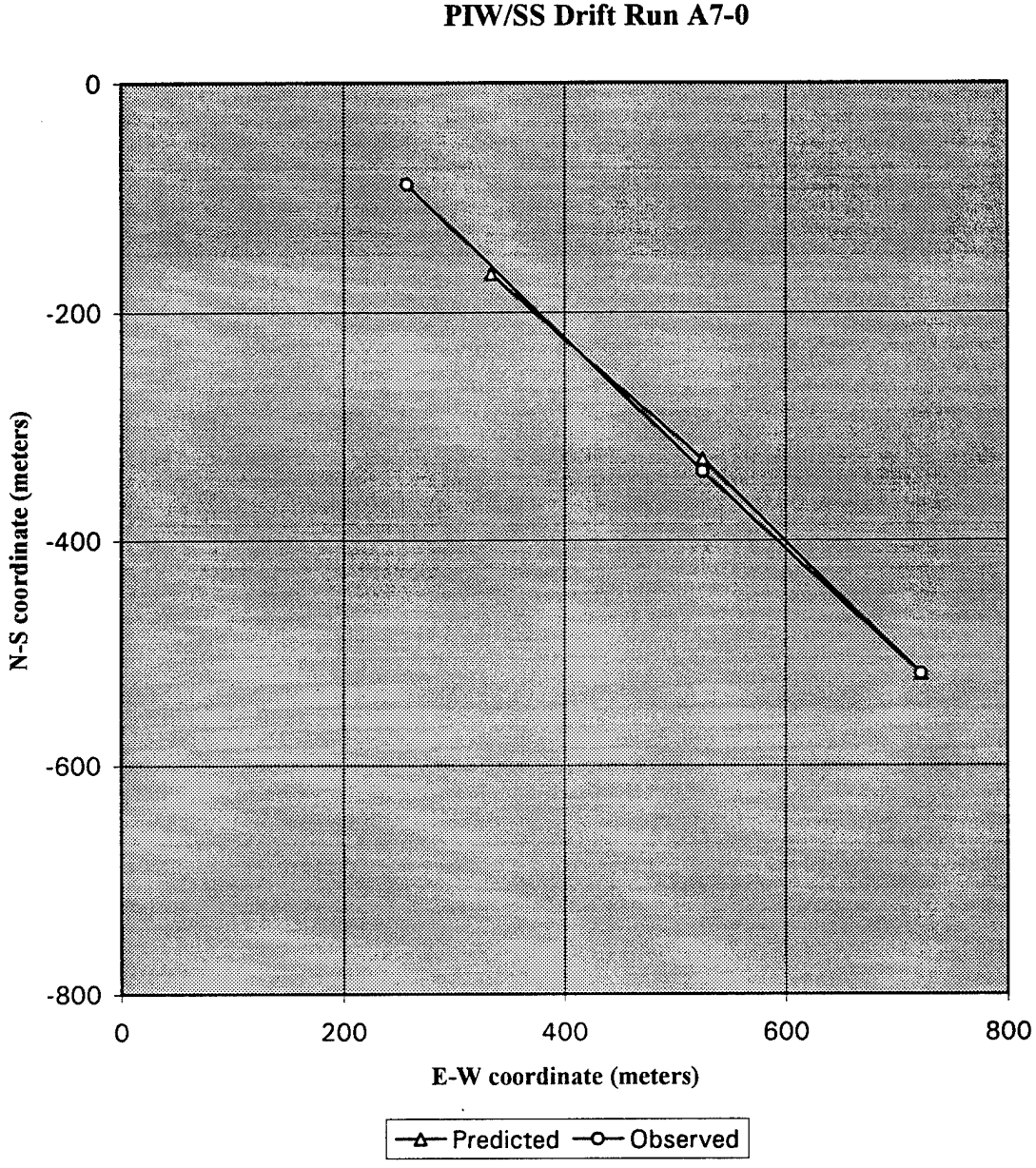
PIW/SS Drift Run A7-0
0
-200
-400
-600
-800
N-S coordinate (meters)
0
200
400
600
800
E-W coordinate (meters)
Predicted
Observed

PIW/SS Leeway Run A8-0

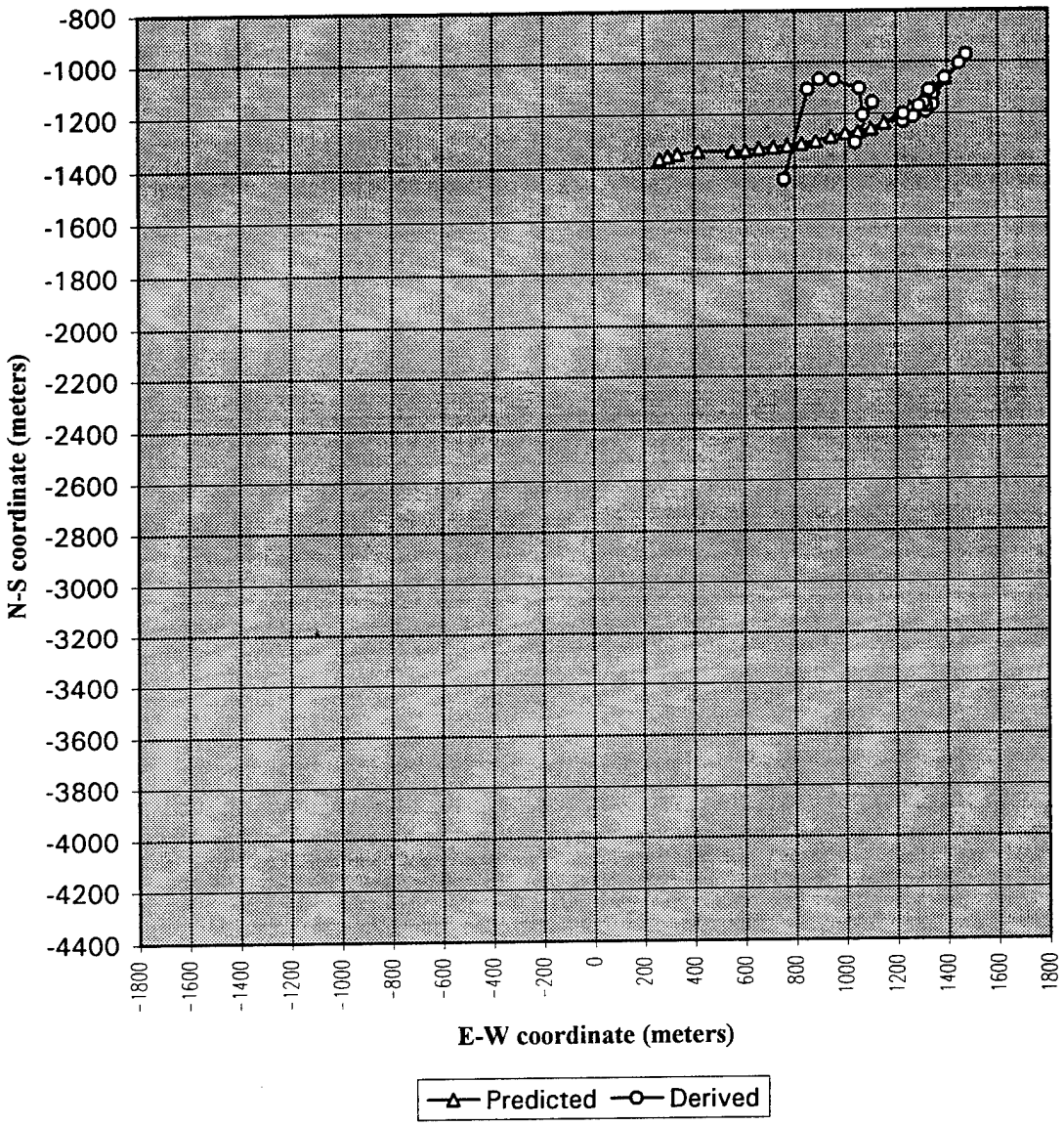

PIW/SS Drift Run A8-0

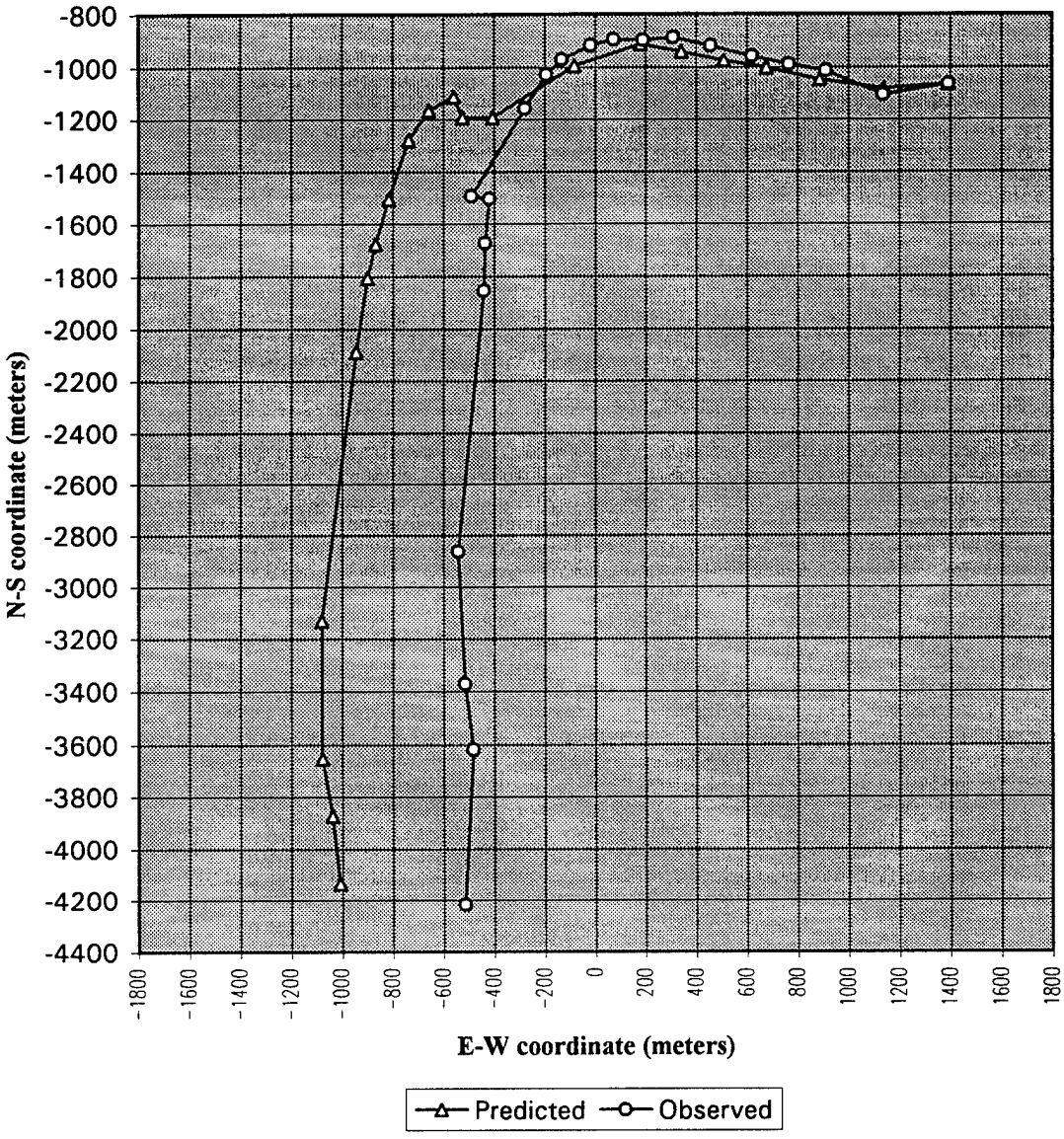

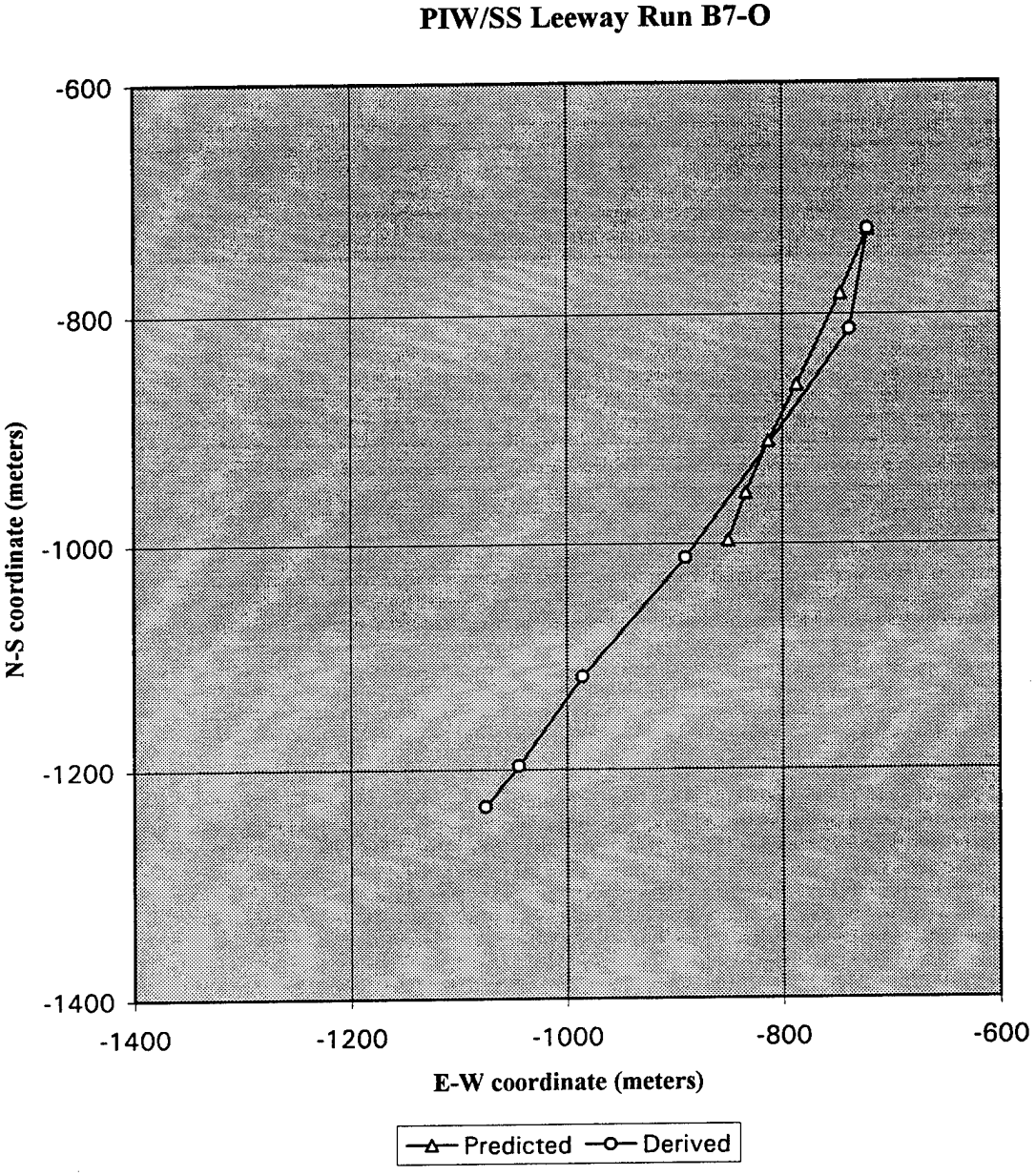
PIW/SS Leeway Run B7-O
-600
-800
-1000
-1200
-1400
N-S coordinate (meters)
-1400
-1200
-1000
-800
-600
E-W coordinate (meters)
Predicted
Derived

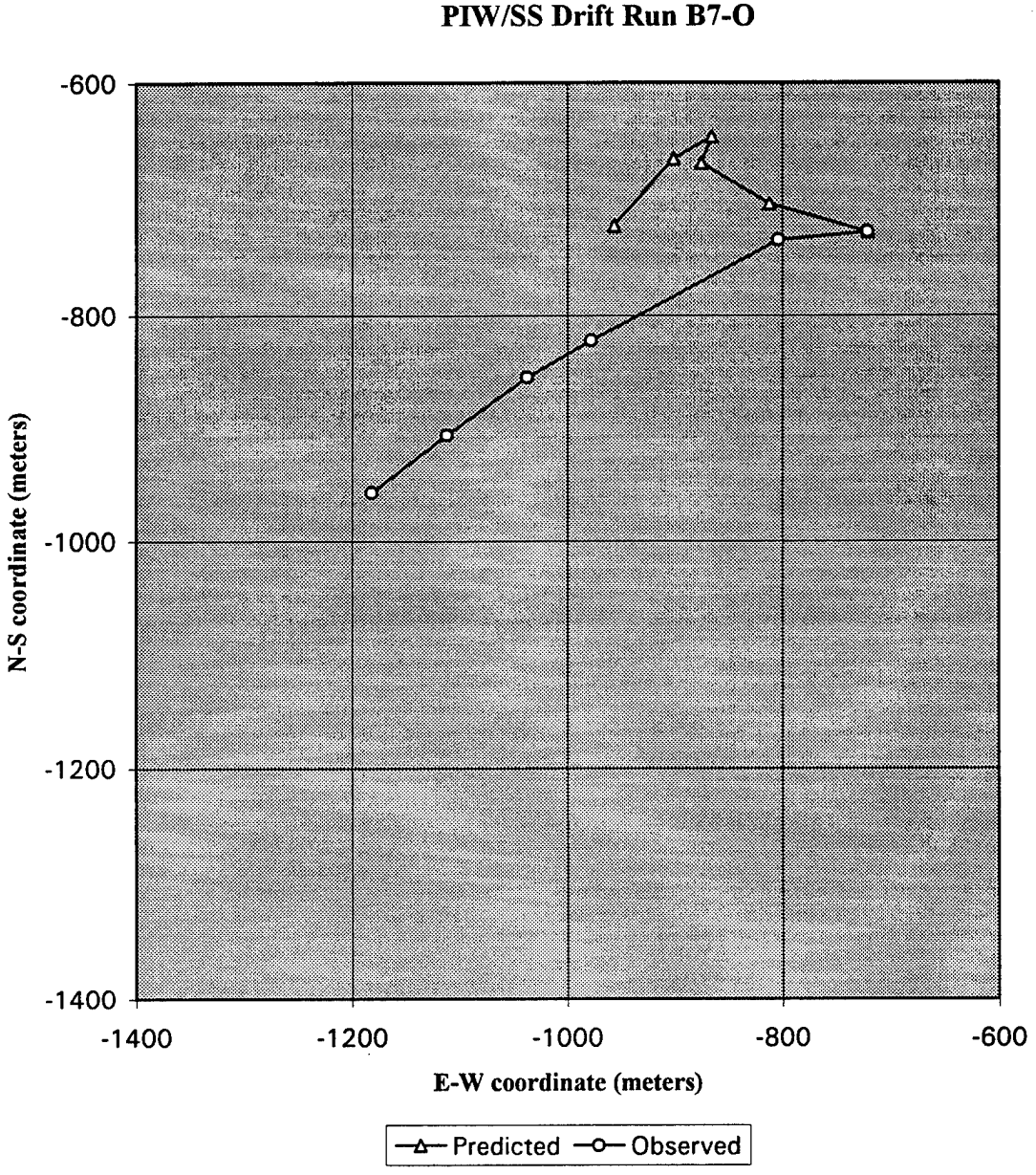
PIW/SS Drift Run B7-O
-600
-800
-1000
-1200
-1400
N-S coordinate (meters)
-1400
-1200
-1000
-800
-600
E-W coordinate (meters)
Predicted
Observed

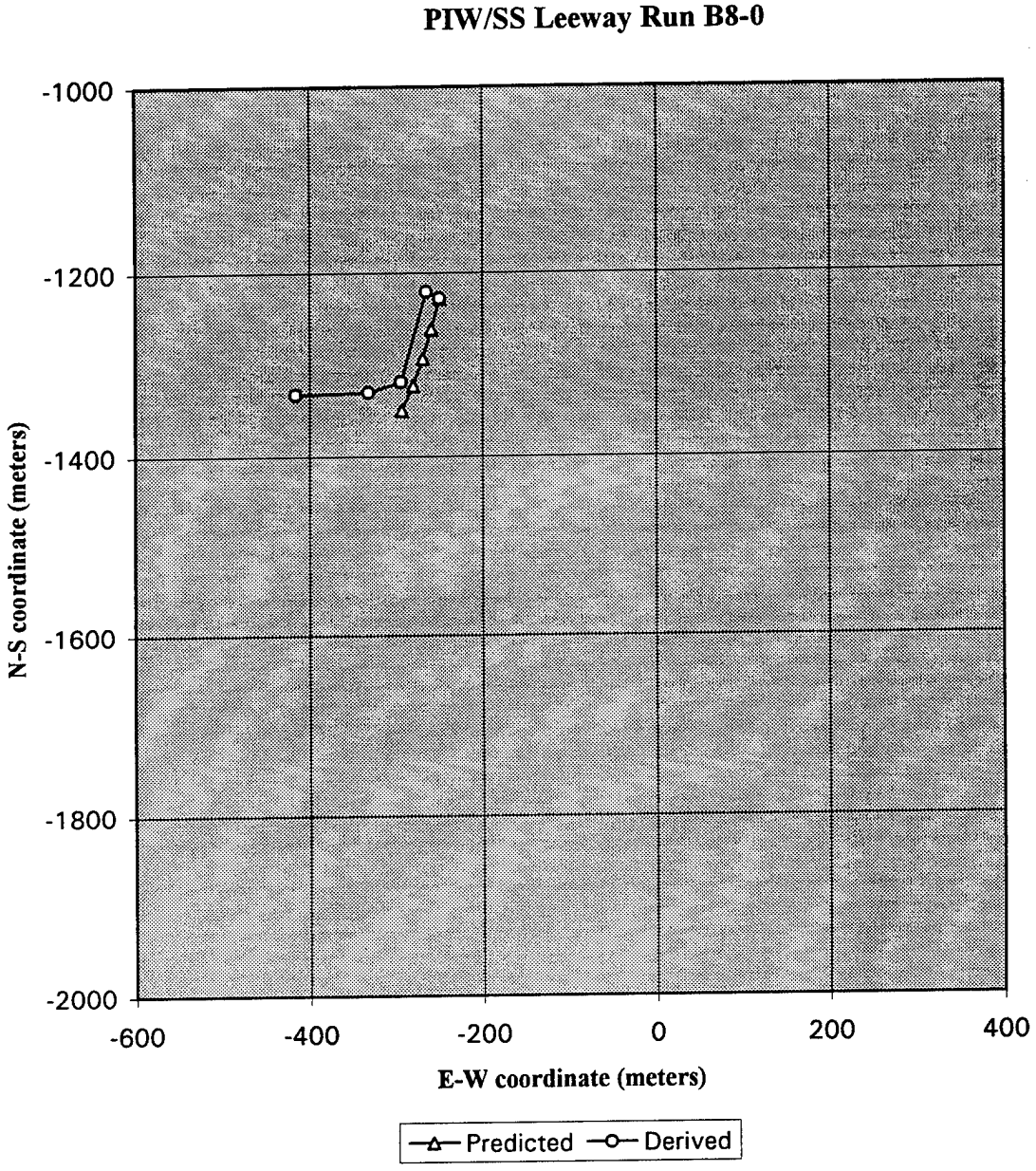
PIW/SS Leeway Run B8-0
-1000
-1200
-1400
-1600
-1800
-2000
N-S coordinate (meters)
-600
-400
-200
0
200
400
E-W coordinate (meters)
Predicted
Derived

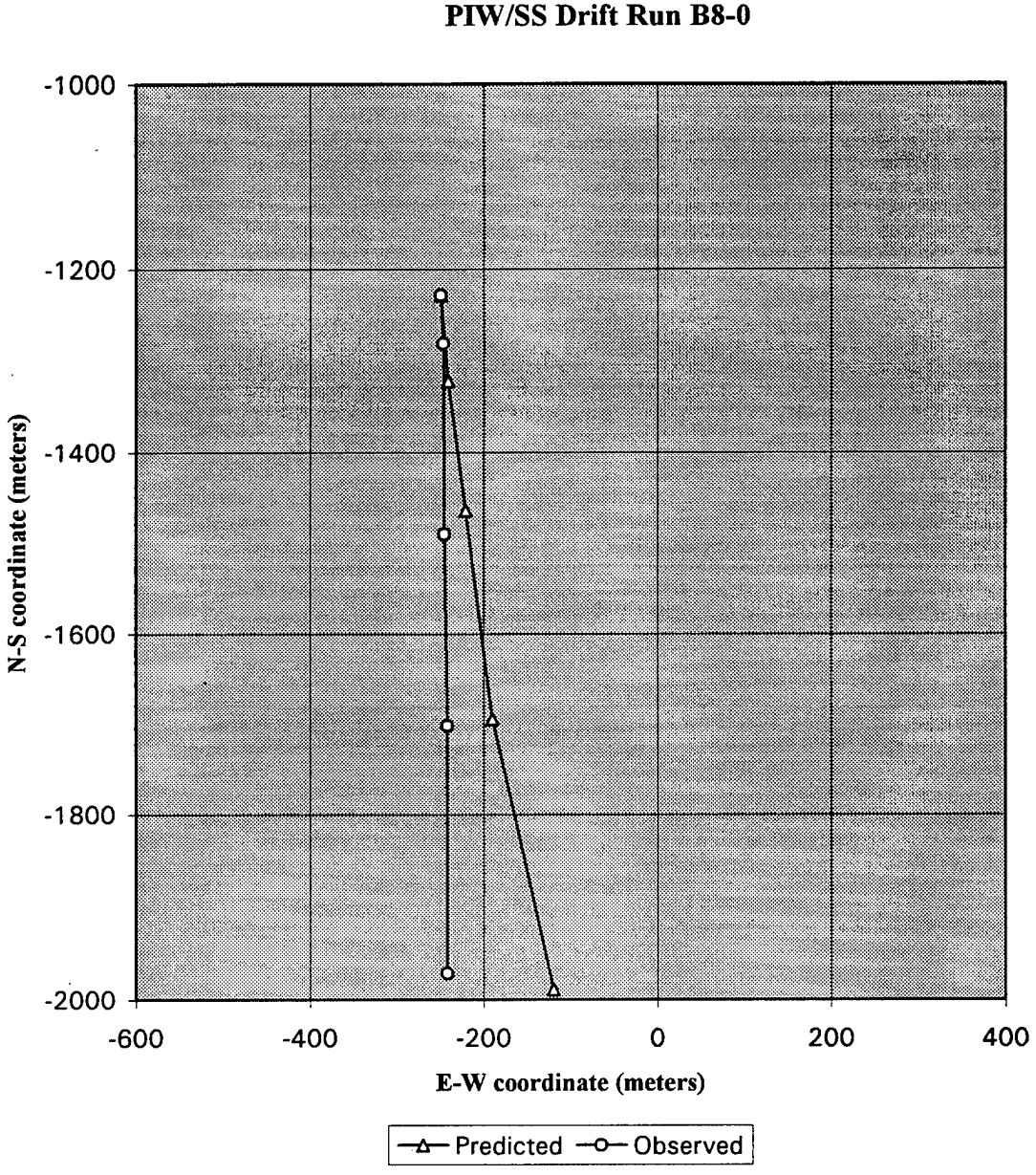
PIW/SS Drift Run B8-0
-1000
-1200
-1400
-1600
-1800
-2000
N-S coordinate (meters)
-600
-400
-200
0
200
400
E-W coordinate (meters)
Predicted
Observed

PIW/SS Leeway Run B9-0

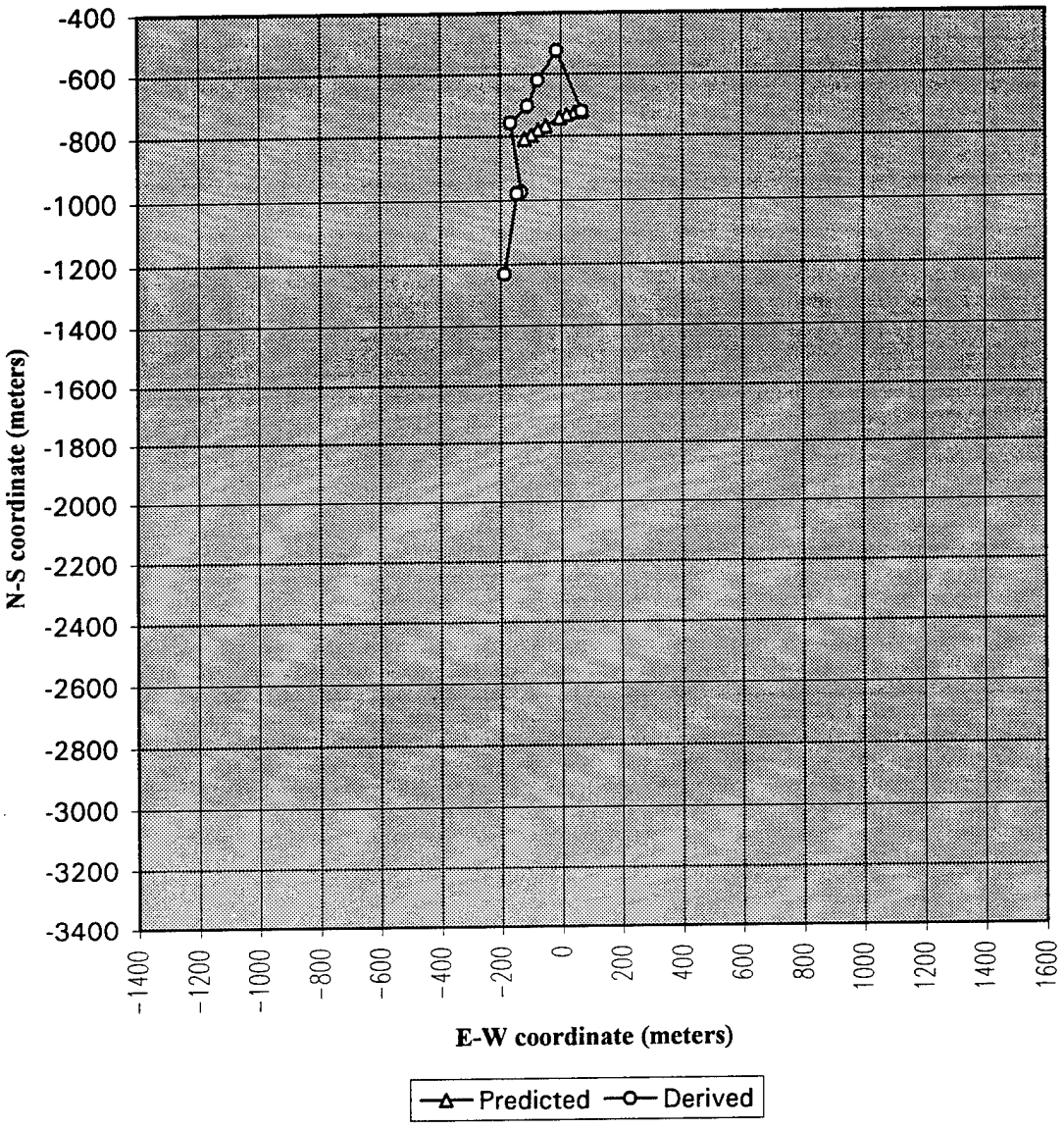

PIW/SS Drift Run B9-0

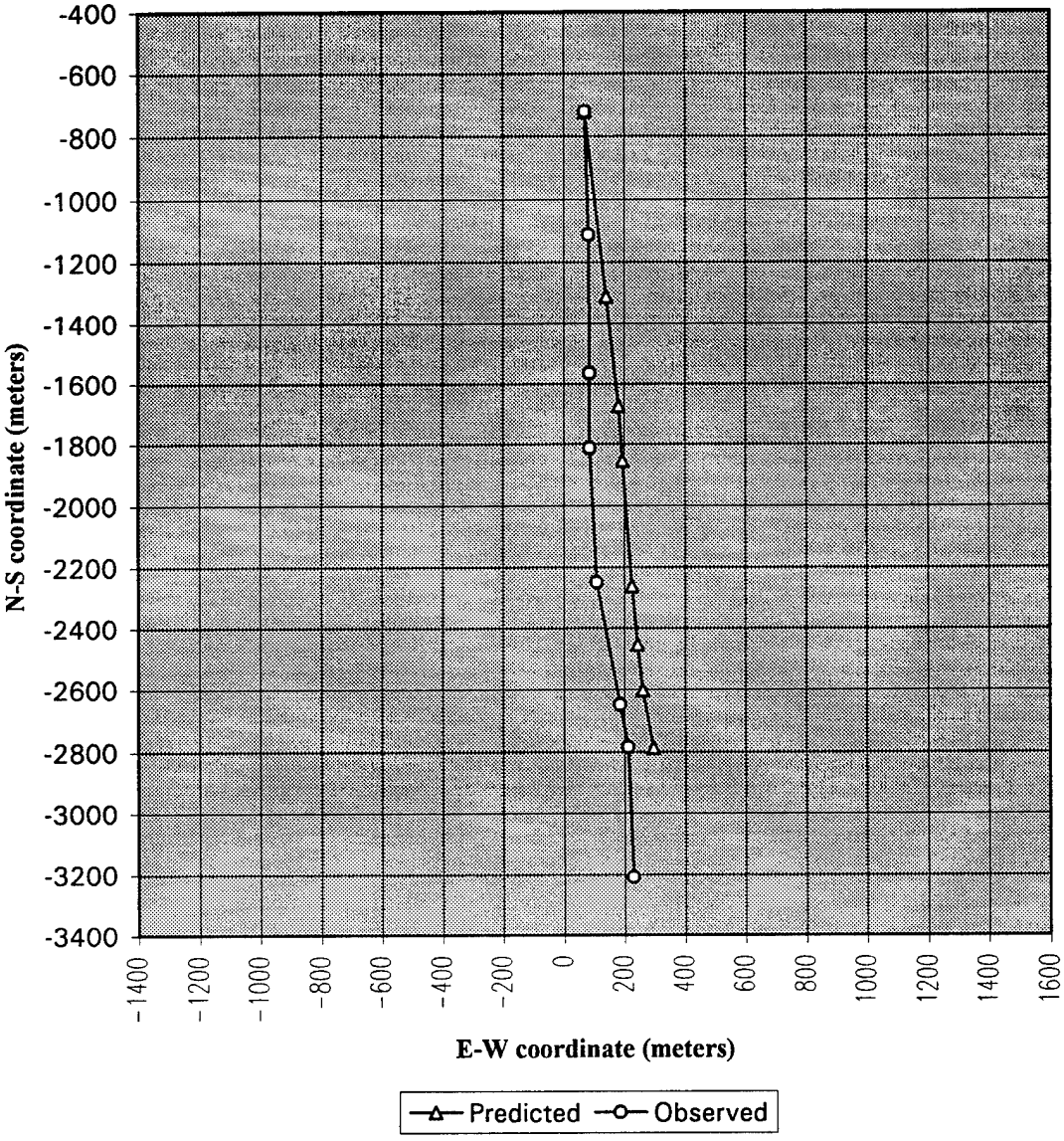

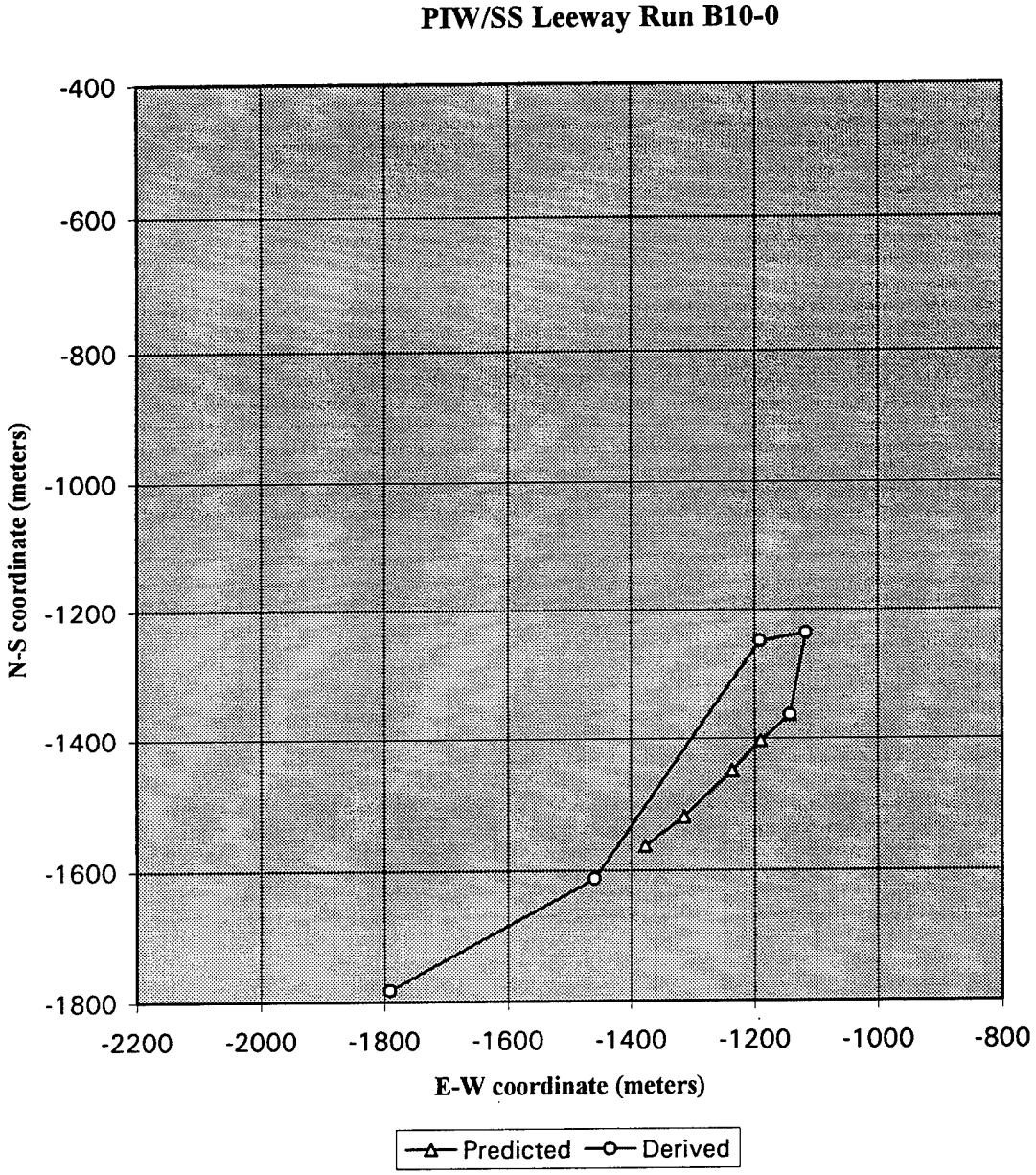
PIW/SS Leeway Run B10-0
-400
-600
-800
-1000
-1200
-1400
-1600
-1800
N-S coordinate (meters)
-2200
-2000
-1800
-1600
-1400
-1200
-1000
-800
E-W coordinate (meters)
Predicted
Derived

PIW/SS Drift Run B10-0

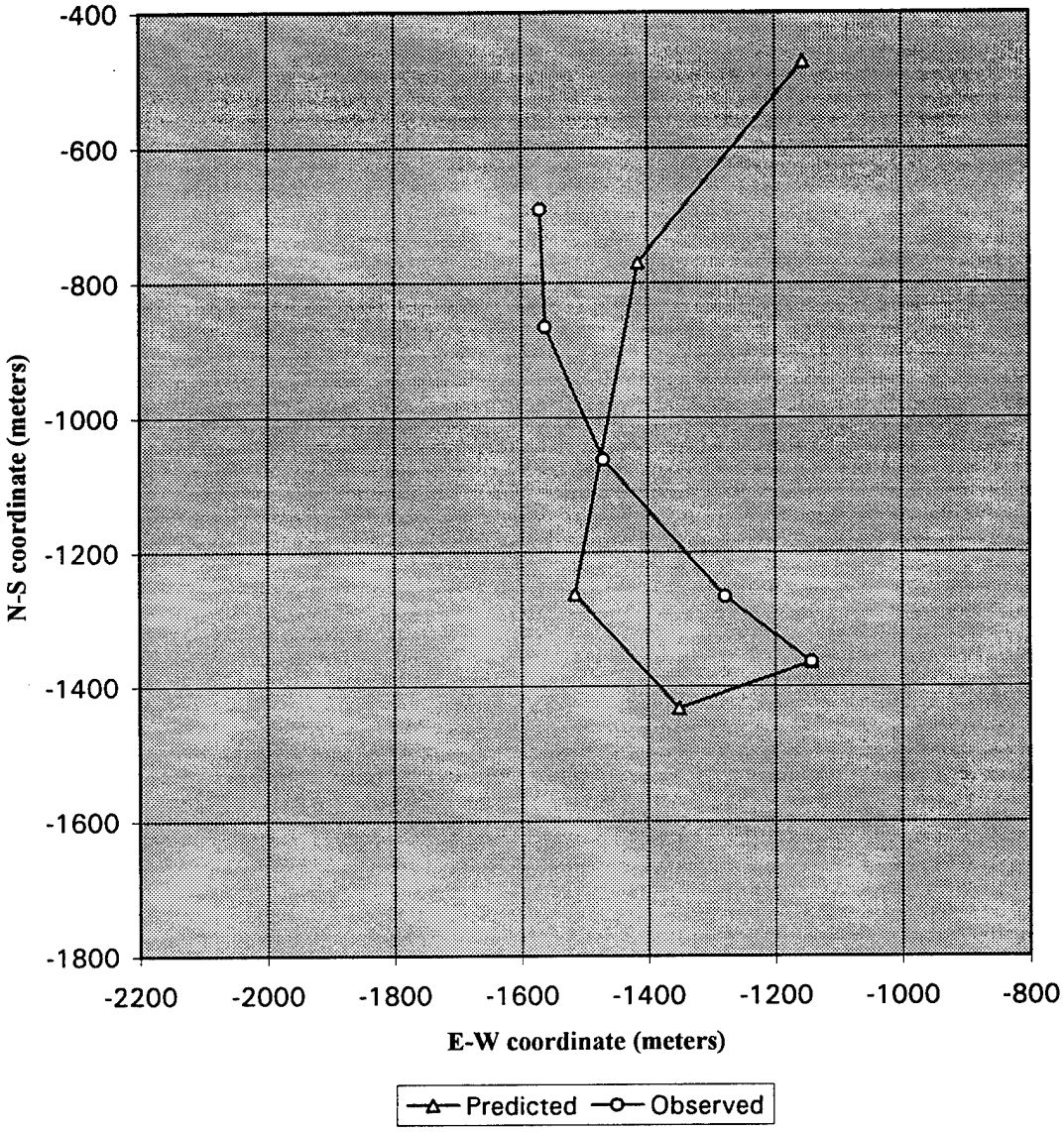

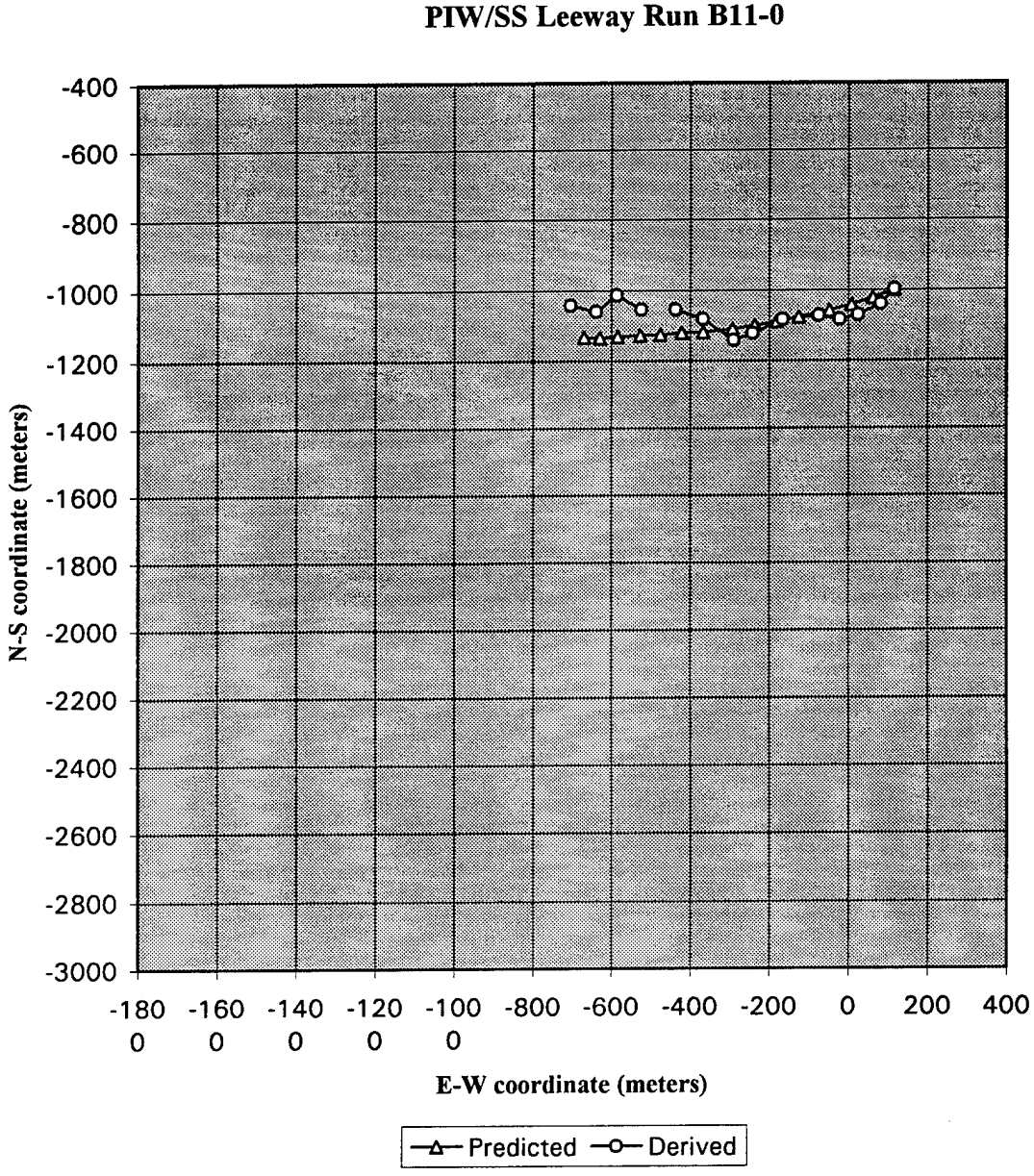
PIW/SS Leeway Run B11-0
-400
-600
-800
-1000
-1200
-1400
-1600
-1800
-2000
-2200
-2400
-2600
-2800
-3000
N-S coordinate (meters)
-180 -160 -140 -120 -100 -800 -600 -400 -200 0 200 400
0 0 0 0 0
E-W coordinate (meters)
Predicted
Derived

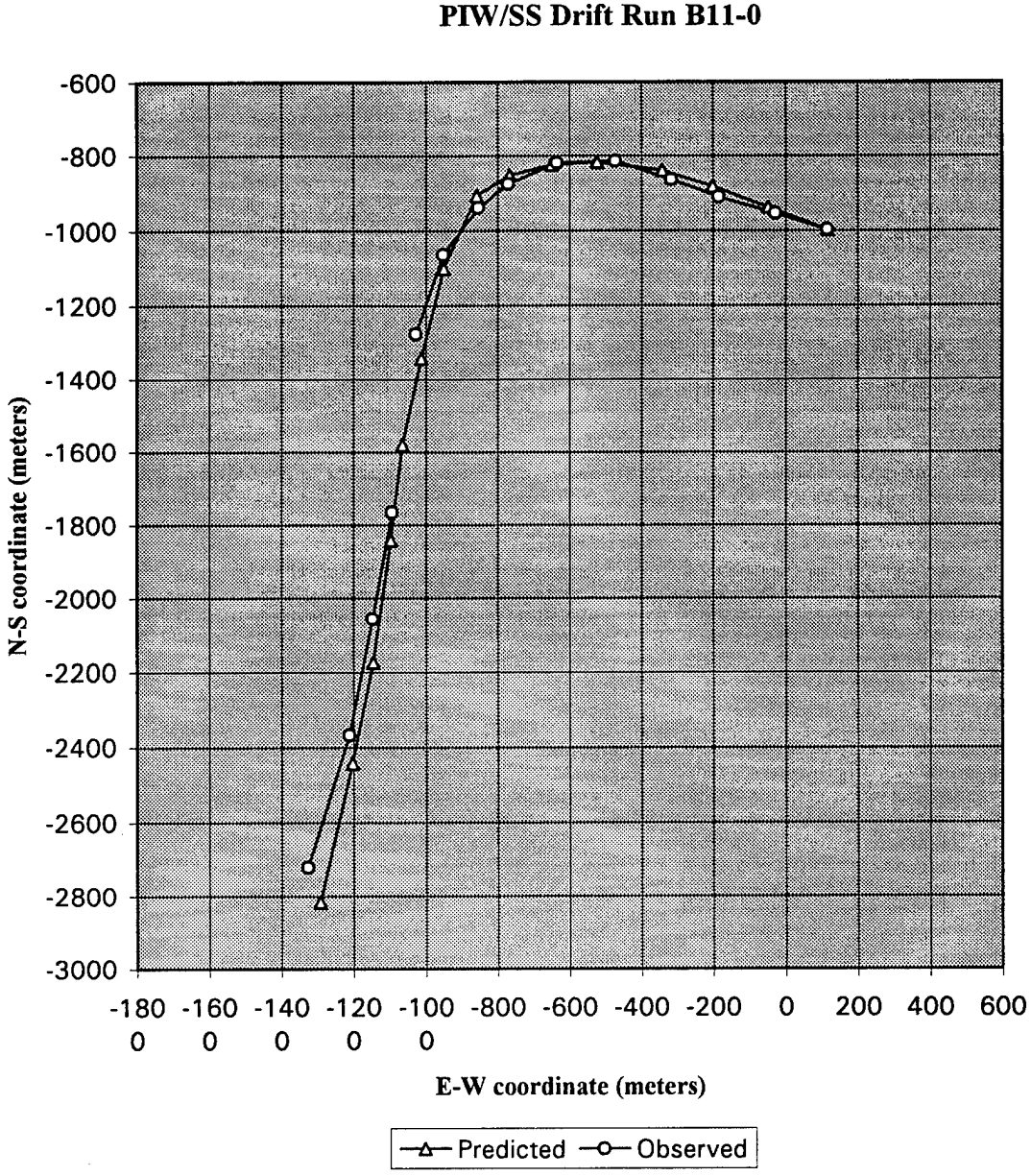
PIW/SS Drift Run B11-0
-600
-800
-1000
-1200
-1400
-1600
-1800
-2000
-2200
-2400
-2600
-2800
-3000
N-S coordinate (meters)
-180 -160 -140 -120 -100 -800 -600 -400 -200 0 200 400 600
0 0 0 0 0
E-W coordinate (meters)
Predicted
Observed